

RESEARCH MEMORANDUM

THE ORIGIN AND DISTRIBUTION OF SUPERSONIC STORE INTERFERENCE
FROM MEASUREMENT OF INDIVIDUAL FORCES ON SEVERAL
WING-FUSELAGE-STORE CONFIGURATIONS

VI.- SWEEP-WING HEAVY-BOMBER CONFIGURATION WITH STORES
OF DIFFERENT SIZES AND SHAPES

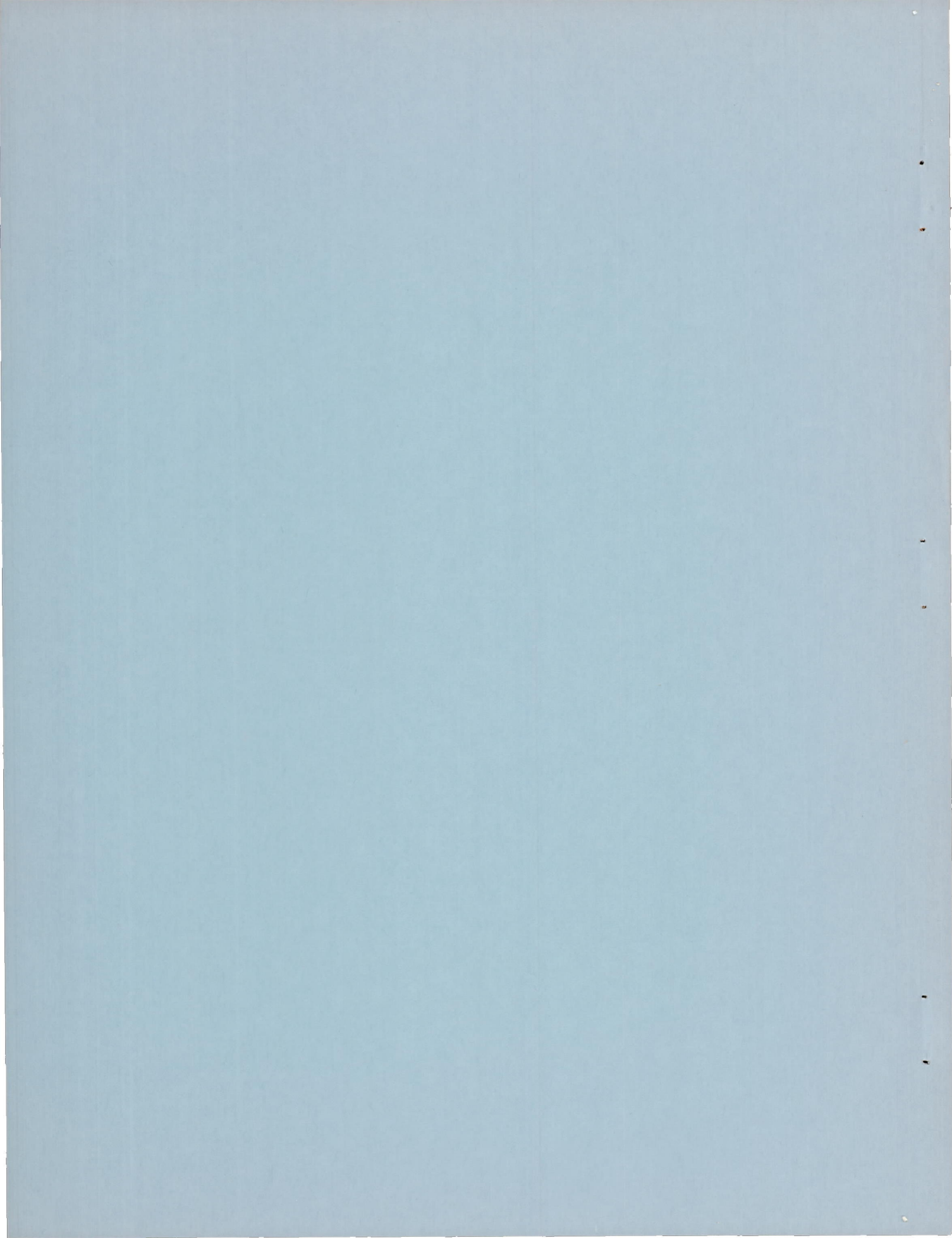
By Norman F. Smith

Langley Aeronautical Laboratory
Langley Field, Va.

Declassified February 8, 1963

NATIONAL ADVISORY COMMITTEE
FOR AERONAUTICS
WASHINGTON

March 8, 1956



NATIONAL ADVISORY COMMITTEE FOR AERONAUTICS

RESEARCH MEMORANDUM

THE ORIGIN AND DISTRIBUTION OF SUPERSONIC STORE INTERFERENCE
FROM MEASUREMENT OF INDIVIDUAL FORCES ON SEVERAL
WING-FUSELAGE-STORE CONFIGURATIONS

VI.- SWEEP-WING HEAVY-BOMBER CONFIGURATION WITH STORES
OF DIFFERENT SIZES AND SHAPES

By Norman F. Smith

SUMMARY

A supersonic wind-tunnel investigation of the origin and distribution of store interference has been performed in the Langley 4- by 4-foot supersonic pressure tunnel at a Mach number of 1.61 in which separate forces on a store, a fuselage, a swept wing, and a swept-wing-fuselage combination were measured. The store was separately sting-mounted on its own six-component internal balance and was traversed through a wide systematic range of spanwise, chordwise, and vertical positions. This report presents data on a configuration which simulated a heavy-bomber airplane with stores of several shapes and sizes.

The drag of the various stores in the presence of the wing-fuselage combination is explained in a qualitative way by buoyancy considerations, that is, by consideration of the position of the nose and afterbody portions of the store in the flow (pressure) field of the wing-fuselage combination. The drag of the wing-fuselage combination in the flow field of the various stores appears to be similarly explained by buoyancy considerations.

The total drag of the complete (wing-fuselage-store) configuration with the small ogive-cylinder or the large parabolic store was lower than with the large ogive-cylinder store for any given store position. The effect of store position, however, remained very large for all stores; consequently, the drag of the configuration with a small store in an unfavorable location in many cases exceeded the drag of the configuration with a large store in a favorable location.

Of the stores investigated, the small store and the finned store encountered larger peak values of lift, side force, and drag coefficients and steeper variations of these coefficients with changes in store position. This is a consequence of the fact that the small store or the fins were more completely submerged in regions in which the interference force was in one direction.

INTRODUCTION

References 1 and 2 present the results of an experimental investigation of stores interference on a simulated heavy-bomber configuration at $M = 1.6$. The store investigated simulated a twin-engine (equivalent frontal area) nacelle (with no provision for internal flow) or a very large external store. Individual forces and moments were measured on the store (6 components) and on the fuselage, wing, and wing-fuselage combination (4 components). A spanwise range of store midpoint positions larger than the wing semispan and a chordwise range of positions nearly equal to the fuselage length were investigated.

The present report covers an investigation of the same swept-wing heavy-bomber model with stores of several sizes and shapes and with a large store with fins. A range of chordwise store positions somewhat smaller than that covered in the work of references 1 and 2 was utilized. The results are compared with the more extensive data on the large ogive-cylinder store from references 1 and 2.

SYMBOLS

$C_{D_{wf}}$	drag coefficient of wing-fuselage combination, Drag/ qS
$C_{L_{wf}}$	lift coefficient of wing-fuselage combination, Lift/ qS
$C_{m_{wf}}$	pitching-moment coefficient of wing-fuselage combination (measured about $\bar{c}/4$), Pitching moment/ $qS\bar{c}$
C_{D_s}	drag coefficient of store, Drag/ qF
$C_{D_{Bs}}$	base drag coefficient of store, $-P_{Bs} \frac{A}{F}$
C_{L_s}	lift coefficient of store, Lift/ qF
C_{m_s}	pitching-moment coefficient of store (measured about store nose, positive when nose is up), Pitching moment/ $qF\bar{l}$
C_{Y_s}	side-force coefficient of store (positive to the right, toward the fuselage for semispan model used), Side force/ qF

C_{n_s}	yawing-moment coefficient of store (positive to the right), Yawing moment/ qFl
C_{D_t}	total drag coefficient of complete (wing-fuselage-store) con- figuration based on wing area, $C_{D_{wf}} + C_{D_s}F/S$
C_{L_t}	total lift coefficient of complete (wing-fuselage-store) con- figuration based on wing area, $C_{L_{wf}} + C_{L_s}F/S$
\bar{c}	mean aerodynamic chord of wing, 6.58 in.
A	area of store base, sq ft
S	total area of wing semispan, 0.5 sq ft
F	maximum frontal area of store, sq ft
q	dynamic pressure, lb/sq ft
P_{B_s}	pressure coefficient on store base, $\frac{P - P_0}{q_0}$
b/2	wing semispan, 12 in.
l	store length, in.
x	chordwise position of store midpoint, measured from fuselage nose, in. (See fig. 1)
y	spanwise position of store center line, measured from fuselage center line, in.
z	vertical position of store center line, measured from wing chord plane, positive downward, in.
α	angle of attack, deg

Subscripts:

wf	wing-fuselage combination
s	store
t	total, for complete wing-fuselage-store configuration

APPARATUS AND TESTS

The general arrangement of the test setup is shown in figure 1. Figure 2 is a photograph of the models (with large ogive-cylinder store shown) and support plate. Figure 3 is a photograph of the various stores investigated. The fins for the large ogive-cylinder store are detailed on figure 4. Complete dimensions of the models are given in figures 1 and 4 and table I. A detailed description of the models and support equipment and a discussion of support interference are given in reference 1. The wing-fuselage combination was the same one used in the tests of references 1 and 2 and simulated a swept-wing heavy-bomber type airplane. The large stores were sized to a frontal area equivalent to a twin-engine nacelle or a large store, while the small store was sized to a frontal area equivalent to a single-engine nacelle or a smaller store.

The ogive-cylinder store (fig. 3), because of its extensive use in this research program (notably refs. 1 and 2), is utilized as a basic or reference configuration with which comparisons are made. The cylindrical-afterbody store utilized the forward half of the ogive-cylinder store, but employed a cylindrical afterbody in place of the original ogive afterbody. This store was designed and tested to aid in the separation of interference effects on the nose and afterbody portions of the store. The finned store was formed by adding four fins (fig. 4) to the ogive-cylinder store. (Fins were oriented at 45° for all tests.) The small ogive-cylinder store (fig. 3) is geometrically similar to the large one, but is 8.8 inches in length. The parabolic store is of the same diameter as the (large) ogive cylinder, but was designed with a parabolic contour and has no cylindrical center section. The fineness ratios of the nose and afterbody of this store are therefore higher than those of the others in the series (see table I) although the overall fineness ratio remained the same as the basic ogive-cylinder store.

The parabolic, small ogive-cylinder store and large ogive-cylinder store with cylindrical afterbody were tested at three chordwise positions, $x = 24, 27,$ and 30 inches, through the range of spanwise and vertical positions. The finned store, on the other hand, was investigated at four chordwise positions, $x = 21, 24, 27,$ and 30 inches, through the range of spanwise positions at only one vertical height, $z = 2.09$ inches. The smaller values of z were precluded because of physical interference of the fins with the wing.

All tests were run with boundary-layer transition fixed on all surfaces as described in reference 1. The angle of attack of the wing-fuselage combination with the store at $z = 2.09$ inches was varied from 0° to 4° , with the stores remaining at $\alpha = 0^\circ$ throughout. The relative accuracies of the data in this report are the same as those listed in references 1 and 2.

The tests were performed in the Langley 4- by 4-foot supersonic pressure tunnel at a Mach number of 1.6 corresponding to a Reynolds number per foot of 2.4×10^6 .

RESULTS AND DISCUSSION

Basic Data

Isolated store and wing-fuselage data.- The forces and moments on the isolated stores are presented in figure 5. The data for the isolated heavy-bomber wing-fuselage combination are presented in figure 6 (taken from refs. 1 and 2).

Chordwise plots.- The basic data for the various stores in the presence of the wing-fuselage combination are presented in figures 7 to 19 as plots of force coefficient against store chordwise position for six spanwise stations. Corresponding force data for the wing-fuselage combination in the presence of these stores and for the complete (wing-fuselage-store) configuration are presented in figures 20 to 29.

The store and wing-fuselage drag data have been corrected to correspond to a base pressure equal to free-stream static pressure. The base-drag coefficients for the stores are presented separately in figures 9 and 10.

The data for the large ogive-cylinder store are from references 1 and 2 and are repeated in the present report because this store was used in this research program as the store for which the most detailed data were obtained.

Drag, lift, pitching moment, yawing moment, and side force for the store, and drag, lift, and pitching moment for the wing-fuselage combination are presented in the form of plots of coefficients against the chordwise position of the store midpoint. Each figure contains a separate plot for each of six spanwise stations (see fig. 1) from near the wing root to beyond the wing tip. Data are presented for approximately half of the spanwise stations (alternate values of x) for which data are presented in references 1 and 2.

The curves for each store were faired on staggered chordwise plots as a "family" as described in detail in reference 1 and 2 in order to obtain a more accurate line between test points.

Discussion

References 1, 2, and 3 have presented analyses of the data for the heavy-bomber configuration with the large ogive-cylinder store, including contour mapping of the forces, and figures showing the contribution of configuration components to interferences and the effect of various parameters such as angle of attack and store vertical height. Because the tests of the heavy-bomber configuration with stores of different shapes and sizes were made with a somewhat abbreviated range of store locations, no such analysis of the data presented herein has been prepared. The analysis presented is limited to some comparisons of the forces on the various stores in the presence of the heavy-bomber configuration and of the forces on the heavy-bomber configuration in the presence of the various stores. Some interpretation of the results in terms of the flow-field analysis and discussions from references 1, 2, and 3 is included.

Drag.- Figure 7 shows that, for any given store position, the drag coefficient of the parabolic store is less than that of the large ogive-cylinder store. The amount of the difference corresponds roughly to the difference in the interference-free values of drag coefficient for these two stores (see fig. 5 or ticks on fig. 7). The drag coefficients for the small ogive cylinder, on the other hand, are for some positions higher and for other positions lower than the drag of the large (geometrically similar) ogive-cylinder store. Figure 8 shows that the drag of the ogive-cylinder store with cylindrical afterbody is, in general, lower than that of the same store with normal afterbody for the three store positions tested. The amount of the differences varies considerably from the difference between the interference-free values of drag for these two stores (see fig. 5 or ticks on fig. 8).

The foregoing interference effects can be explained by buoyancy considerations as shown in reference 1. For example, figure 11 shows the drag curves for $y = 7.8$ from figures 7 and 8. Shown below these data are scale sketches of the various stores in two chordwise positions in the flow field of the wing. The flow field of the wing is divided into regions of positive and negative static pressures according to the measured variation of static pressure along the store center line shown in the curve below the sketches. This information was taken from figure 35 of reference 1.

Examination of the position of the nose and afterbody sections of the various stores in the flow field of the wing in figure 11 (with attention to the rough magnitude of the pressures as well as to the sign) serves to explain the drags of the four stores relative to their isolated drags at either value of x as well as the changes which occur between the two values of x .

The drag of the finned store (fig. 8) is considerably higher than that of the unfinned store, principally as a result of fin drag.

In figures 20 and 21 in the region of the drag peak, the drag of the wing-fuselage combination is shown to be generally higher in the presence of the large ogive-cylinder store than in the presence of the other stores. This result is due to the greater adverse interference of this large store. In the region to the rear of this peak, the wing-fuselage drag is in some cases lower in the presence of the other stores. This result is due to the greater beneficial interference of this large store.

The fact that the store of smaller size produced smaller interference effects on the wing-fuselage combination was noted previously for a small store in reference 4 and is explained (from the standpoint of the buoyancy concept discussed in ref. 1) by the fact that this store produces an interference pressure field which is of lesser extent and intensity. The same explanation applies to the smaller interferences measured for the higher fineness-ratio (parabolic) store.

The drag of the wing-fuselage combination is shown in figure 21 to be consistently lower in the presence of the finned store. The reasons for this are not understood at present.

The total drags of the wing-fuselage-store configuration are lower for all store positions for the configurations which include the stores of smaller size or higher fineness ratio than for those which include the basic, large ogive-cylinder store (fig. 22). This result stems from the lower interference drags produced and incurred by these stores.

The changes in total drag which occur with changes in store position remain large and of similar magnitude, however, for all stores. Consequently, the total drag of the wing-fuselage combination with the small ogive-cylinder store or the parabolic store in an unfavorable location in many cases exceeded the total drag of the configuration with the large ogive-cylinder store in a favorable location.

Lift.- Figures 12 and 13 show that only small differences exist in C_{L_s} for the three large (unfinned) stores. The small ogive-cylinder store and the finned store, however, show very much higher values of C_{L_s} for some store positions and generally steeper gradients with variations in x . These effects are the result of the fact that the small store or the fins of the finned store can be more completely submerged in a region in which lift is generated (due to pressure gradient or flow deviation or both) in one direction. The large store, on the other hand, tends to extend through several such regions so that lower peak values of lift coefficient result. This same effect is noted in references 3 and 4 for

other tests of the small and large ogive-cylinder store. It will be noted that at angles of attack other than zero, the values of store lift presented represent only interference values, since the angle of attack of the store remained at 0° . The store lift due to store angle of attack must also be considered in applying these data to conditions where the store angle of attack is a finite value.

The lift of the wing-fuselage combination in the presence of the various stores is shown in figures 24 and 25, while the total lift of the wing-fuselage-store configuration is shown in figures 26 and 27. The effect of the four large stores on wing-fuselage lift is shown to be roughly comparable. The small ogive-cylinder store, however, is shown to produce smaller interference lift on the wing-fuselage combination at inboard store positions and slightly negative interference lifts at the outboard positions.

The effects of the various stores on the total lift of the configuration also follow the trends outlined above for wing-fuselage lift because the variations of store lift are small compared to those of the wing-fuselage combination.

Pitching moment.- The store pitching-moment data (figs. 14 and 15) show that the largest variations in store pitching moment are obtained with the finned store. The small ogive-cylinder store also incurs larger values of pitching-moment coefficient than do the larger (unfinned) stores for some positions. Both effects are explained by the discussion of similar lift results in the preceding section.

The pitching moments of the wing-fuselage combination are seen in figures 28 and 29 to be not materially affected by store configuration.

Side force.- Store side force is shown in references 2 and 3 to be generally the most important component from the standpoint of store-support loads. Figures 16 and 17 show that the side force encountered by a store is greatly affected by its size or its use of fins. The large values of side force encountered for some positions by the small ogive-cylinder store and by the finned store are, as was discussed for lift, the result of the submergence of the small store or fins in regions of force in one direction. From an examination of the side force on the fins (the difference between the curves for the large ogive-cylinder store with and without fins, fig. 17), it can be seen that the regions of force in one direction are relatively narrow and sharply defined. The region of store midpoint locations for fin forces toward the tip is roughly the region of the wing plan form, while the regions of store midpoint locations for fin forces toward the wing root are the regions ahead of and behind the wing plan form. The largest loads encountered are in the direction of the tip, even at a wing angle of attack of zero, and these loads become larger as the wing angle of attack is increased and the spanwise flow associated with wing lift increases.

The fact that store loads can be greatly affected by changes in store size, addition of tail fins, or changes in store location indicates that care must be used in estimating such loads, particularly in the use of data from a specific installation in the calculation of loads for a configuration even slightly different.

Yawing moment.- The store yawing-moment coefficients for the various stores (figs. 18 and 19) are presented with reference to the store nose, and therefore reflect closely the store side force. The discussion of store side force in the previous section therefore also applies, in general, to the yawing moment.

CONCLUSIONS

A wind-tunnel investigation at a Mach number of 1.61 has been made wherein separate forces and moments were measured on a swept-wing heavy-bomber configuration and on stores of several shapes and sizes for a very wide range of store positions. A limited analysis of the results indicates the following conclusions:

- (1) The drag of the various stores in the presence of the wing-fuselage combination is explained in a qualitative way by buoyancy considerations; that is, by consideration of the position of the nose and afterbody portions of the store in the flow (pressure) field of the wing-fuselage combination.
- (2) The drag of the wing-fuselage combination in the flow field of the various stores appears to be similarly explained by buoyancy considerations. The interference drag is lower in the presence of the smaller store and higher fineness-ratio store as a consequence of the smaller or lower intensity pressure fields which these stores impose upon the wing-fuselage combination.
- (3) The total drag of the complete (wing-fuselage-store) configuration was lower with the small ogive-cylinder or the large parabolic store than with the large ogive-cylinder store for any given store position. The effect of store position, however, remained very large for all stores; consequently, the total drag of the configuration with a small store in an unfavorable location in many cases exceeded the total drag of the configuration with a large store in a favorable location.
- (4) Of the stores investigated, the small store and the finned store encountered larger peak values of lift, side force, and drag coefficients and steeper variations of these coefficients with changes in store

position. This is a consequence of the fact that the small store or the fins were more completely submerged in regions in which the interference force is in one direction.

Langley Aeronautical Laboratory,
National Advisory Committee for Aeronautics,
Langley Field, Va., November 17, 1955.

REFERENCES

1. Smith, Norman F., and Carlson, Harry W.: The Origin and Distribution of Supersonic Store Interference From Measurement of Individual Forces on Several Wing-Fuselage-Store Configurations. I.- Swept-Wing Heavy-Bomber Configuration With Large Store (Nacelle). Lift and Drag; Mach Number, 1.61. NACA RM L55A13a, 1955.
2. Smith, Norman F., and Carlson, Harry W.: The Origin and Distribution of Supersonic Store Interference From Measurement of Individual Forces on Several Wing-Fuselage-Store Configurations. II.- Swept-Wing Heavy-Bomber Configuration With Large Store (Nacelle). Lateral Forces and Pitching Moments; Mach Number, 1.61. NACA RM L55E26a, 1955.
3. Smith, Norman F., and Carlson, Harry W.: Some Effects of Configuration Variables on Store Loads at Supersonic Speeds. NACA RM L55E05, 1955.
4. Smith, Norman F., and Carlson, Harry W.: The Origin and Distribution of Supersonic Store Interference From Measurement of Individual Forces on Several Wing-Fuselage-Store Configurations. III.- Swept-Wing Fighter-Bomber Configuration With Large and Small Stores. Mach Number, 1.61. NACA RM L55H01, 1955.

TABLE I.- PERTINENT MODEL DIMENSIONS

Fuselage:

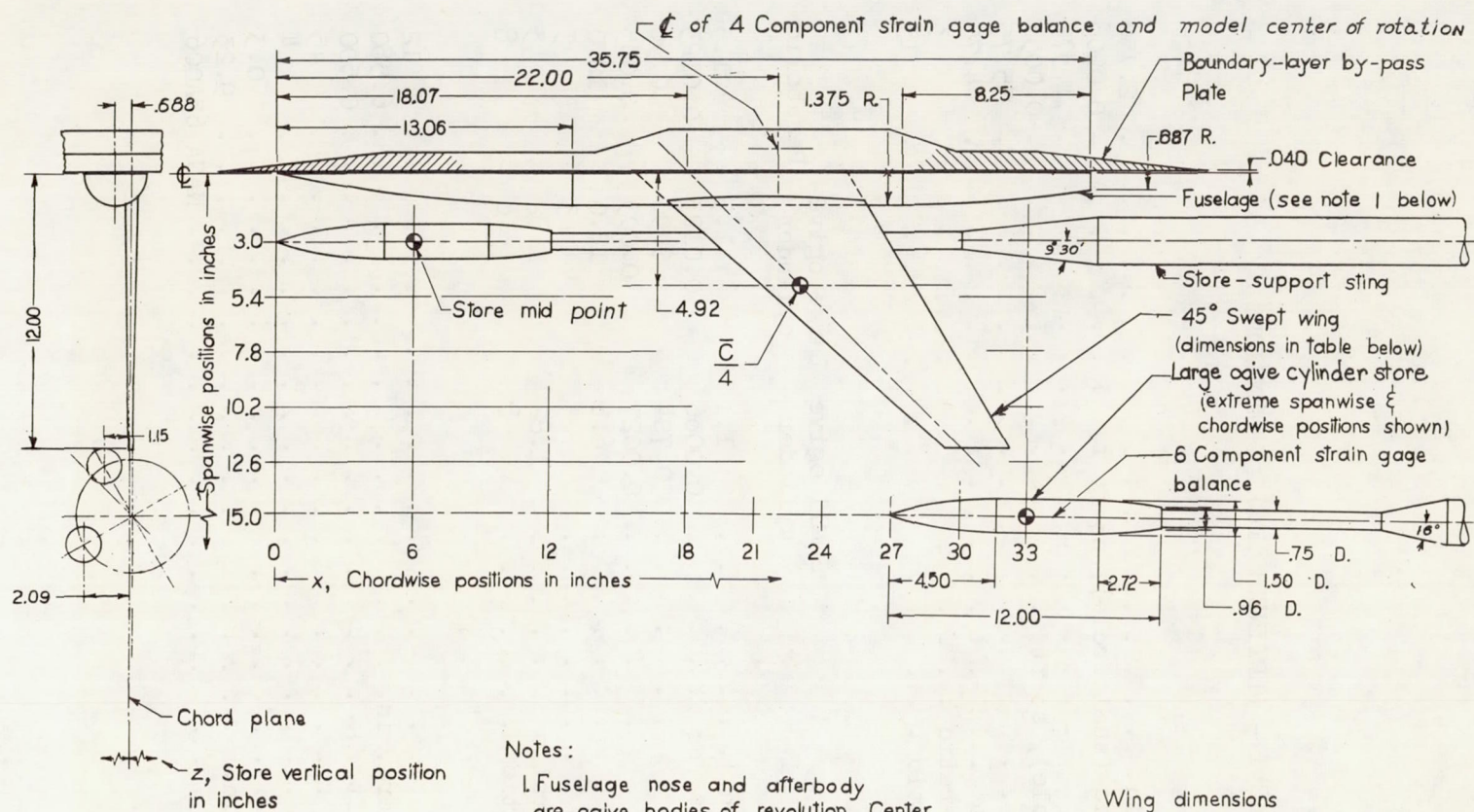
Maximum diameter, in.	2.750
Maximum frontal area (semicircle), sq ft	0.0206
Base diameter, in.	1.372
Base area (semicircle), sq ft	0.0051
Overall length	35.75
Nose fineness ratio	4.75
Afterbody fineness ratio	3
Overall fineness ratio	13

Store:

	Small ogive cylinder	Large ogive cylinder	Parabolic
Maximum diameter, in.	1.1	1.5	1.5
Maximum frontal area, sq ft	0.0066	0.0123	0.0123
Base diameter	0.704	0.96	0.96
Base area, sq ft	0.0027	0.005	0.005
Overall length, in.	8.8	12.0	12.0
Nose fineness ratio	3	3	5
Afterbody fineness ratio	1.82	1.82	3
Overall fineness ratio	8	8	8

Swept wing:

Semispan, in.	12
Mean aerodynamic chord, in.	6.580
Area, semispan, sq ft	0.500
Sweep (c/4), deg	45
Aspect ratio	4
Taper ratio	0.3
Center-line chord, in.	9.23
Airfoil section	NACA 65A006



Notes:

1. Fuselage nose and afterbody are ogive bodies of revolution. Center sections are cylindrical
2. All dimensions in inches.

Wing dimensions

Semi-span	12
Sweep $\frac{\xi}{4}$	45°
Aspect ratio	4
Taper ratio	0.3
ϕ Chord	9.23
Section	65A-006

Figure 1.- Layout of models showing dimensions of components and ranges of store positions investigated.

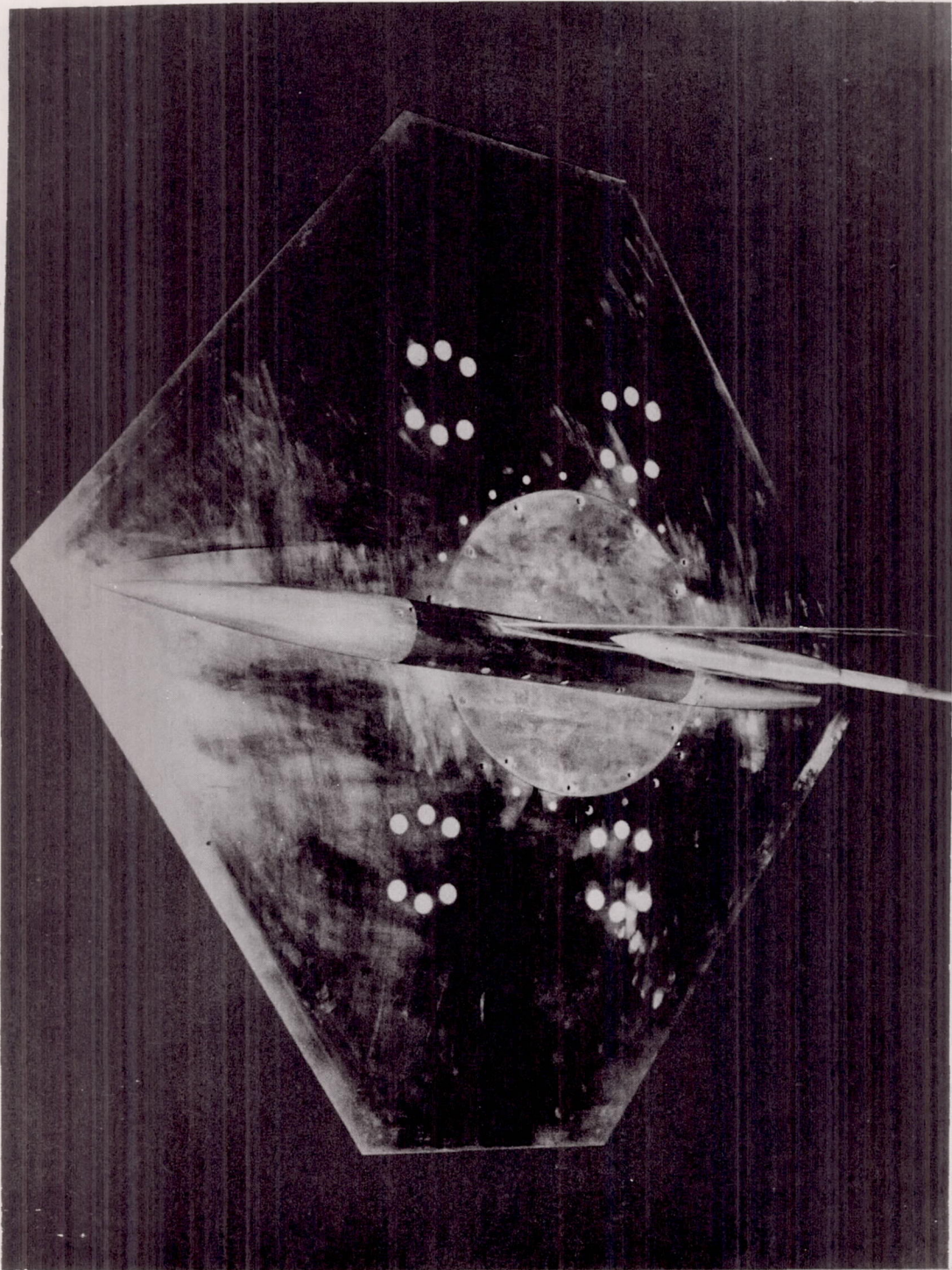
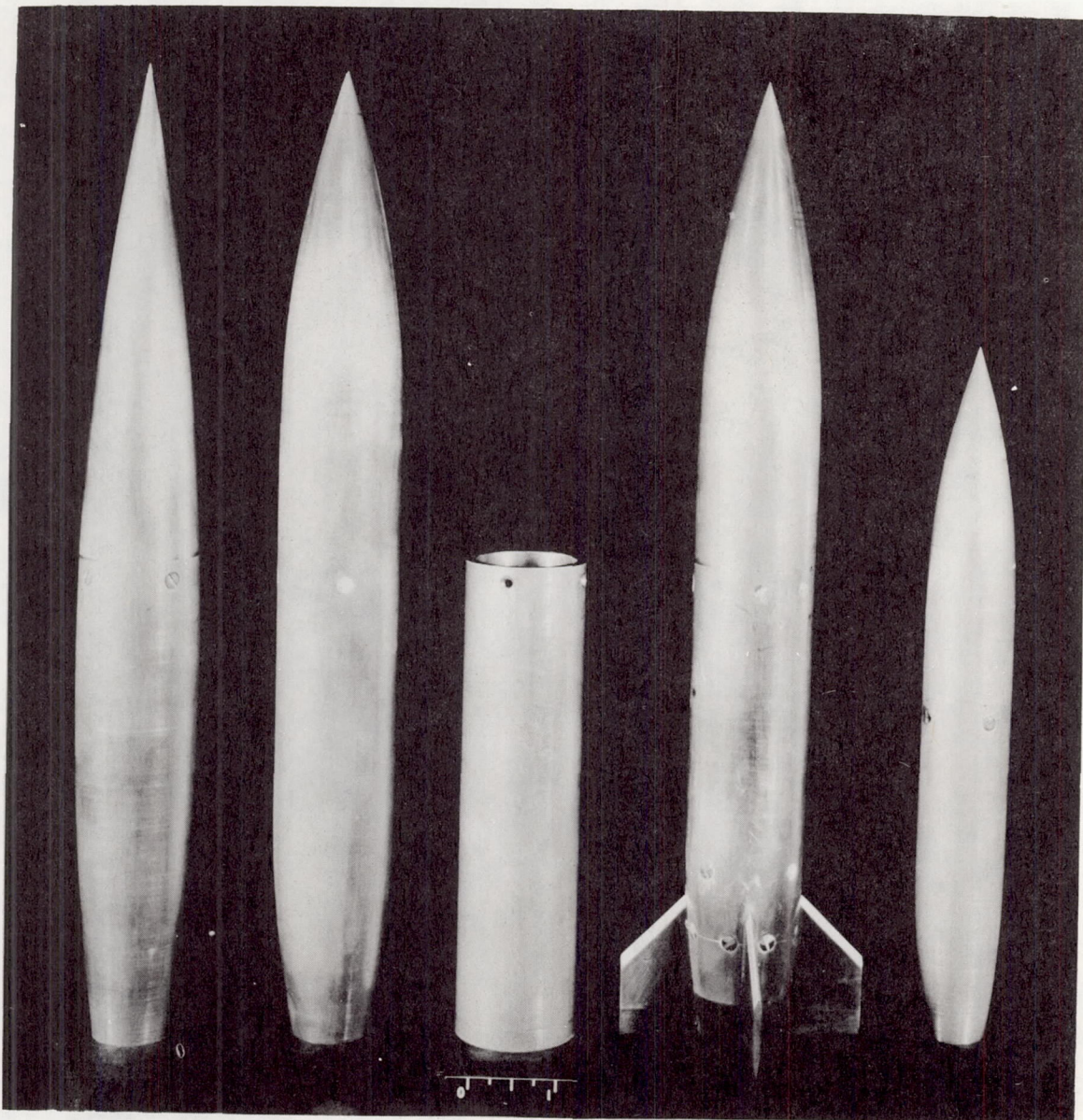


Figure 2.- Photograph of models and mounting plate. Store shown is large ogive-cylinder. (Transition strips not shown.)

L-87526



Parabolic
store

Large Ogive-
Cylinder Store
(references
1 and 2)

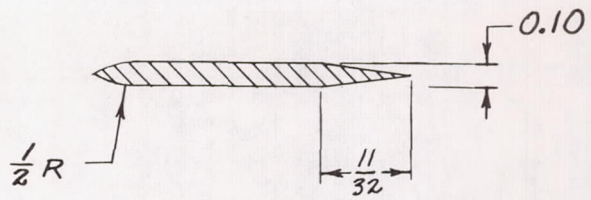
Cylindrical
afterbody
for ogive-
cylinder
store

Large ogive-cylinder
store with fins

Small ogive-
cylinder store

Figure 3.- Photograph of store models tested. (Scale shown is in inches.)

L-89220



Section A-A
(all corners rounded)

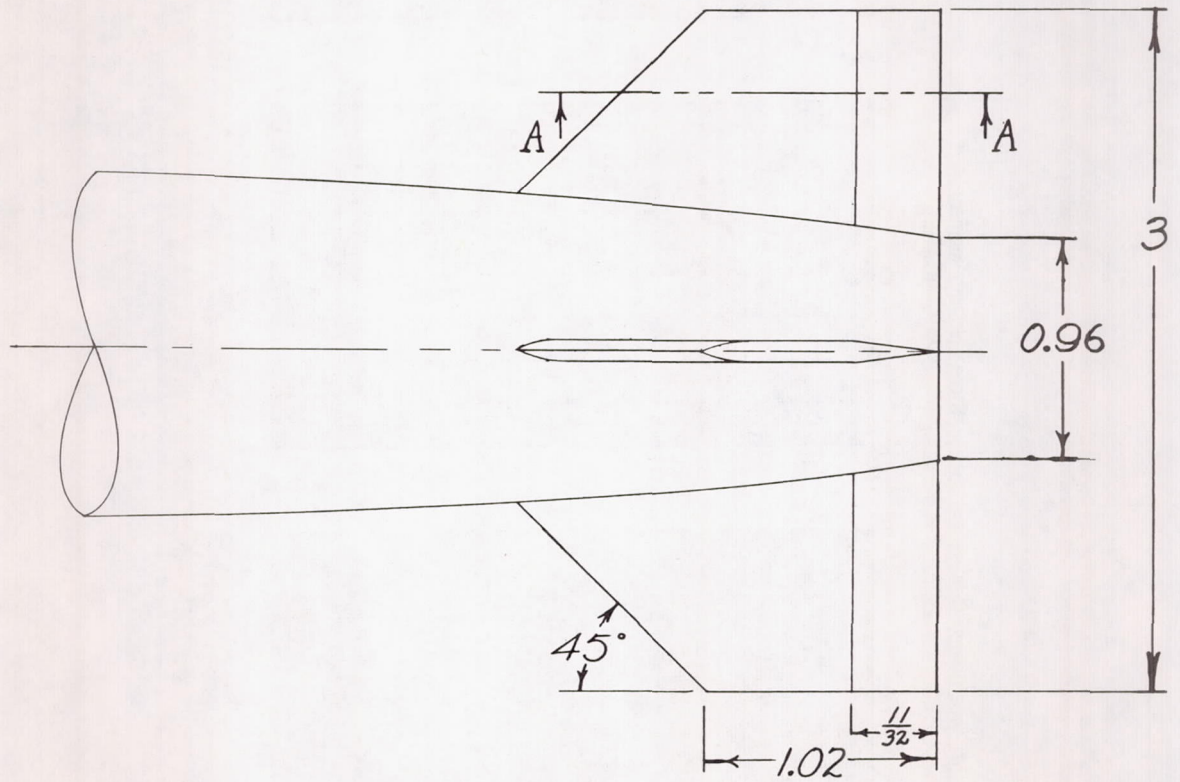
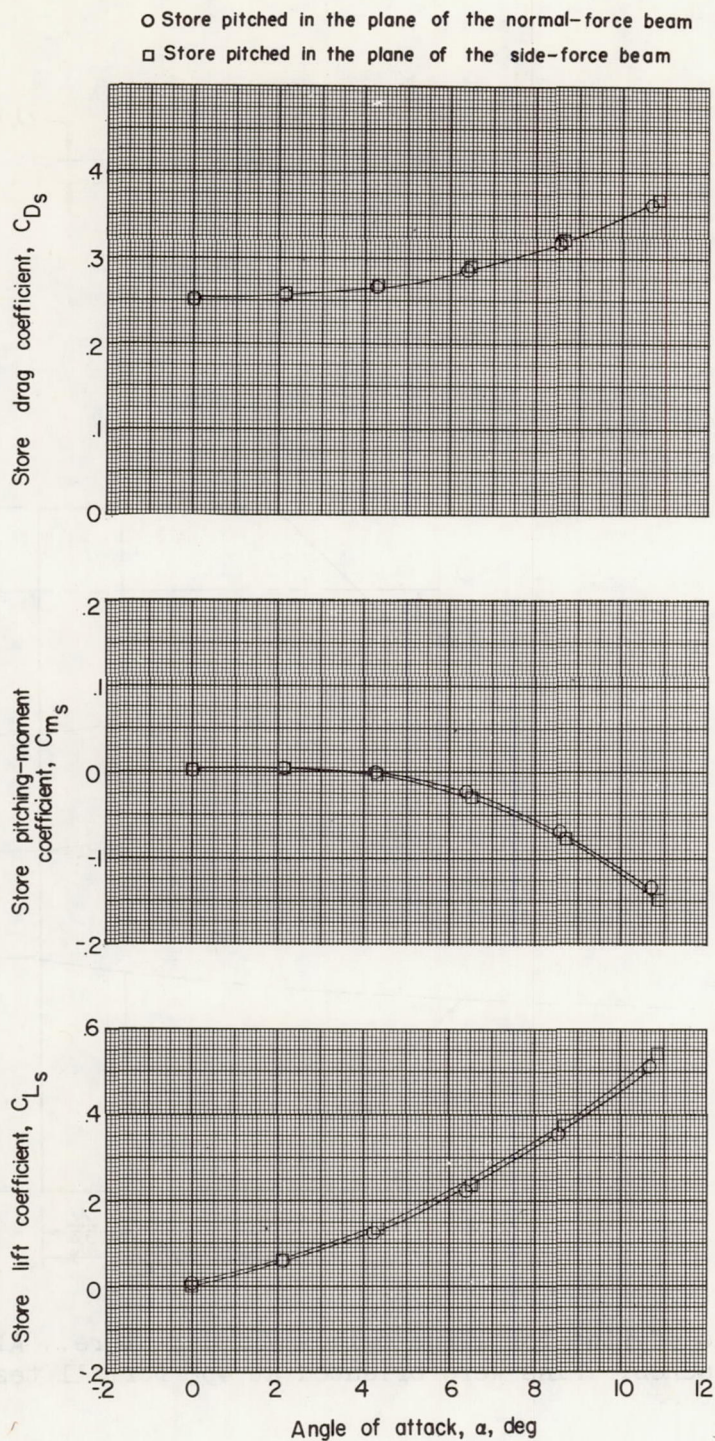
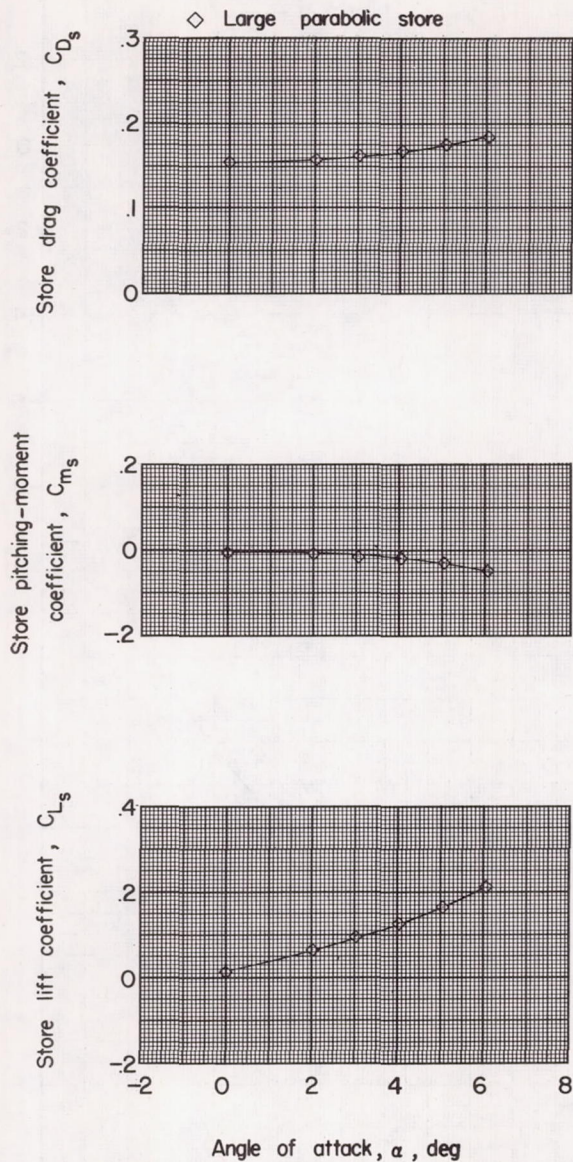


Figure 4.- Details of fins for large ogive-cylinder store. All dimensions are in inches. Fins were oriented at 45° for all tests.



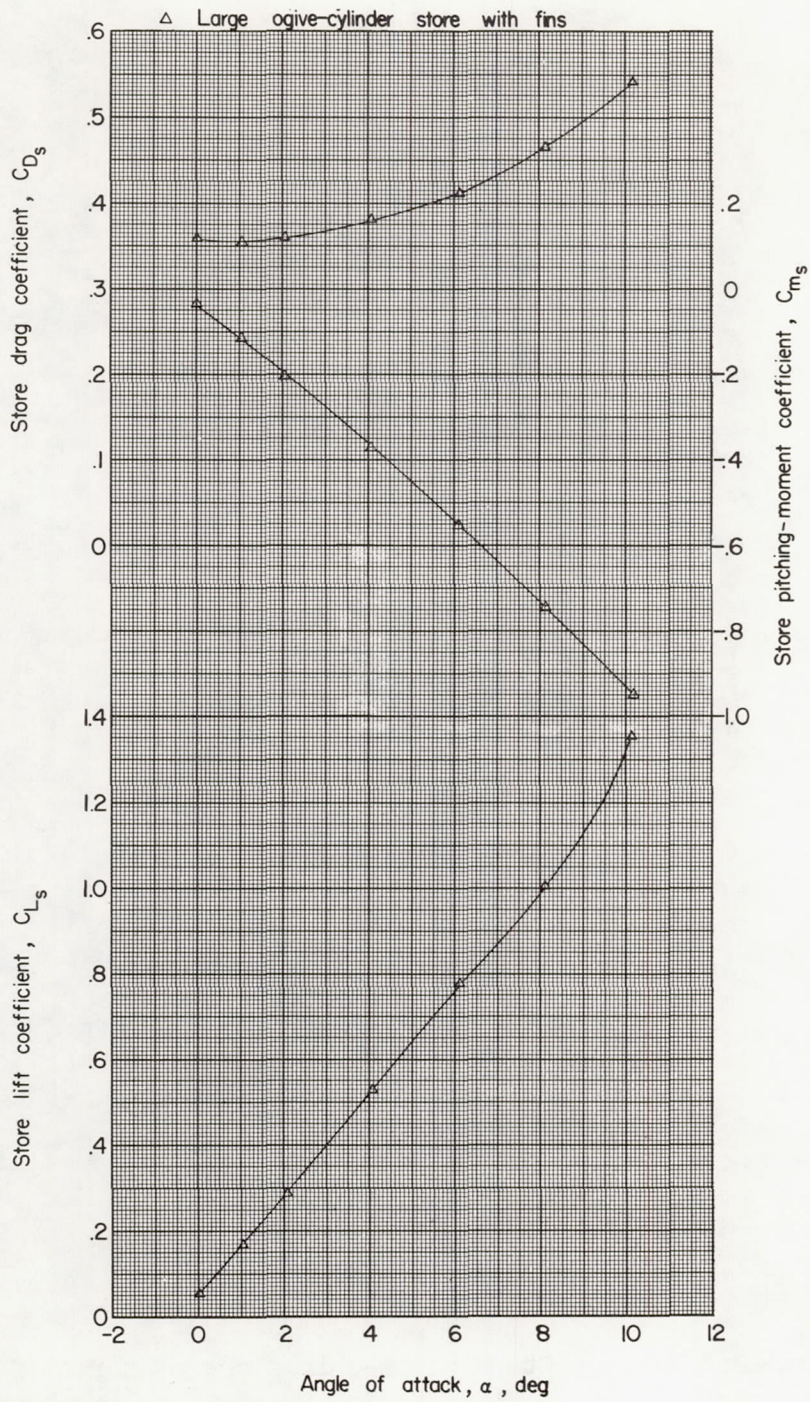
(a) Large and small ogive-cylinder stores.

Figure 5.- Lift, drag, and pitching-moment characteristics of the isolated stores.



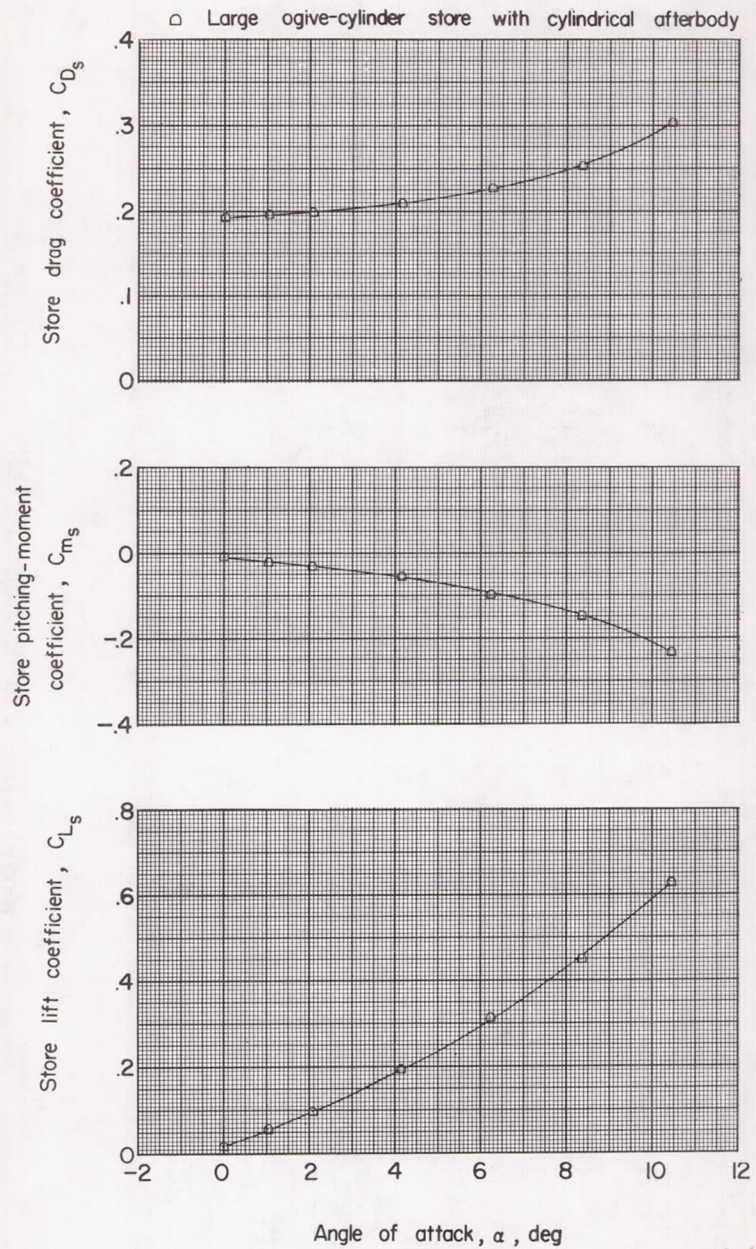
(b) Large parabolic store. Store pitched in plane of normal-force beams.

Figure 5.- Continued.



(c) Large ogive-cylinder store with fins. Store pitched in plane of normal-force beams.

Figure 5.- Continued.



(d) Large ogive-cylinder store with cylindrical afterbody. Store pitched in plane of normal-force beams.

Figure 5.- Concluded.

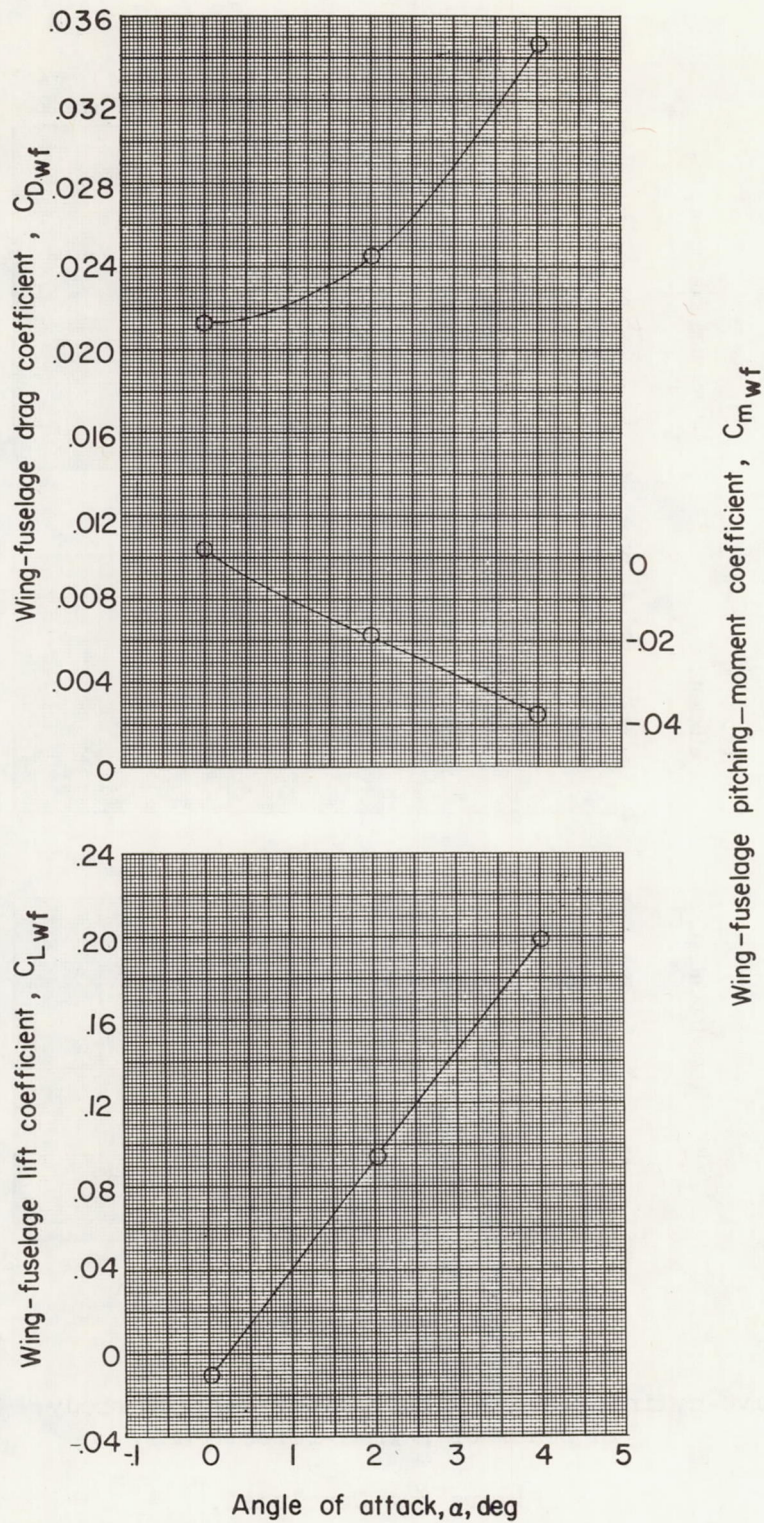
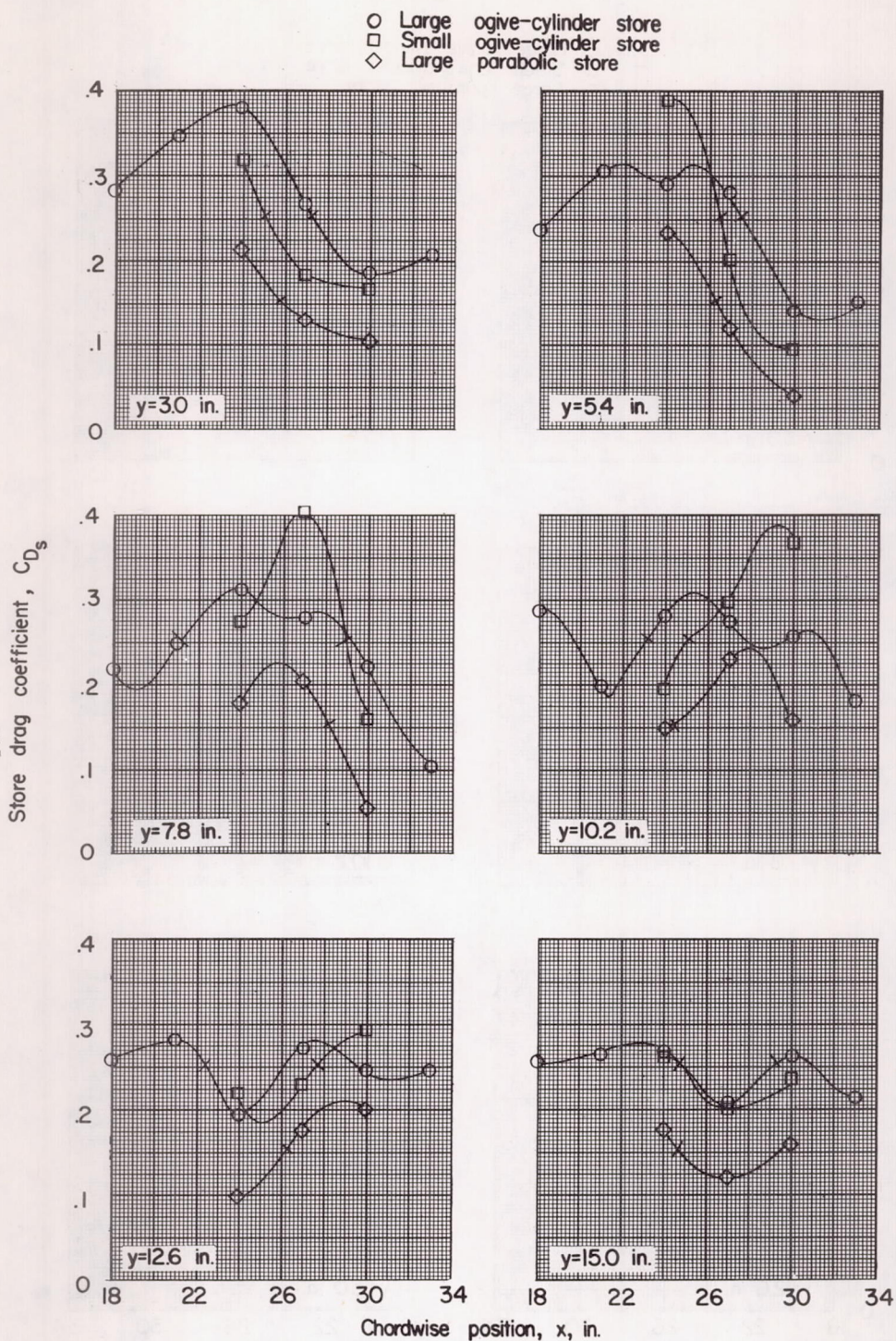


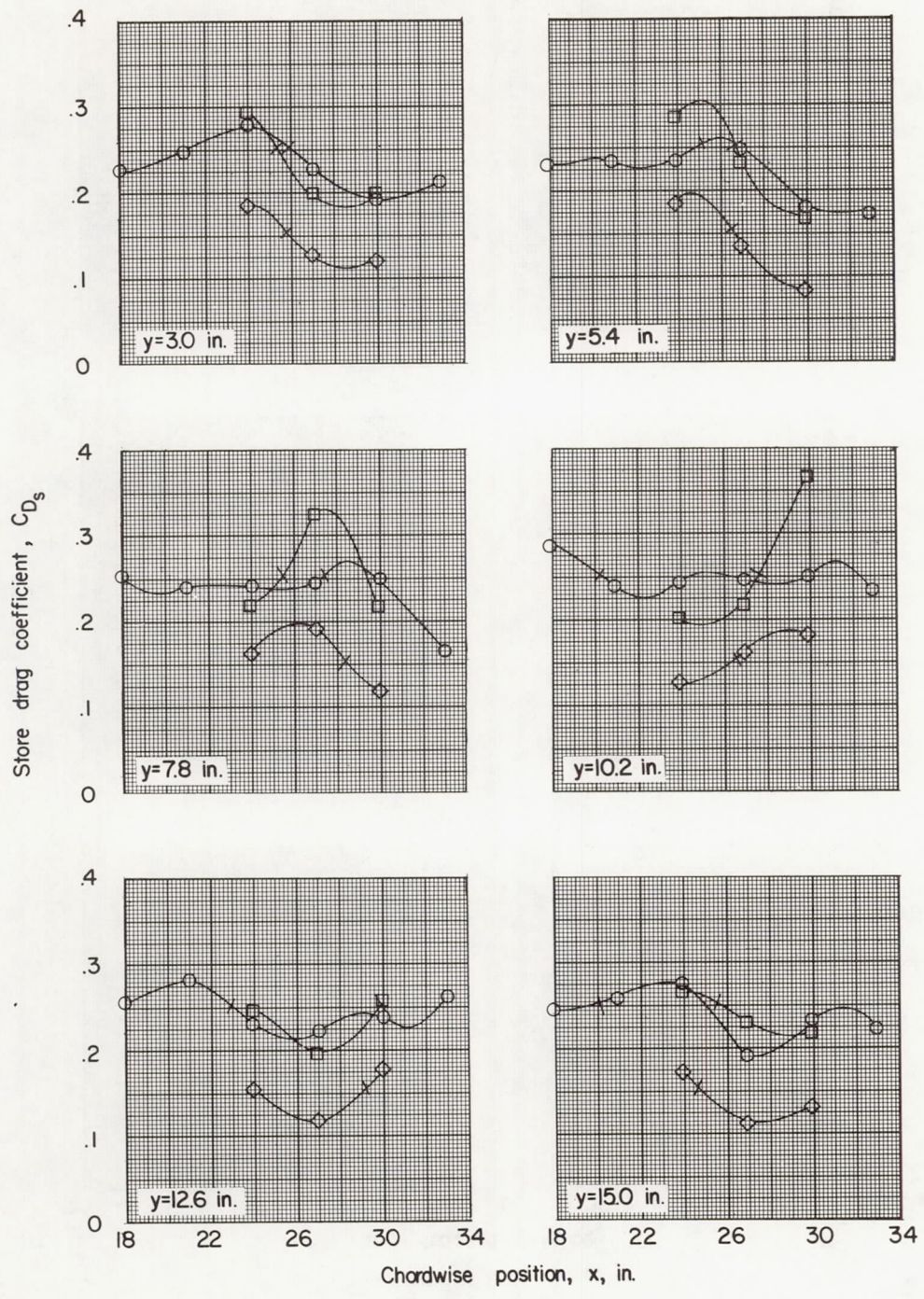
Figure 6.- Lift, drag, and pitching-moment characteristics of isolated wing-fuselage combination (from refs. 1 and 2).



(a) $z = 1.15$ inches; $\alpha = 0^\circ$.

Figure 7.- Drag of stores of different shapes and sizes in presence of wing-fuselage combination. (Tick marks indicate values of drag coefficient for isolated stores. See fig. 5.)

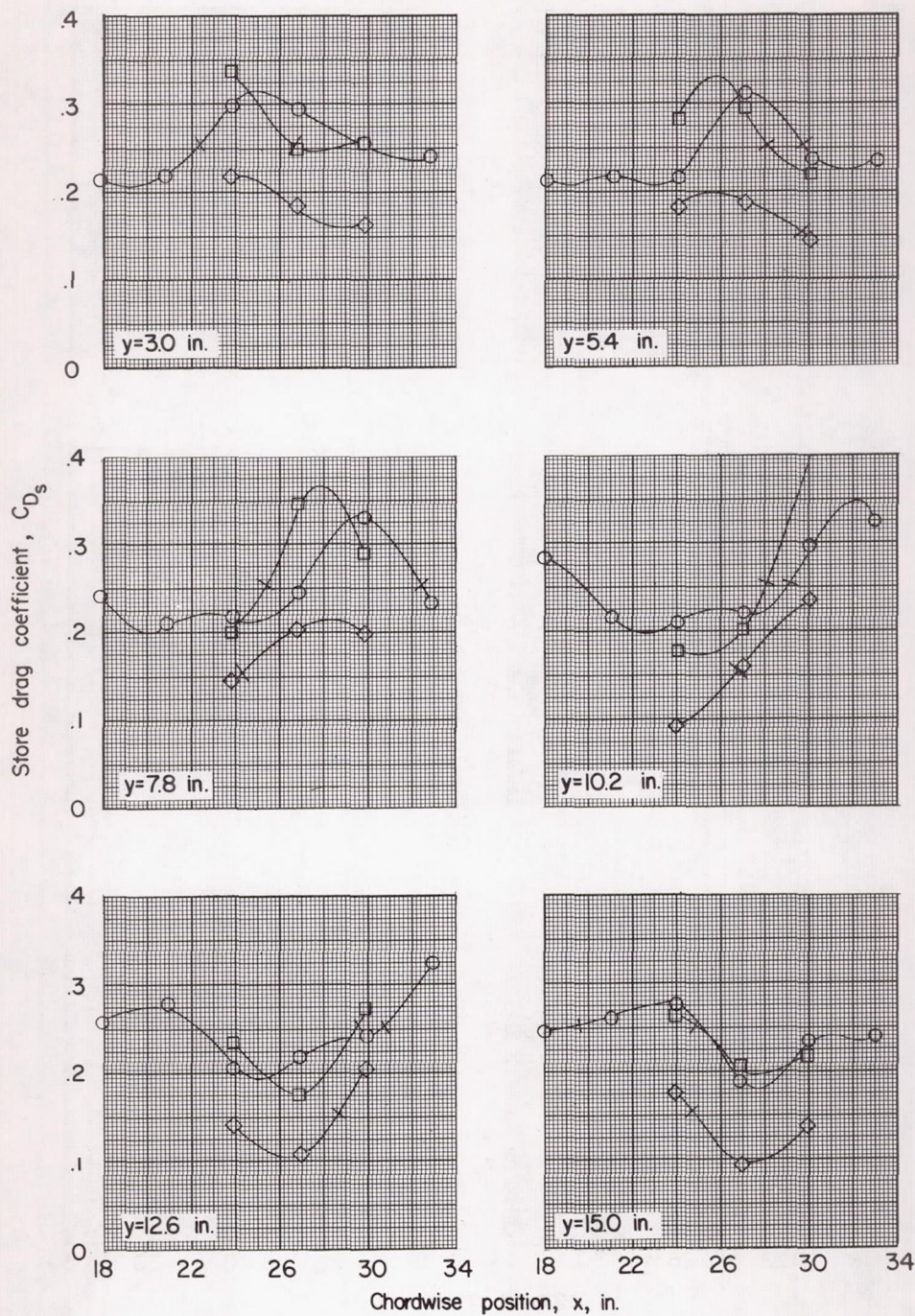
○ Large ogive-cylinder store
 □ Small ogive-cylinder store
 ◇ Large parabolic store



(b) $z = 2.09$ inches; $\alpha = 0^\circ$.

Figure 7.- Continued.

○ Large ogive-cylinder store
 □ Small ogive-cylinder store
 ◇ Large parabolic store



(c) $z = 2.09$ inches; $\alpha = 4^\circ$.

Figure 7.- Concluded.

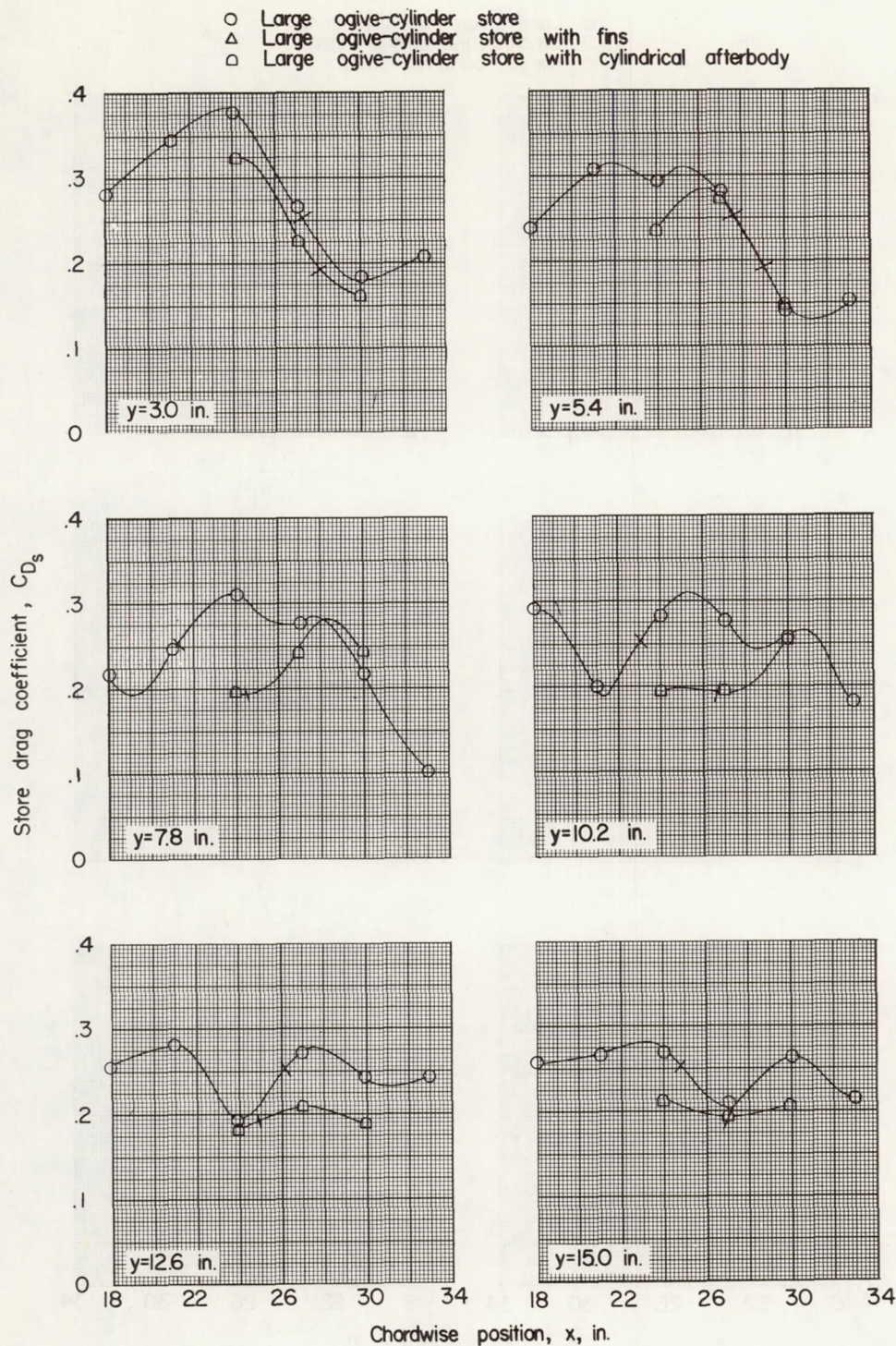
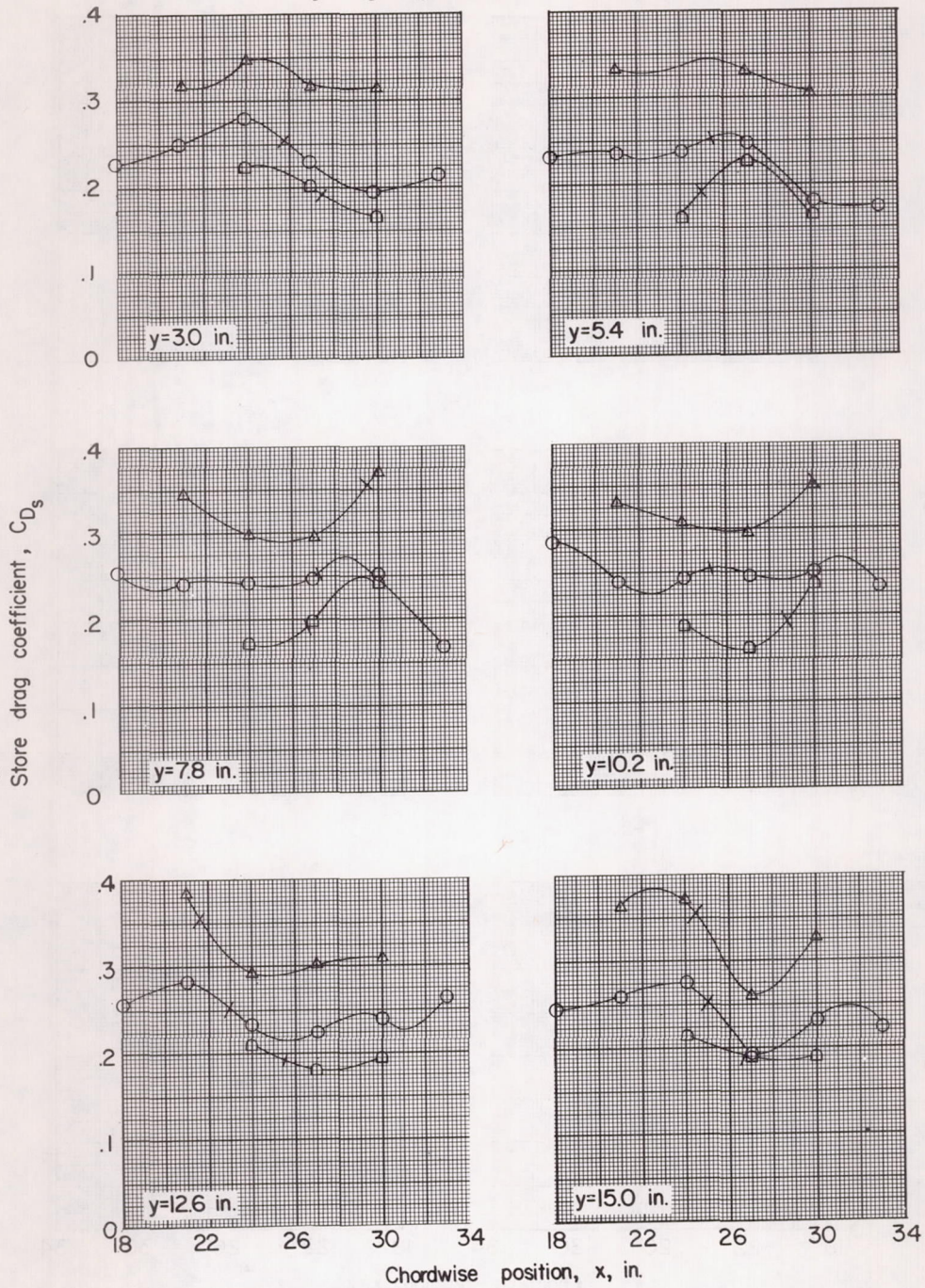
(a) $z = 1.15$ inches; $\alpha = 0^\circ$.

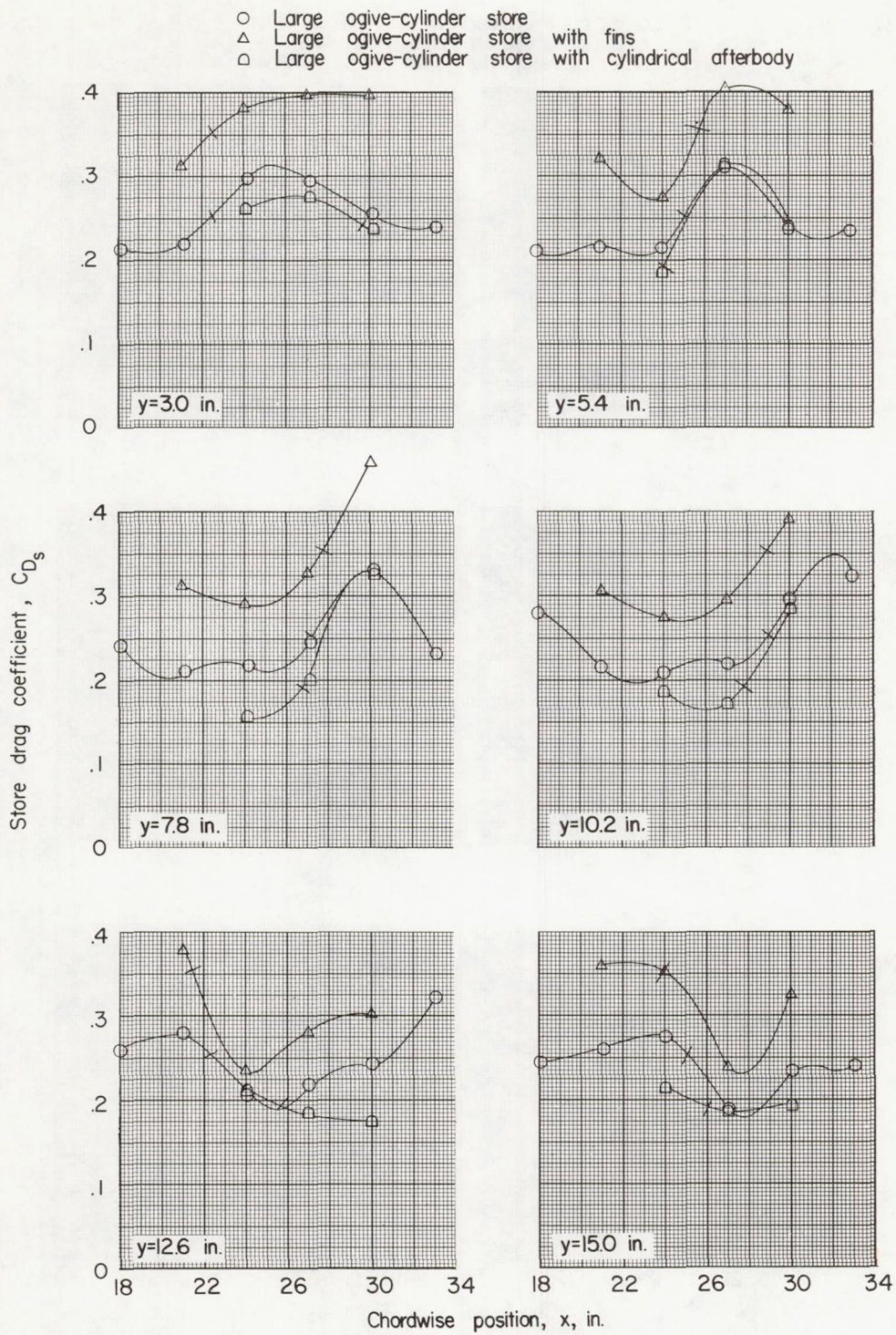
Figure 8.- Drag of large ogive-cylinder store with various afterbody configurations in presence of wing-fuselage combination. (Tick marks indicate values of drag coefficient for isolated stores. See fig. 5.)

- Large ogive-cylinder store
- △ Large ogive-cylinder store with fins
- ◻ Large ogive-cylinder store with cylindrical afterbody



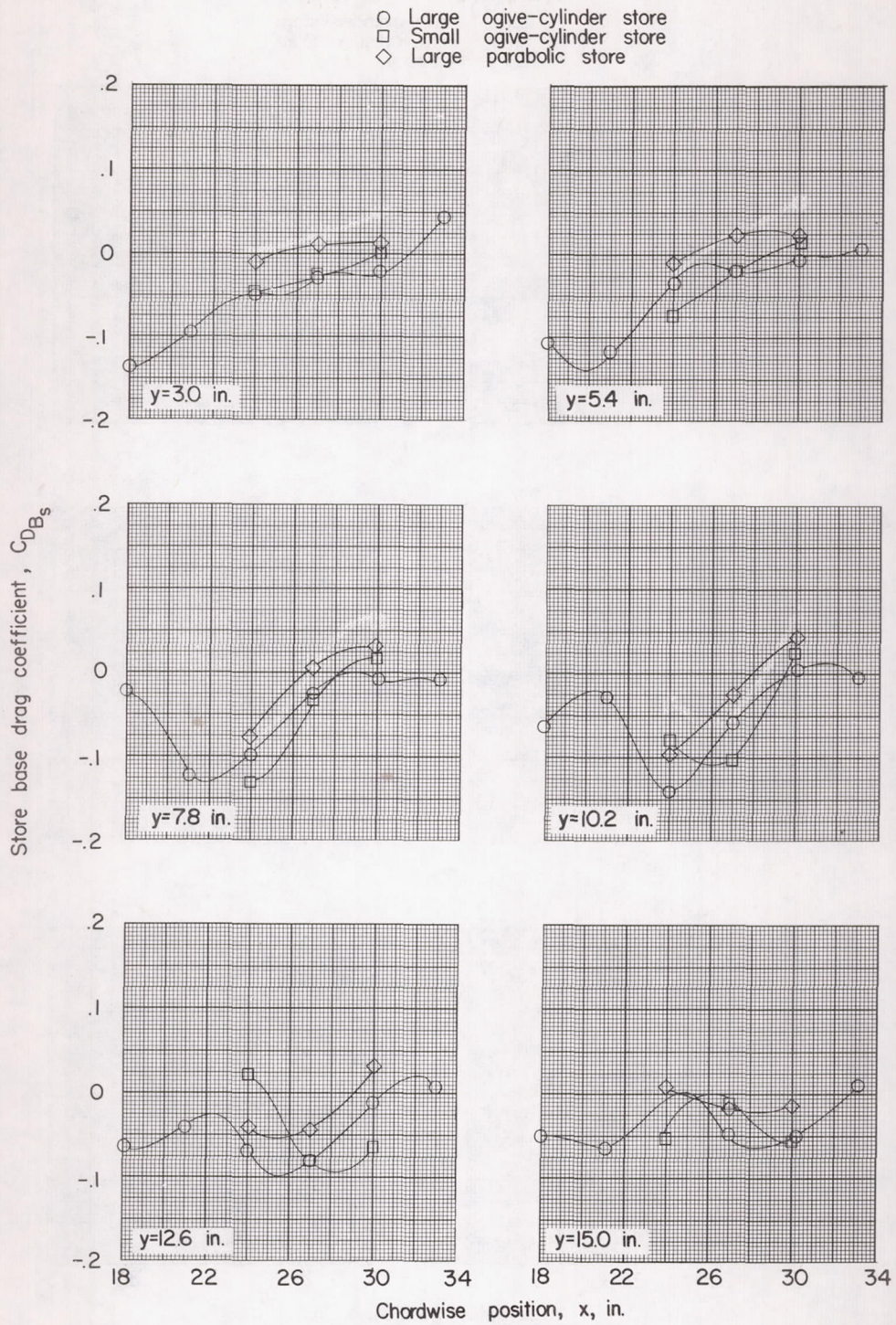
(b) $z = 2.09$ inches; $\alpha = 0^\circ$.

Figure 8.- Continued.



(c) $z = 2.09$ inches; $\alpha = 4^\circ$.

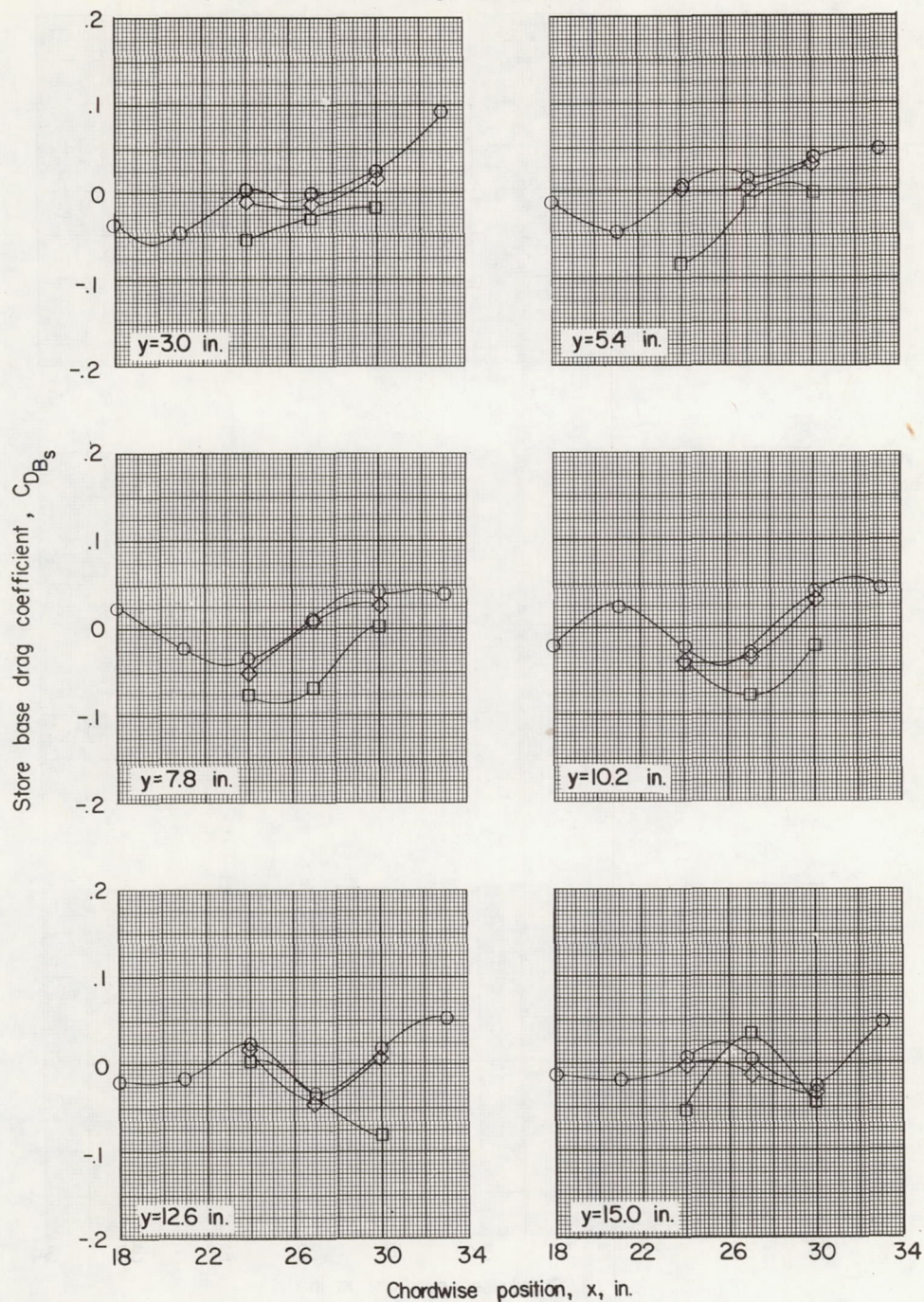
Figure 8.- Concluded.



(a) $z = 1.15$ inches; $\alpha = 0^\circ$.

Figure 9.- Base drag of stores of different shapes and sizes in presence of wing-fuselage combination.

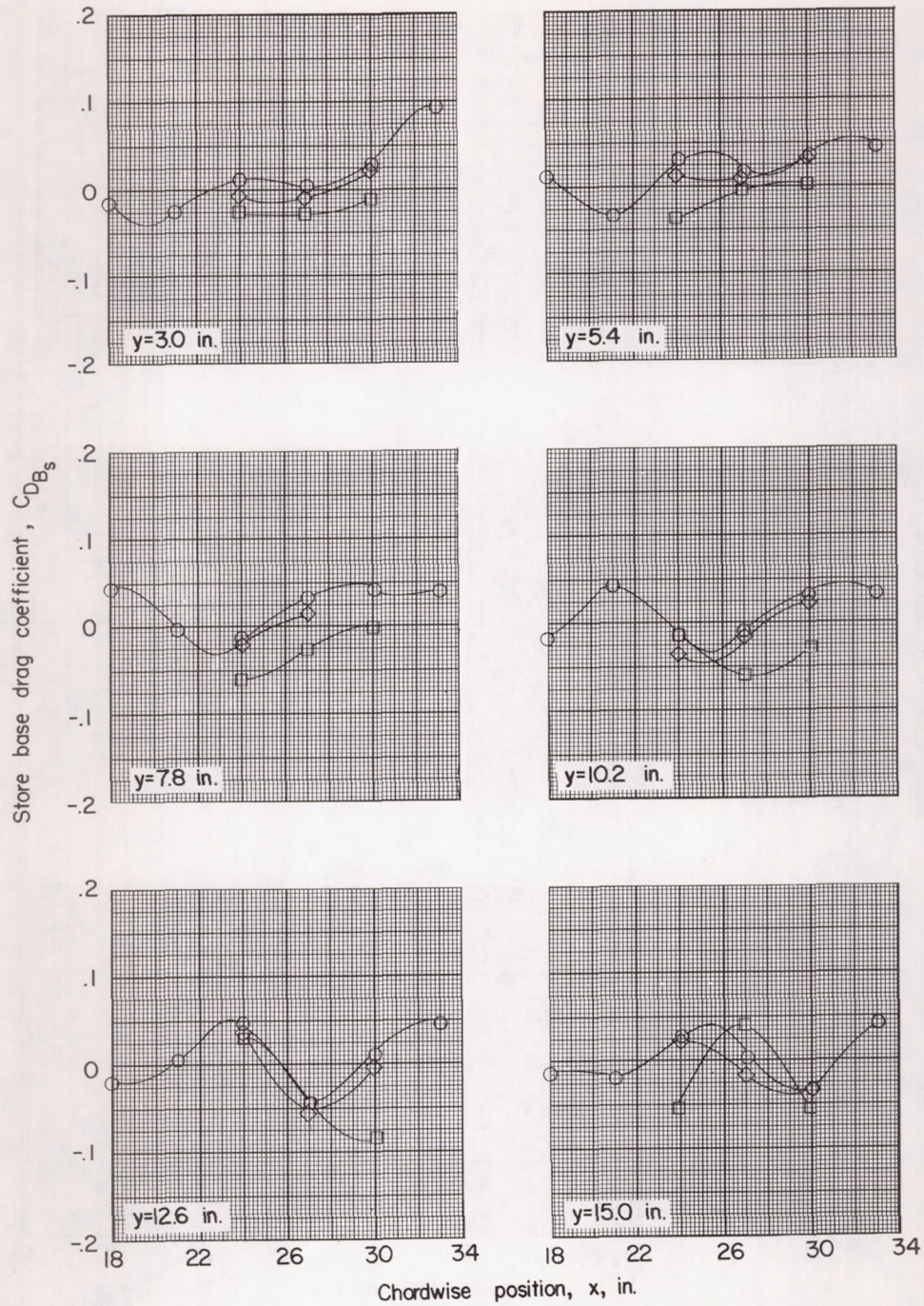
- Large ogive-cylinder store
- Small ogive-cylinder store
- ◇ Large parabolic store



(b) $z = 2.09$ inches; $\alpha = 0^\circ$.

Figure 9.- Continued.

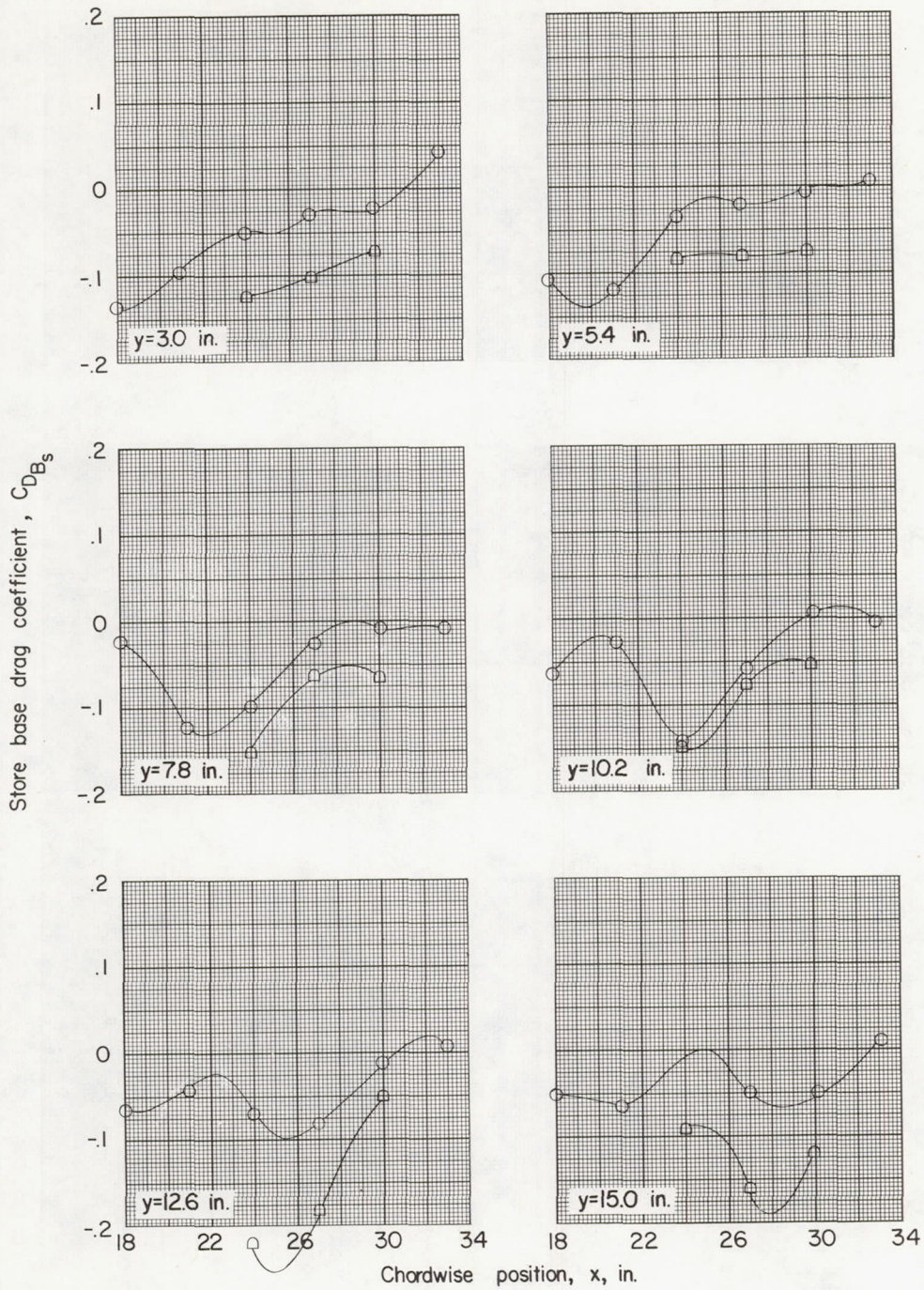
○ Large ogive-cylinder store
 □ Small ogive-cylinder store
 ◇ Large parabolic store



(c) $z = 2.09$ inches; $\alpha = 4^\circ$.

Figure 9.- Concluded.

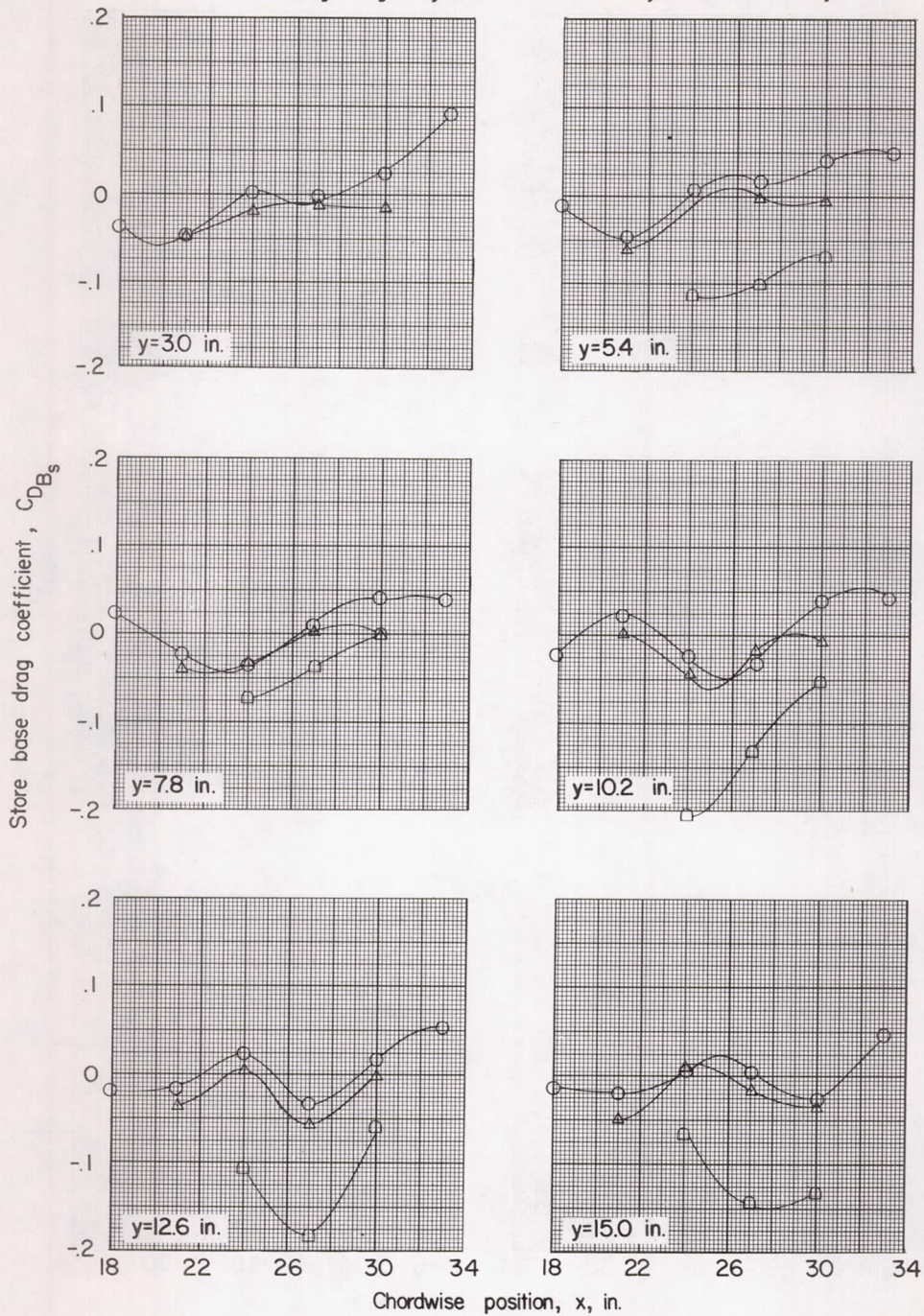
- Large ogive-cylinder store
- △ Large ogive-cylinder store with fins
- Large ogive-cylinder store with cylindrical afterbody



(a) $z = 1.15$ inches; $\alpha = 0^\circ$.

Figure 10.- Base drag of large ogive-cylinder store with various afterbody configurations in presence of wing-fuselage combination.

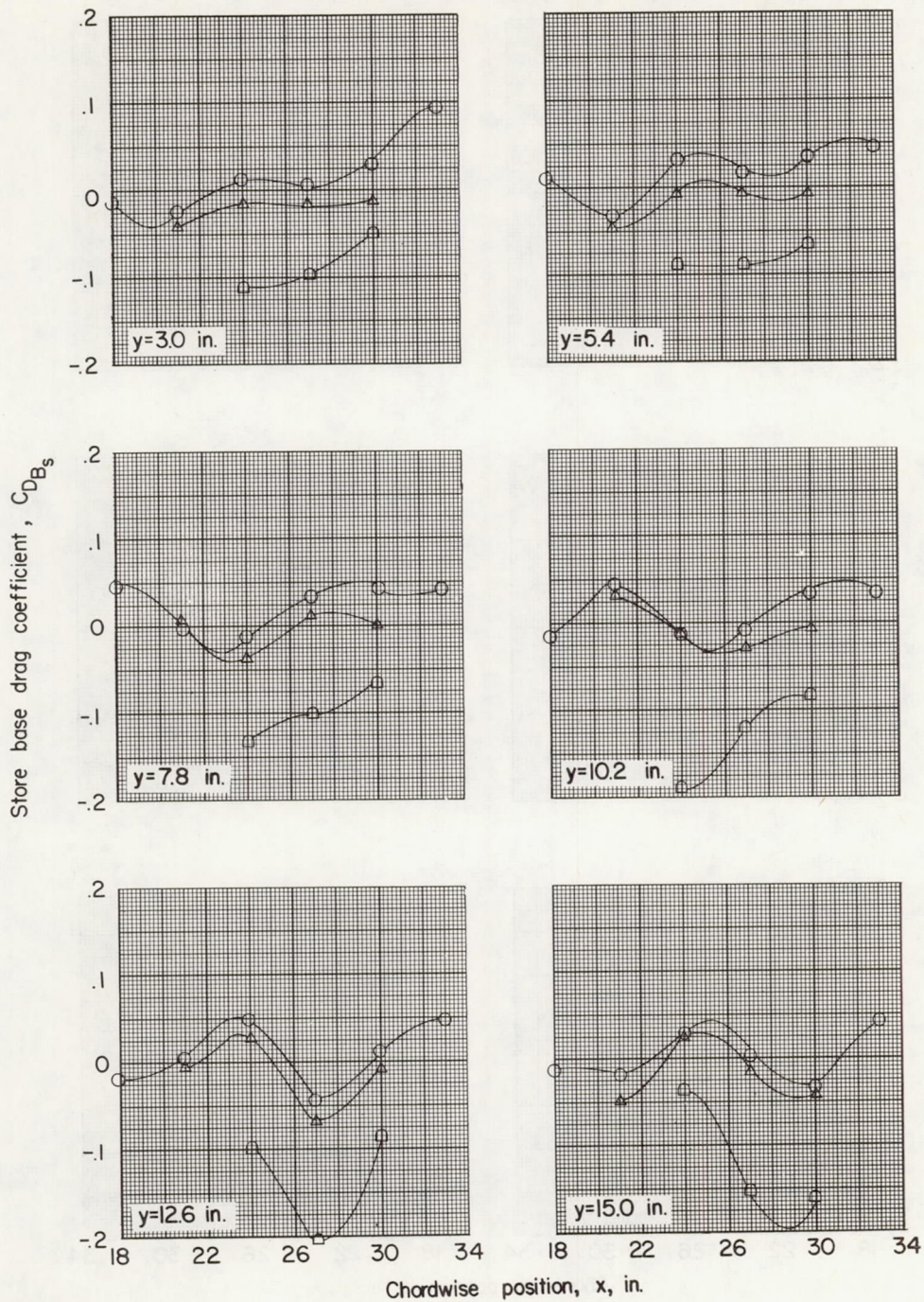
- Large ogive-cylinder store
- △ Large ogive-cylinder store with fins
- Large ogive-cylinder store with cylindrical afterbody



(b) $z = 2.09$ inches; $\alpha = 0^\circ$.

Figure 10.- Continued.

- Large ogive-cylinder store with fins
- △ Large ogive-cylinder store with cylindrical afterbody
- Large ogive-cylinder store with cylindrical afterbody



(c) $z = 2.09$ inches; $\alpha = 4^\circ$.

Figure 10.- Concluded.

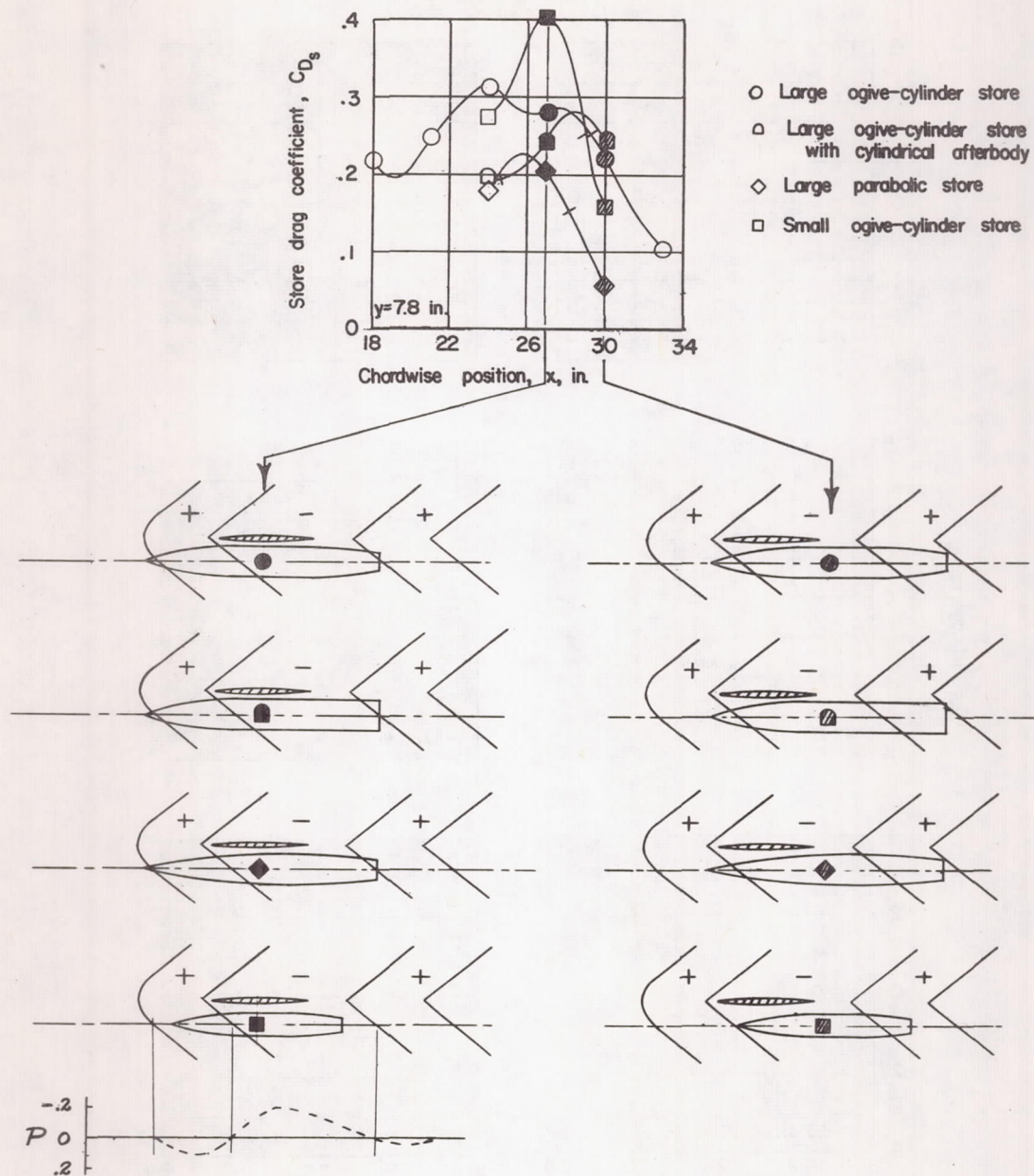


Figure 11.- Comparison of drags of various stores in terms of effective-pressure field of the wing alone. (Pressure-field information from ref. 1. Tick marks indicate values of drag coefficient for isolated stores. See fig. 5.)

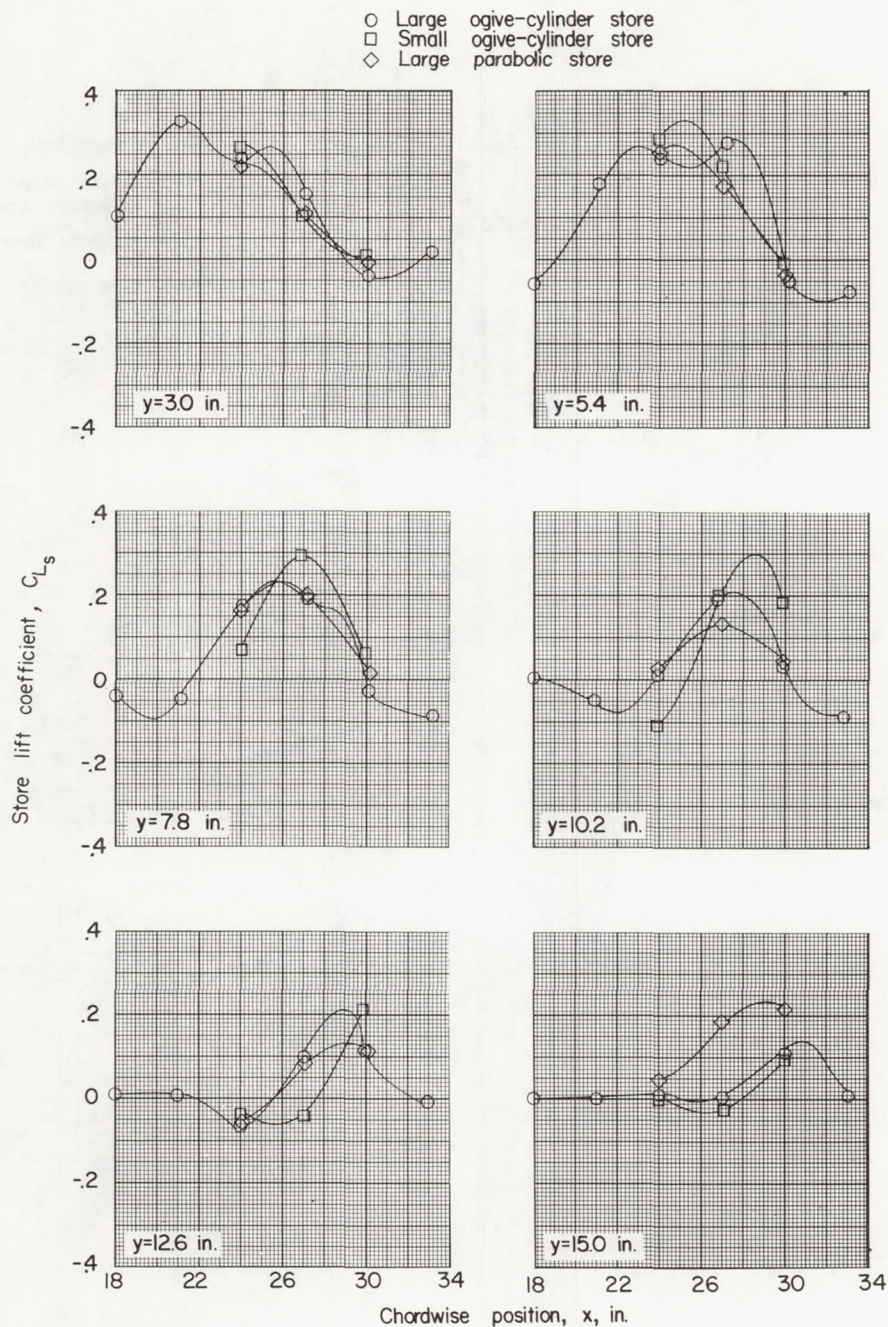
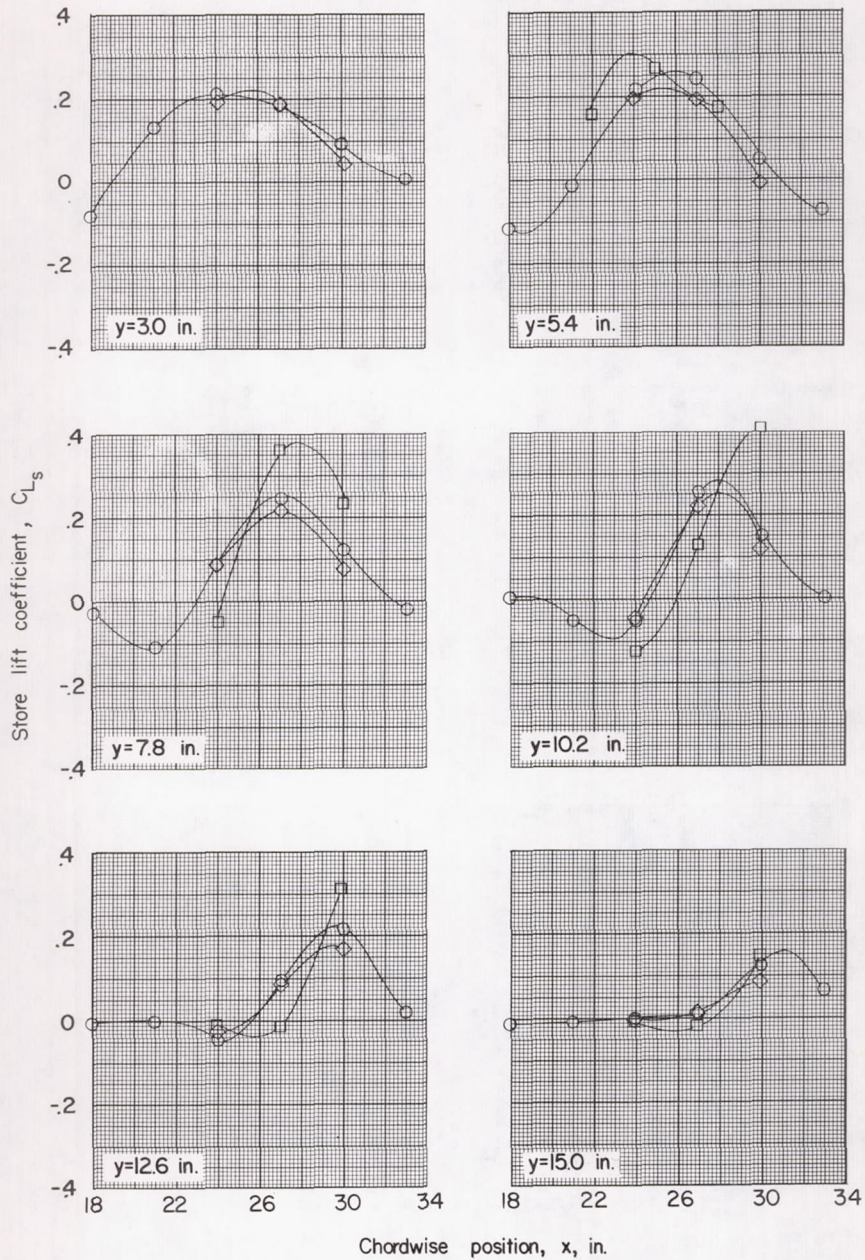


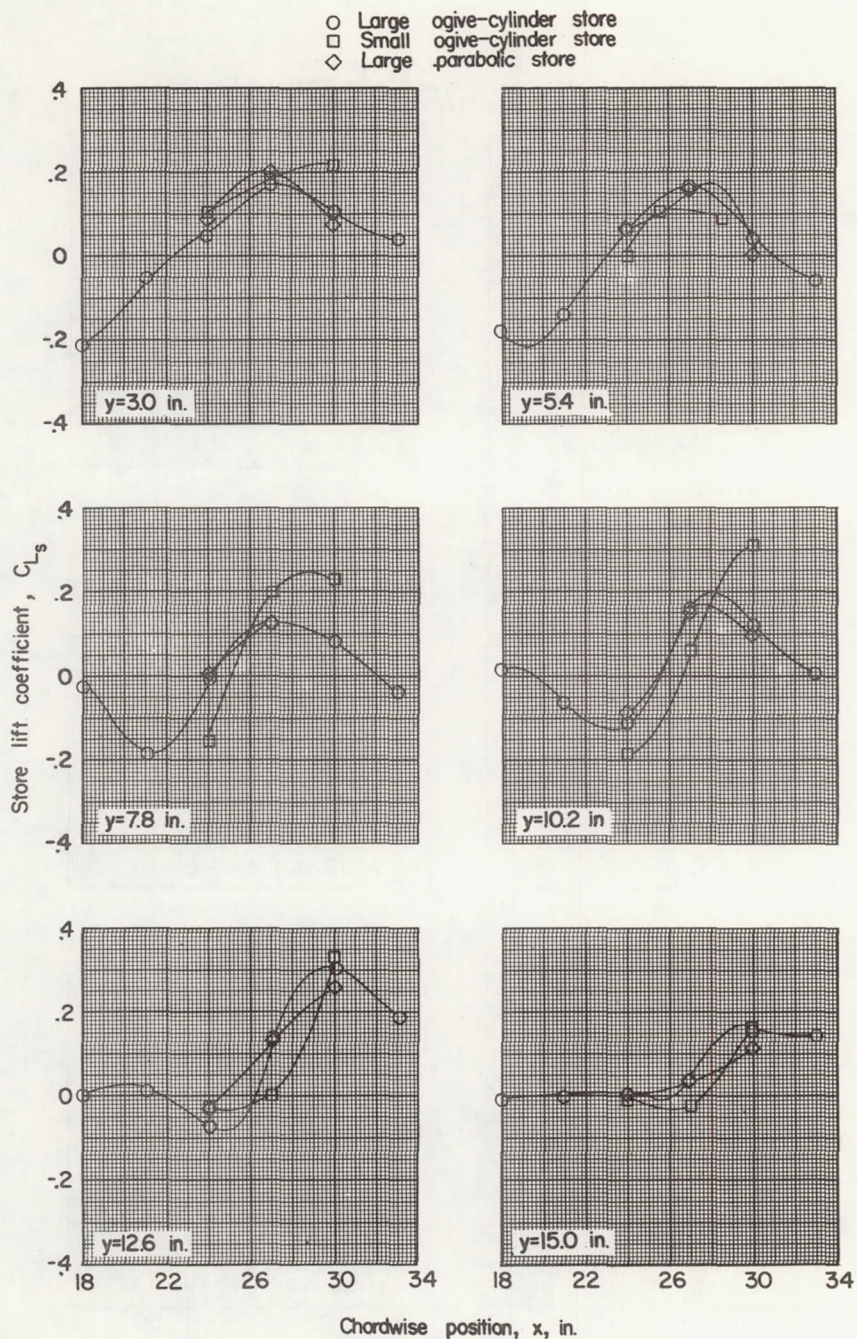
Figure 12.- Lift of stores of different shapes and sizes in presence of wing-fuselage combination.

○ Large ogive-cylinder store
 □ Small ogive-cylinder store
 ◇ Large parabolic store



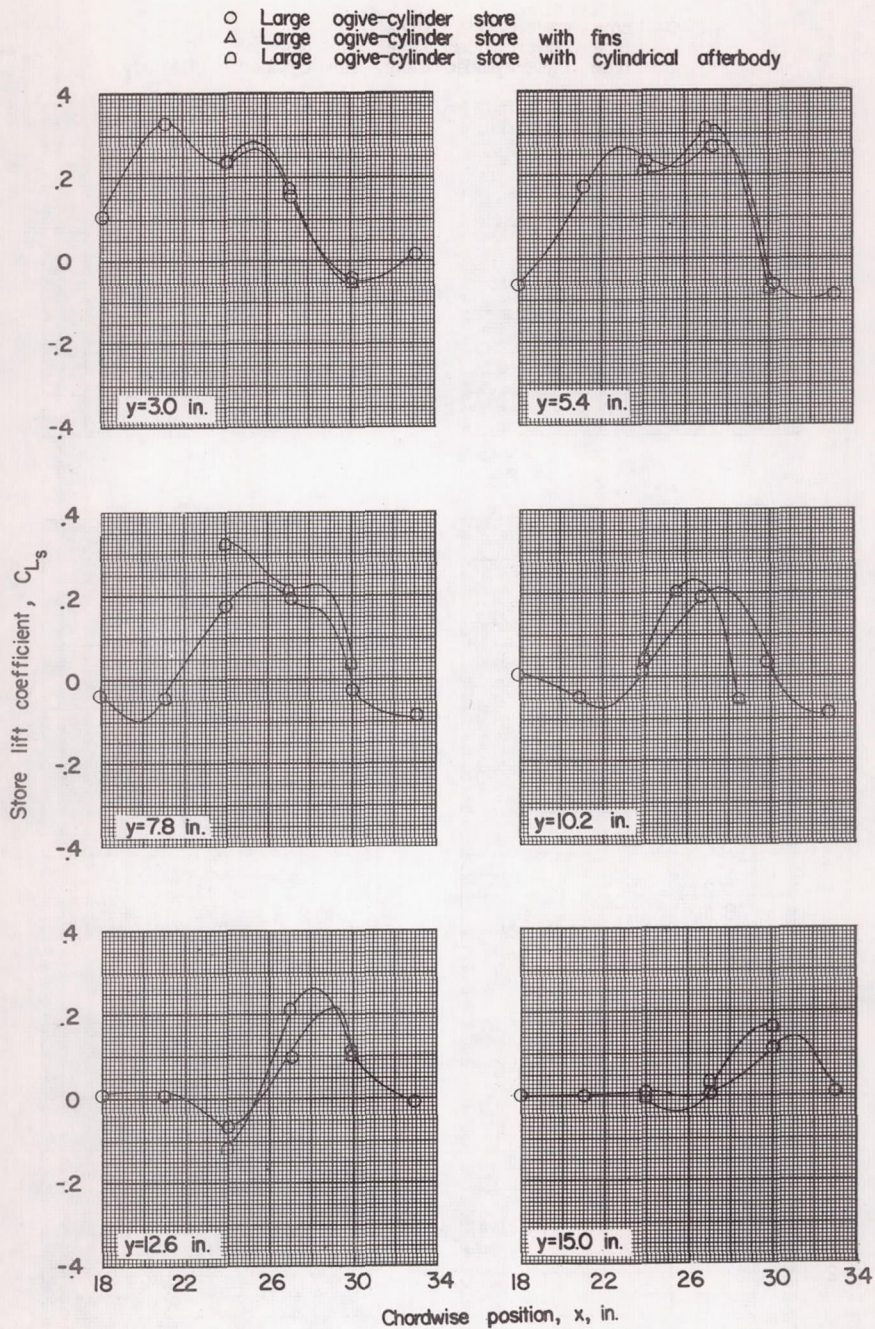
(b) $z = 2.09$ inches; $\alpha = 0^\circ$.

Figure 12.- Continued.



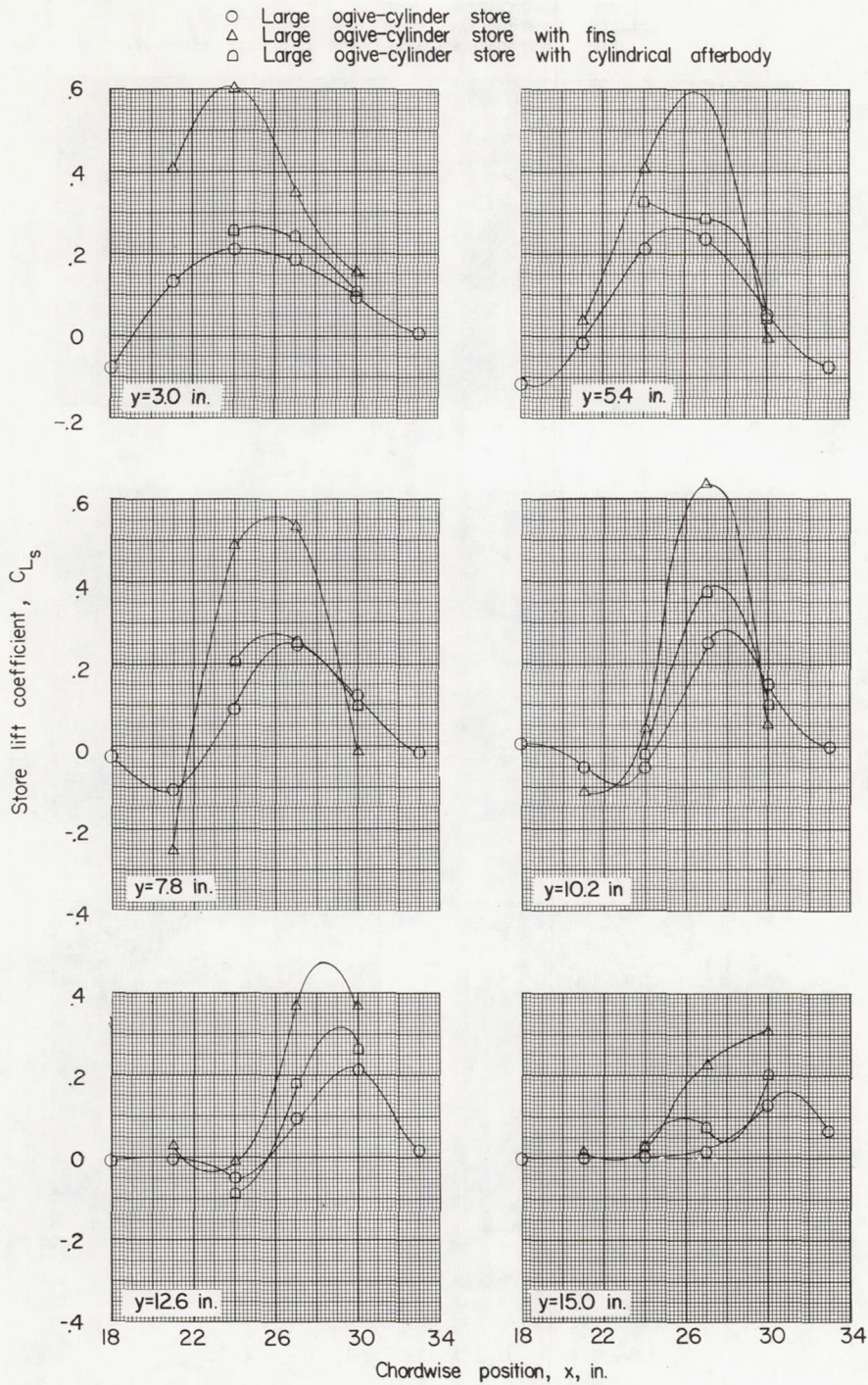
(c) $z = 2.09$ inches; $\alpha = 4^\circ$.

Figure 12.- Concluded.



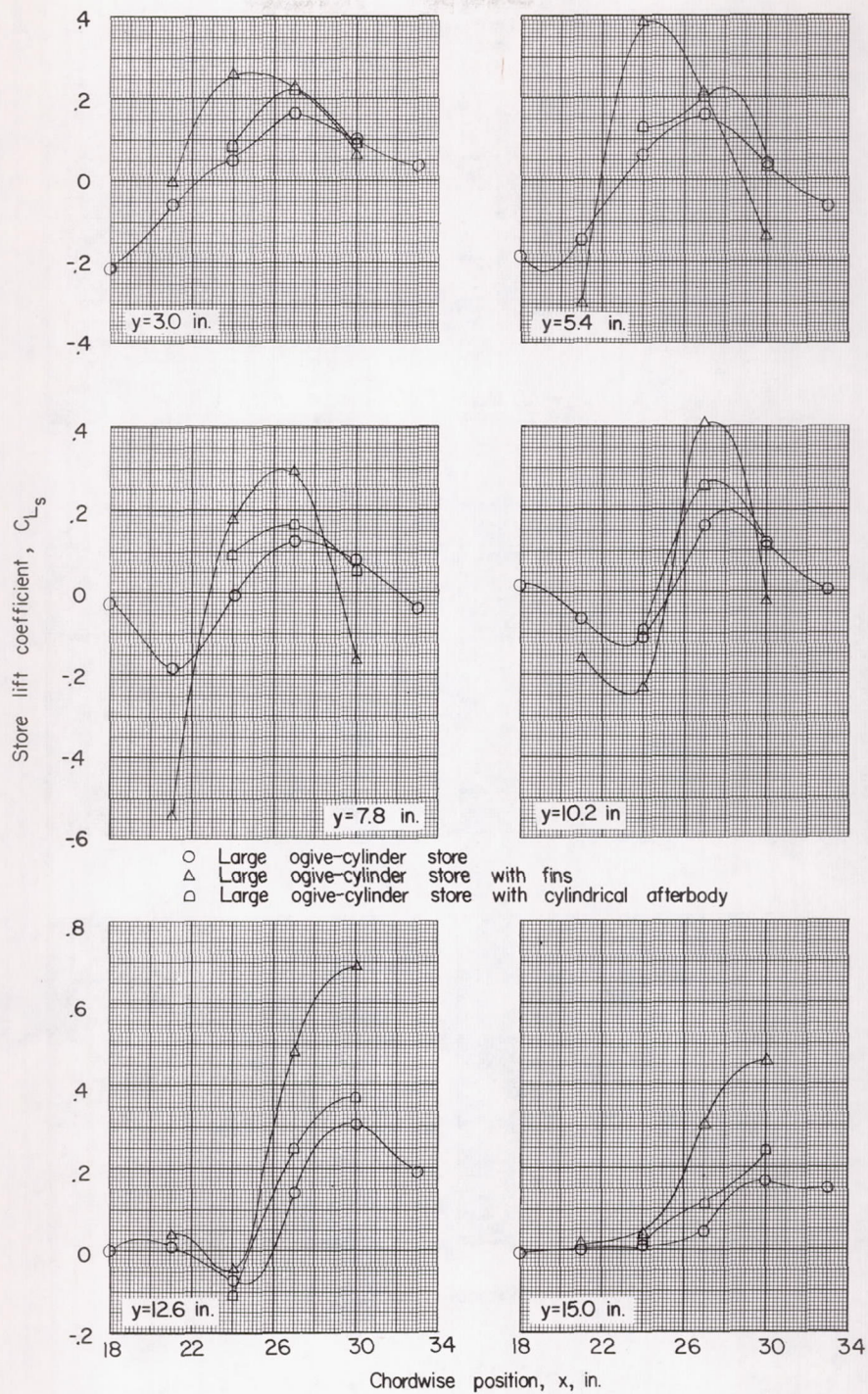
(a) $z = 1.15$ inches; $\alpha = 0^\circ$.

Figure 13.- Lift of large ogive-cylinder store with various afterbody configurations in presence of wing-fuselage combination.



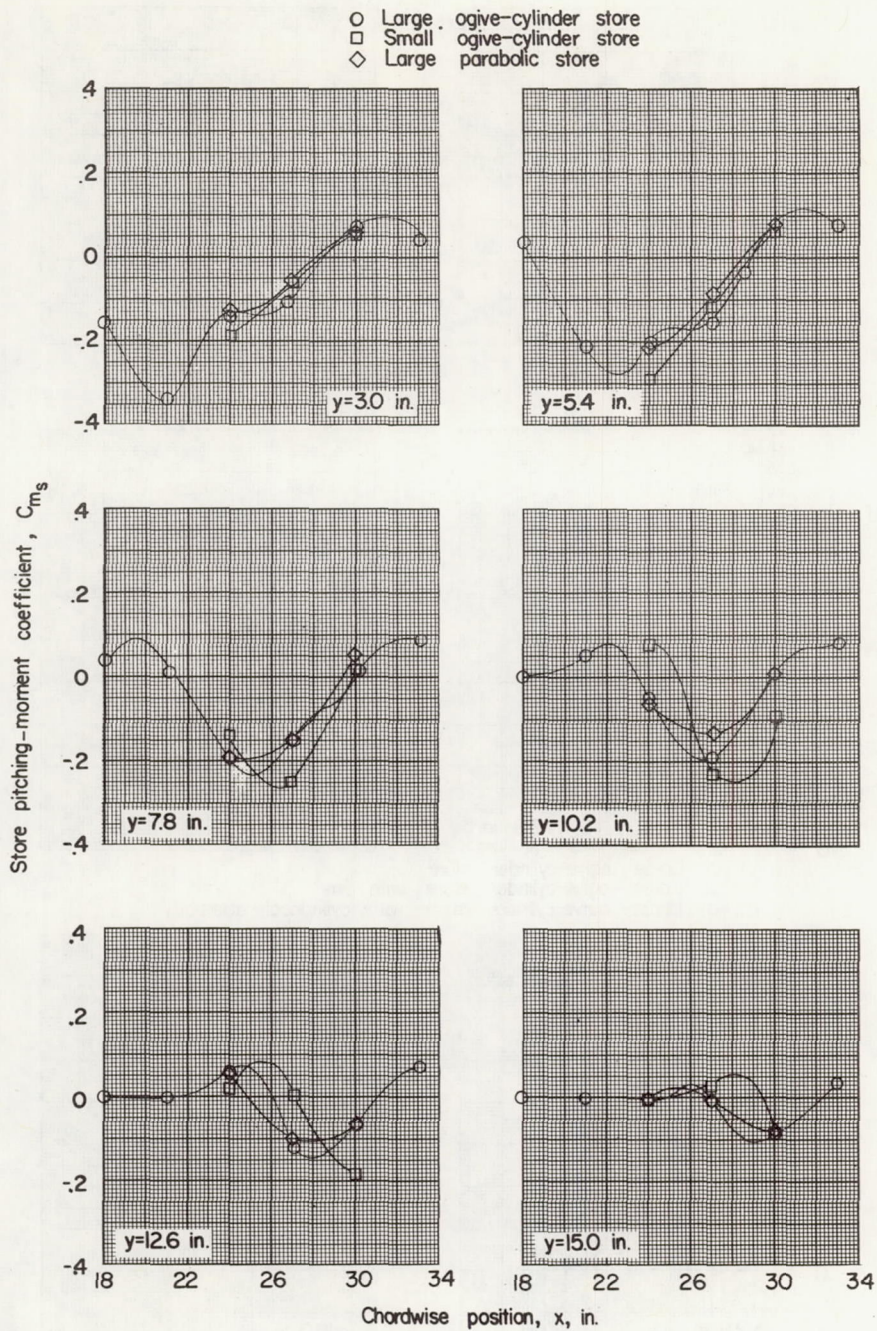
(b) $z = 2.09$ inches; $\alpha = 0^\circ$.

Figure 13.- Continued.



(c) $z = 2.09$ inches; $\alpha = 4^\circ$.

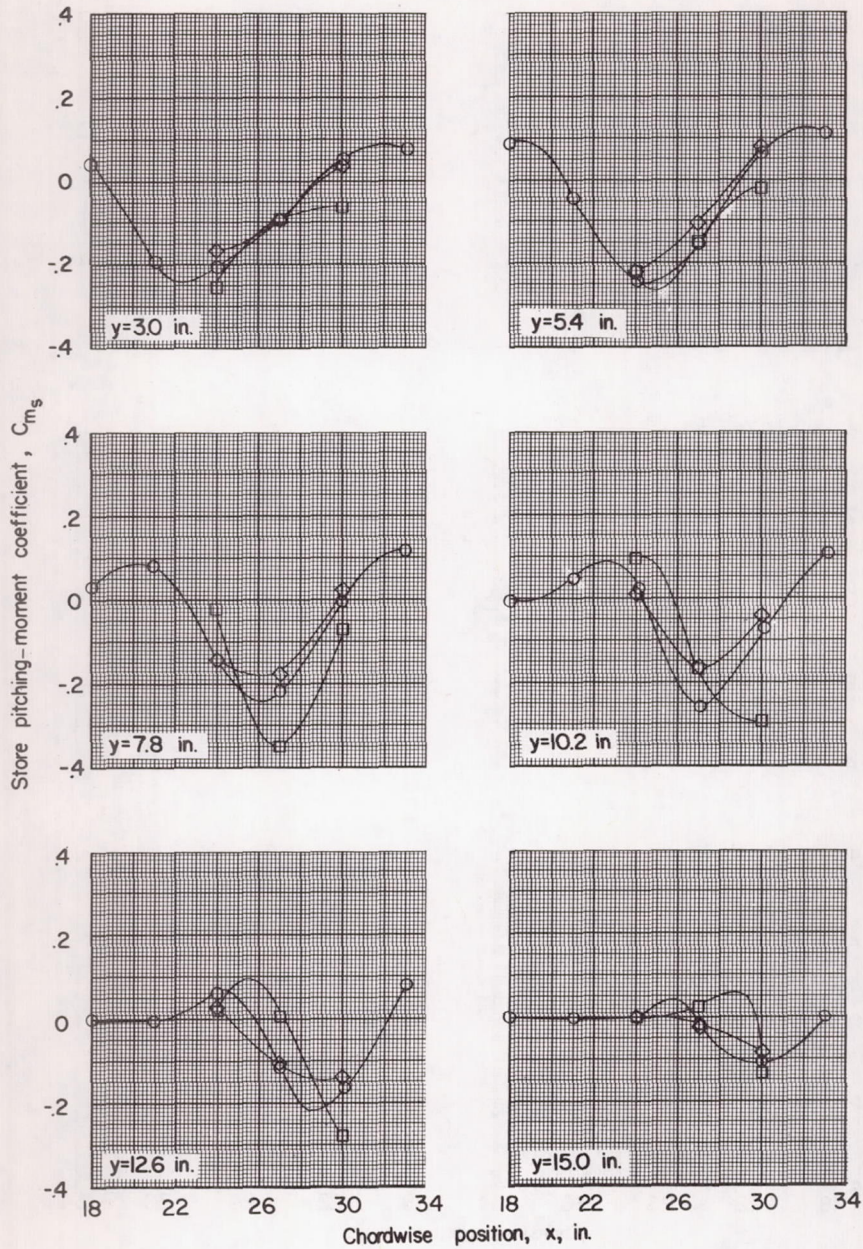
Figure 13.- Concluded.



(a) $z = 1.15$ inches; $\alpha = 0^\circ$.

Figure 14.- Pitching moment of stores of different shapes and sizes in presence of wing-fuselage combination. (Center of moments is store nose.)

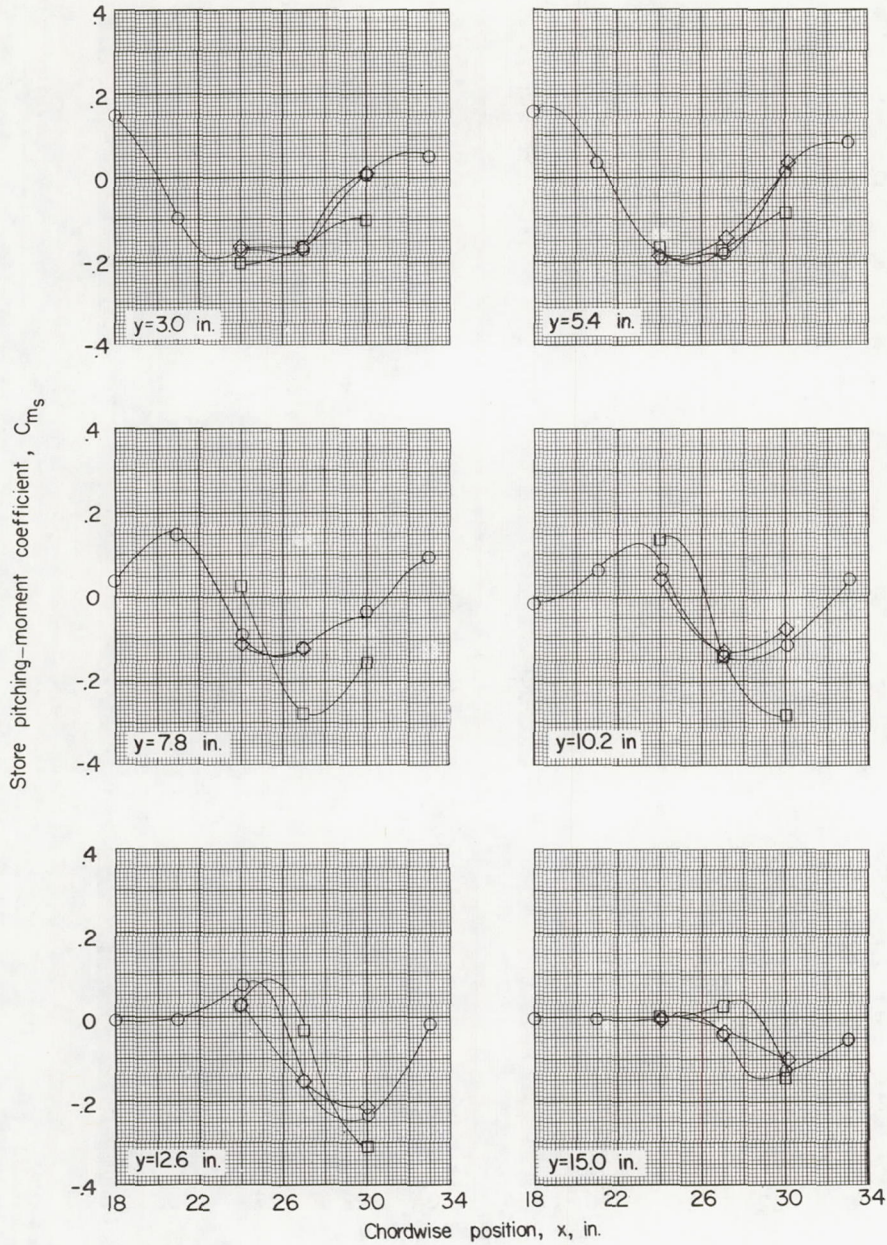
○ Large ogive-cylinder store
 □ Small ogive-cylinder store
 ◇ Large parabolic store



(b) $z = 2.09$ inches; $\alpha = 0^\circ$.

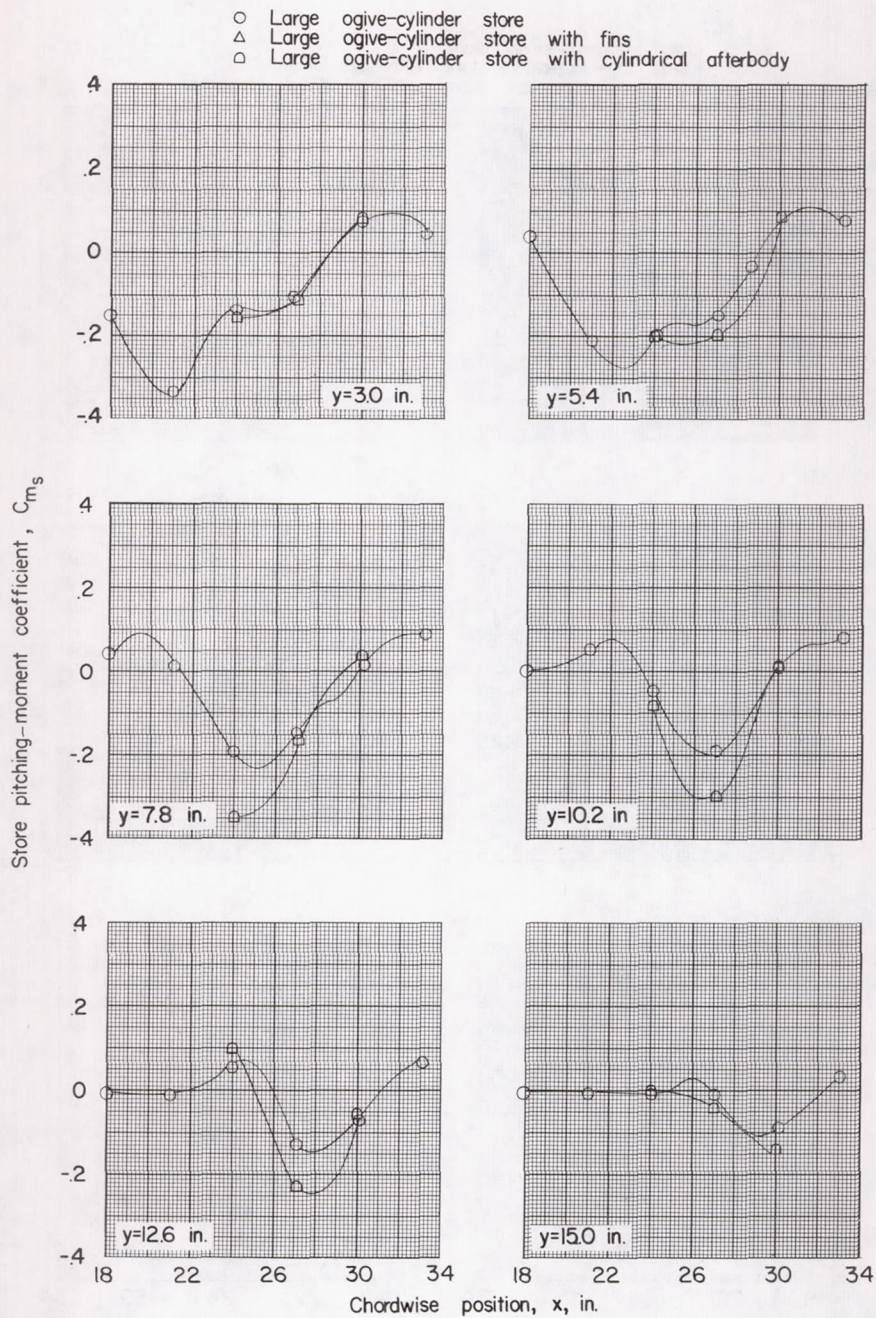
Figure 14.- Continued.

○ Large ogive-cylinder store
 □ Small ogive-cylinder store
 ◇ Large parabolic store



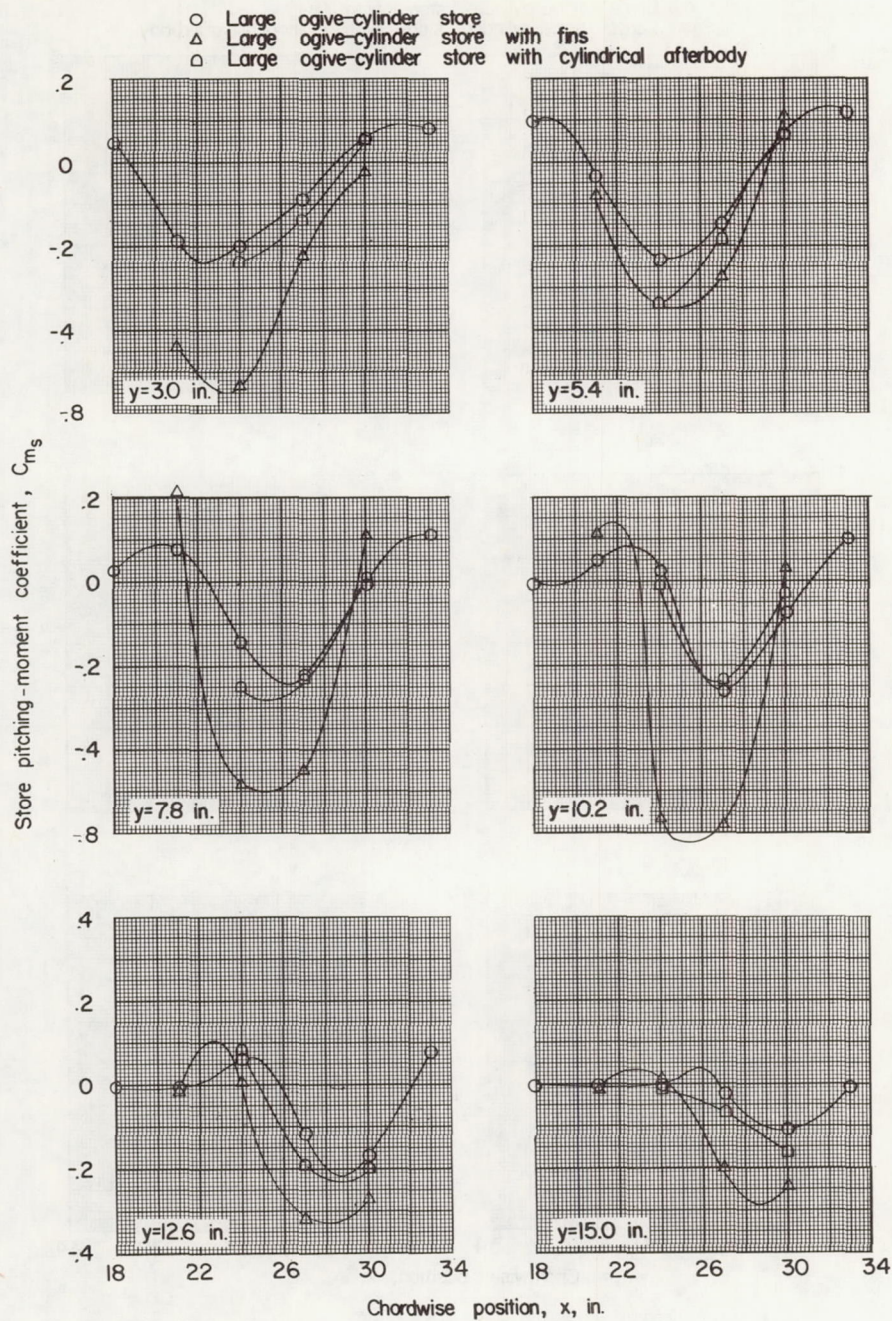
(c) $z = 2.09$ inches; $\alpha = 4^\circ$.

Figure 14.- Concluded.



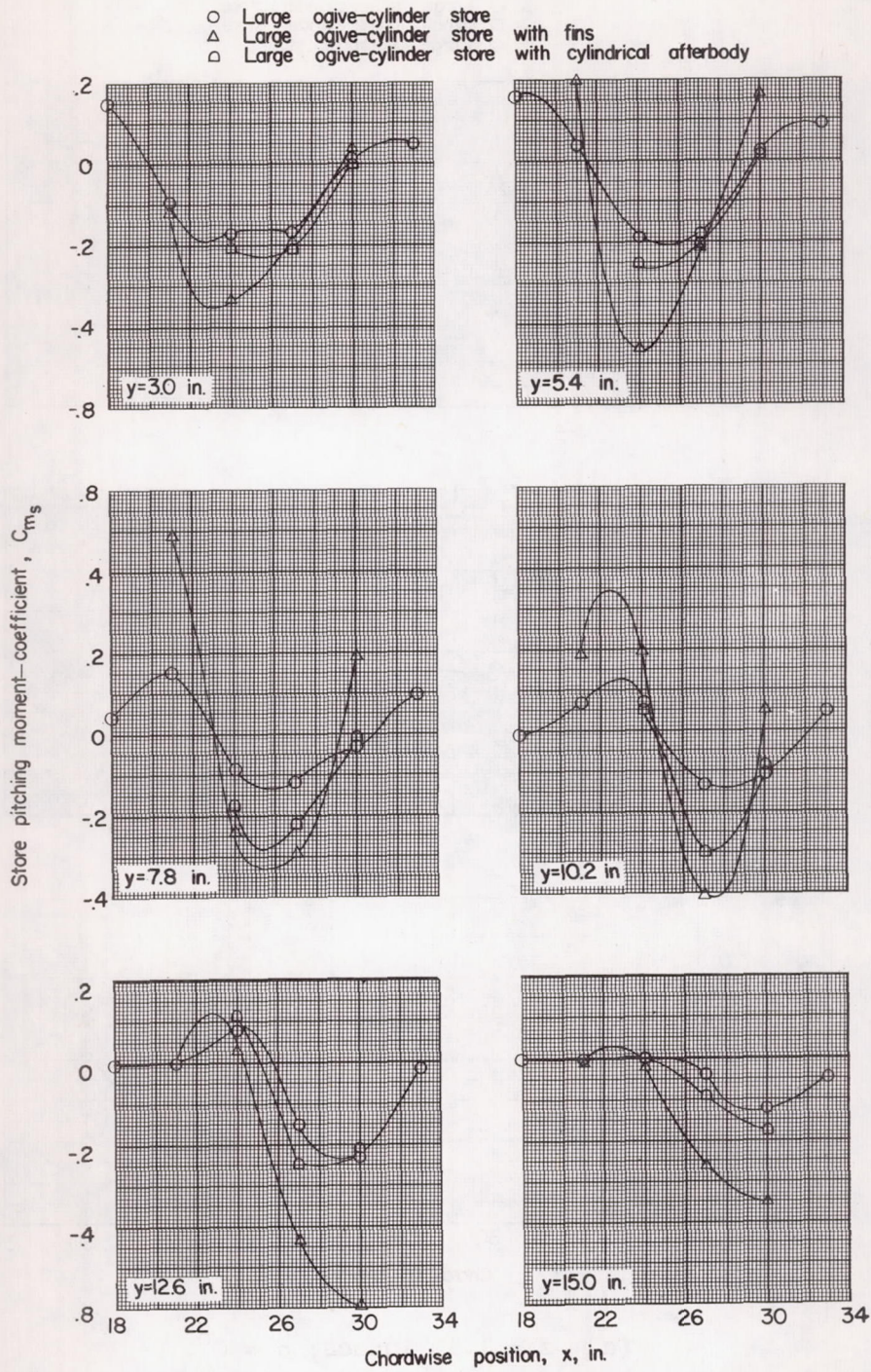
(a) $z = 1.15$ inches; $\alpha = 0^\circ$.

Figure 15.- Pitching moment of large ogive-cylinder store with various afterbody configurations in presence of wing-fuselage combination. (Center of moments is store nose.)



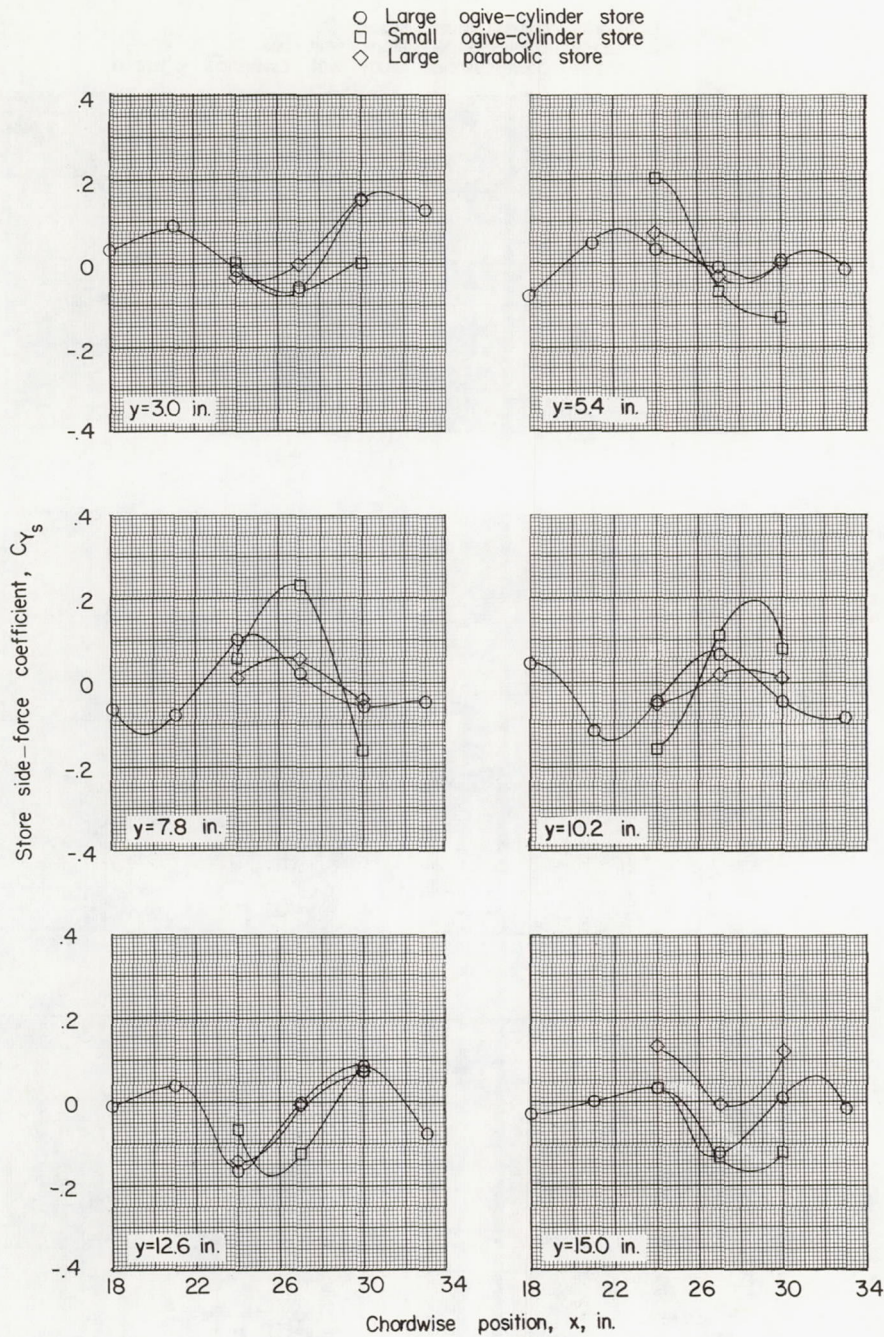
(b) $z = 2.09$ inches; $\alpha = 0^\circ$.

Figure 15.- Continued.



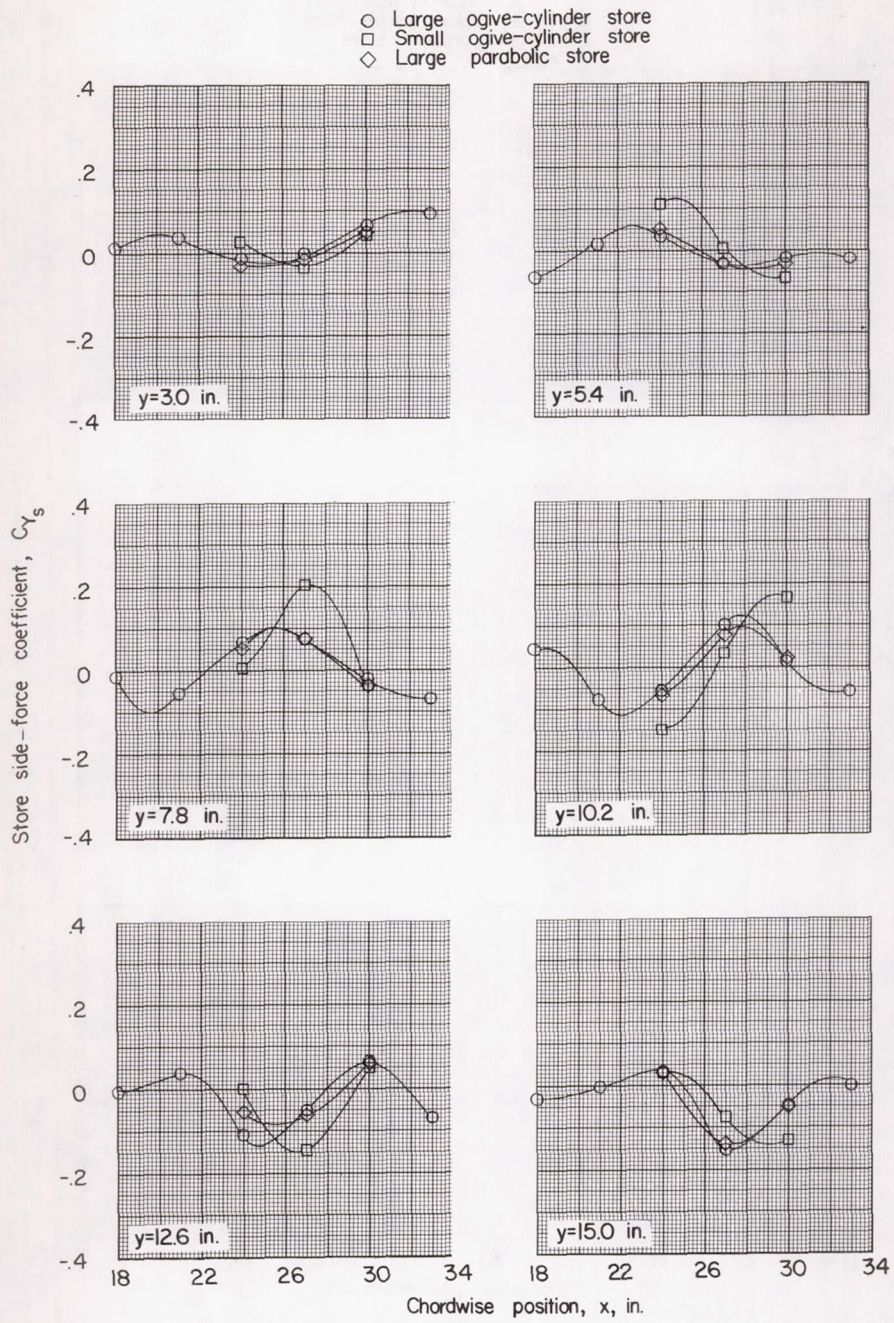
(c) $z = 2.09$ inches; $\alpha = 4^\circ$.

Figure 15.- Concluded.



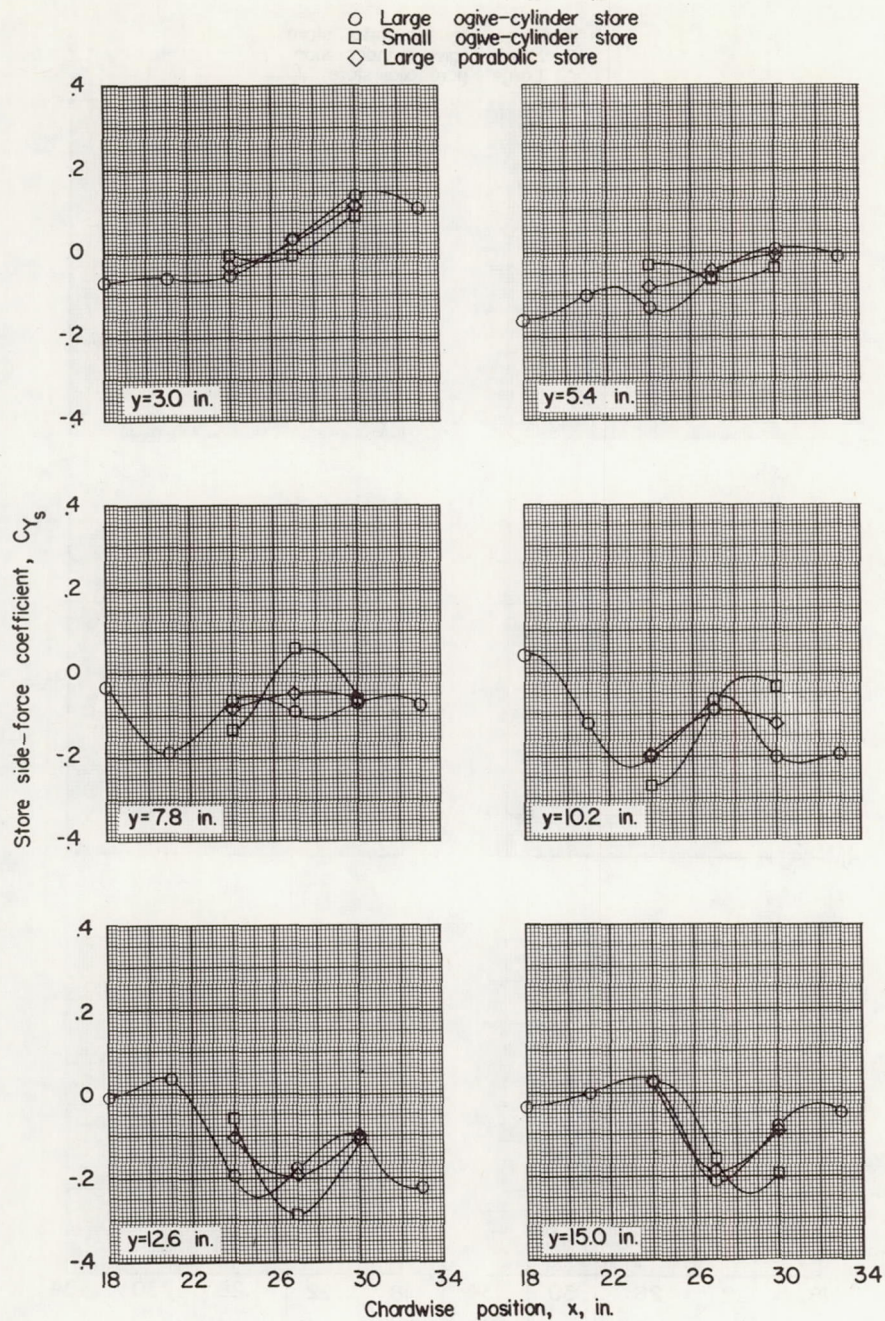
(a) $z = 1.15$ inches; $\alpha = 0^\circ$.

Figure 16.- Side force of stores of different shapes and sizes in presence of wing-fuselage combination.



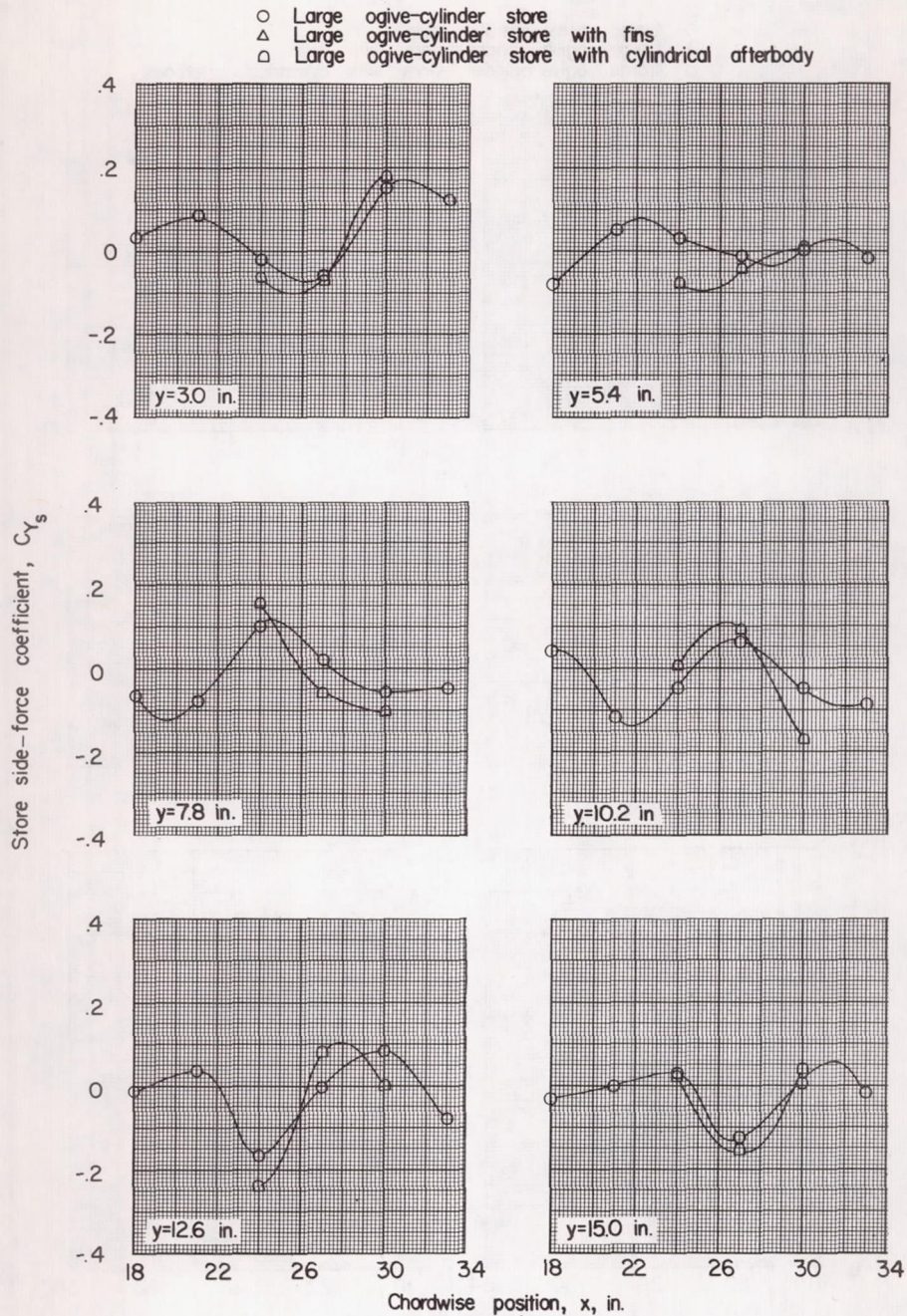
(b) $z = 2.09$ inches; $\alpha = 0^\circ$.

Figure 16.- Continued.



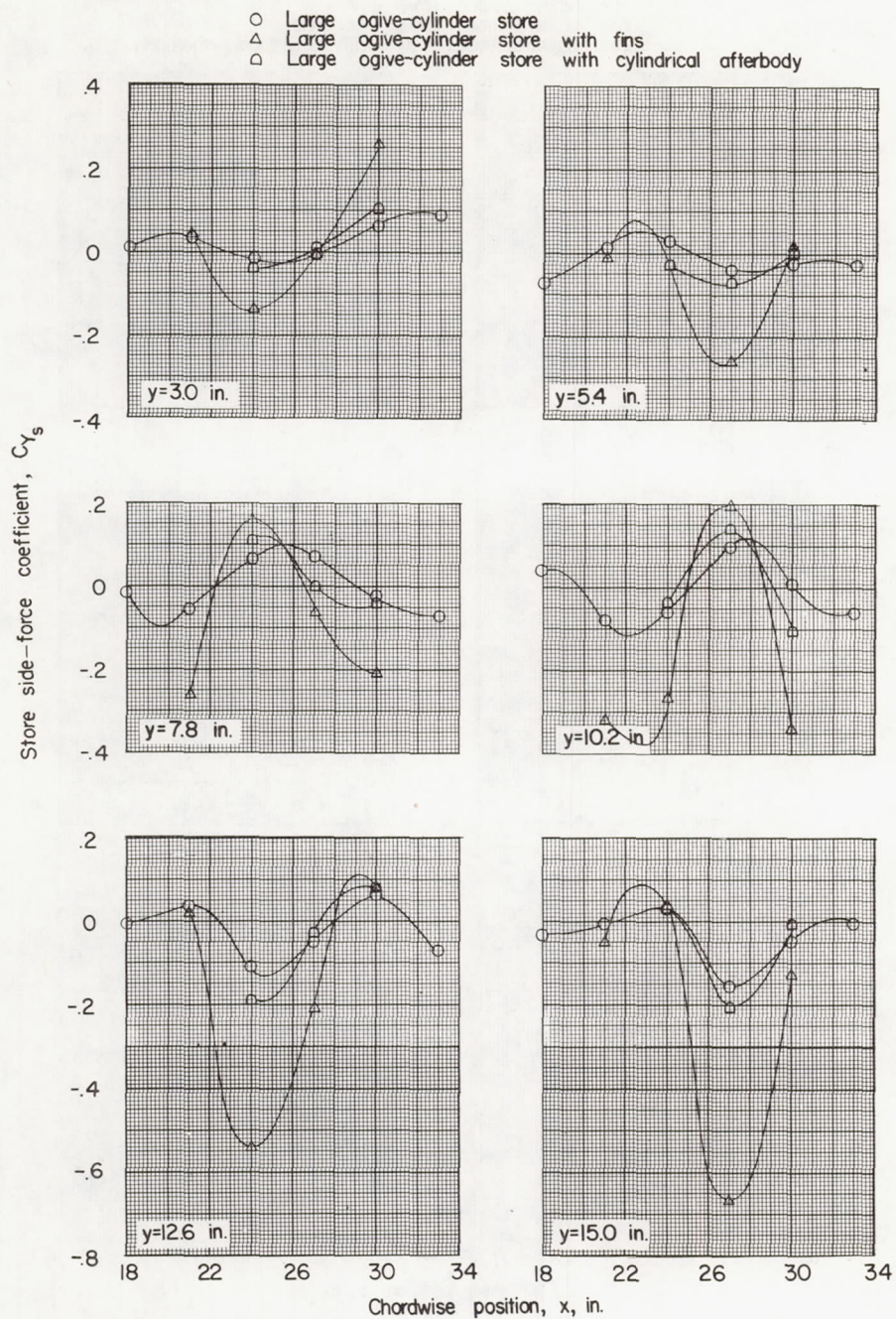
(c) $z = 2.09$ inches; $\alpha = 4^\circ$.

Figure 16.- Concluded.



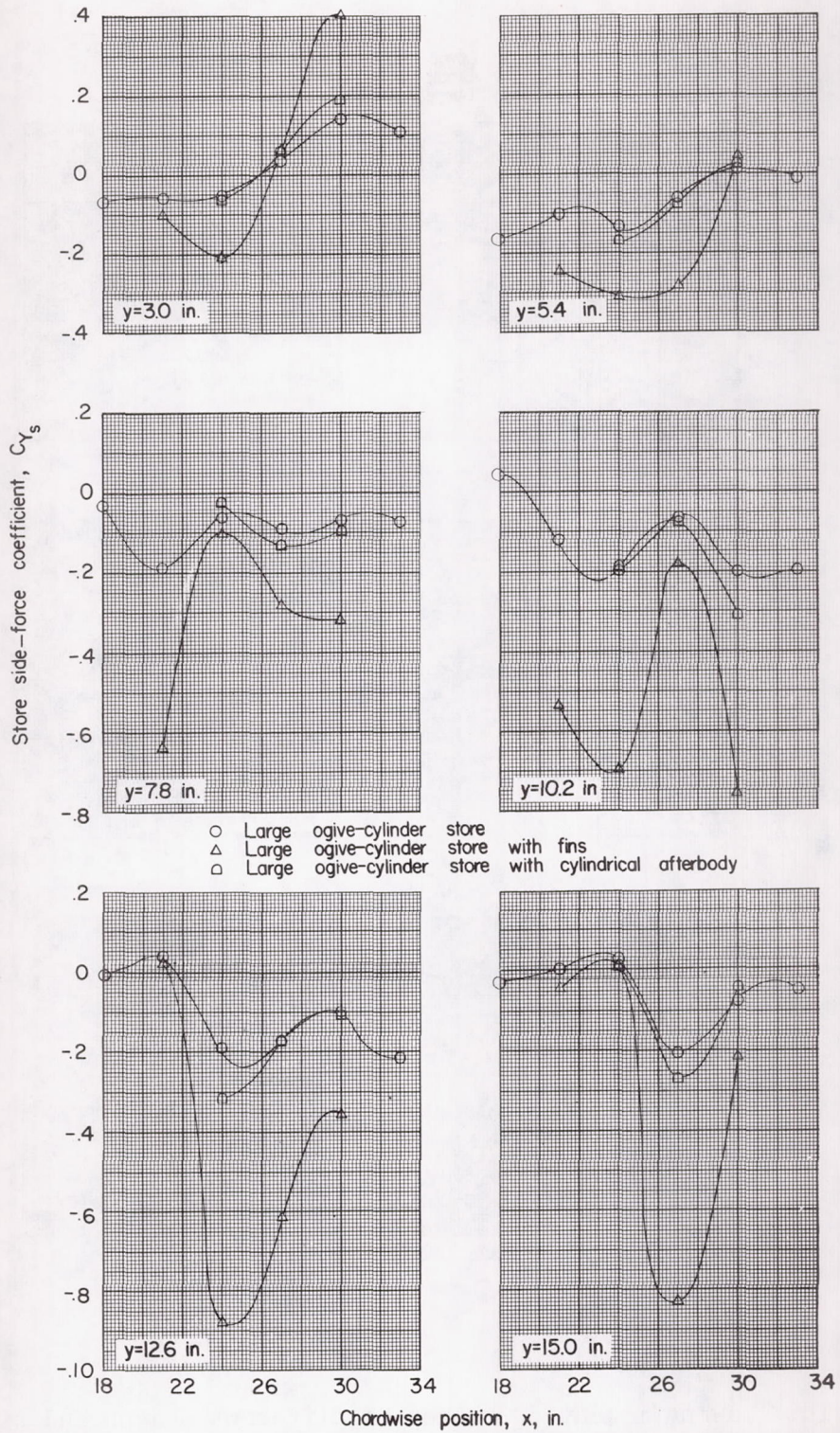
(a) $z = 1.15$ inches; $\alpha = 0^\circ$.

Figure 17.- Side force of large ogive-cylinder store with various after-body configurations in presence of wing-fuselage combination.



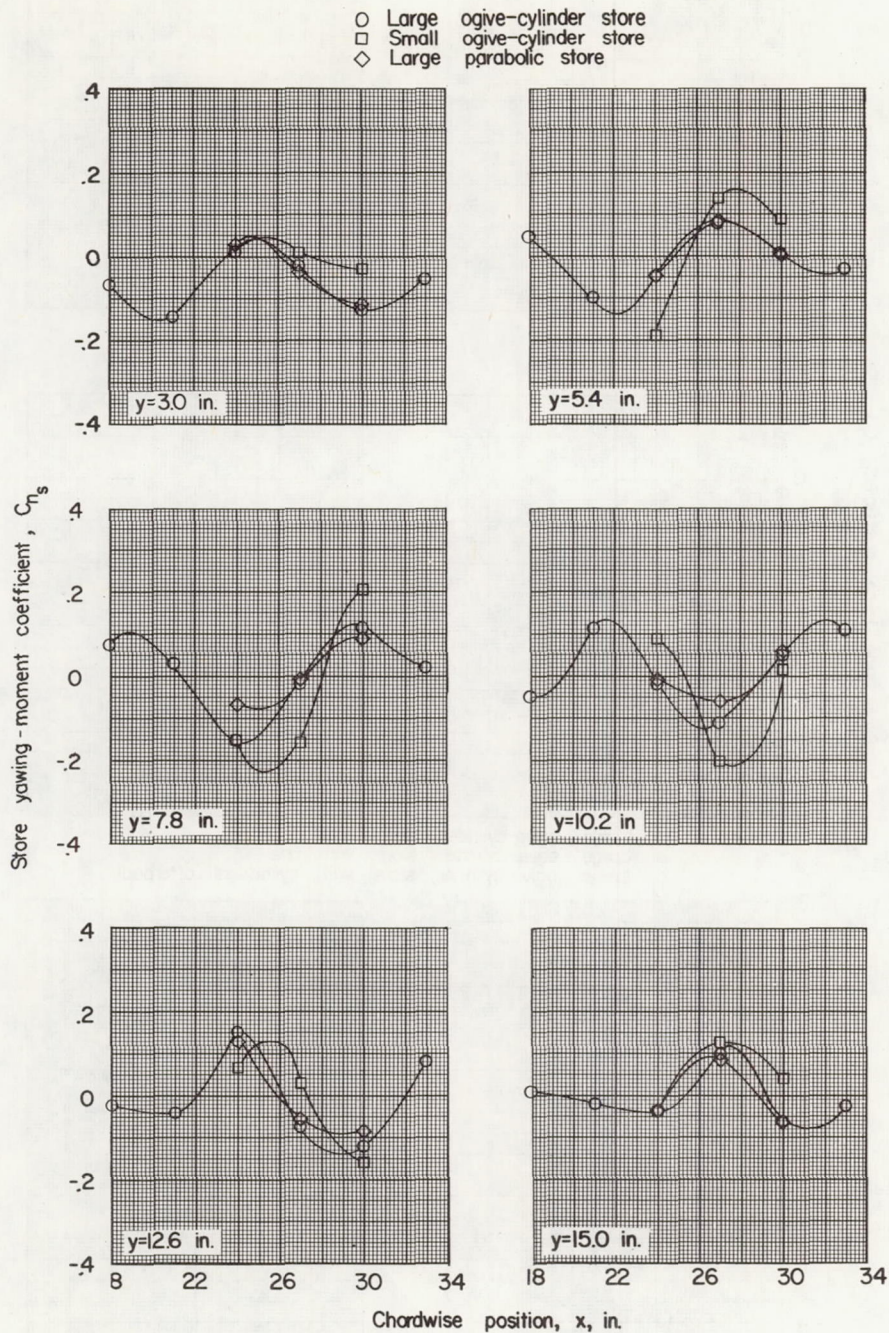
(b) $z = 2.09$ inches; $\alpha = 0^\circ$.

Figure 17.- Continued.



(c) $z = 2.09$ inches; $\alpha = 4^\circ$.

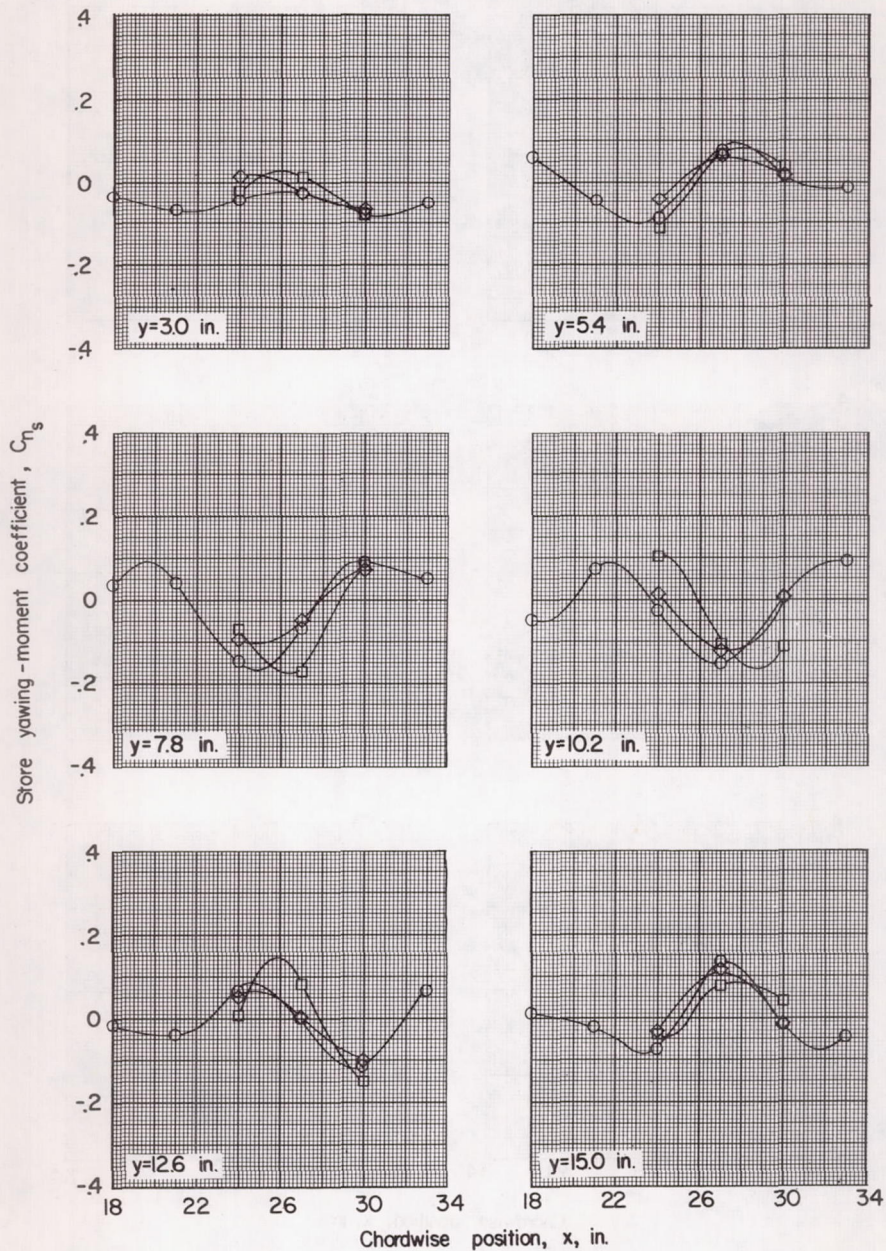
Figure 17.- Concluded.



(a) $z = 1.15$ inches; $\alpha = 0^\circ$.

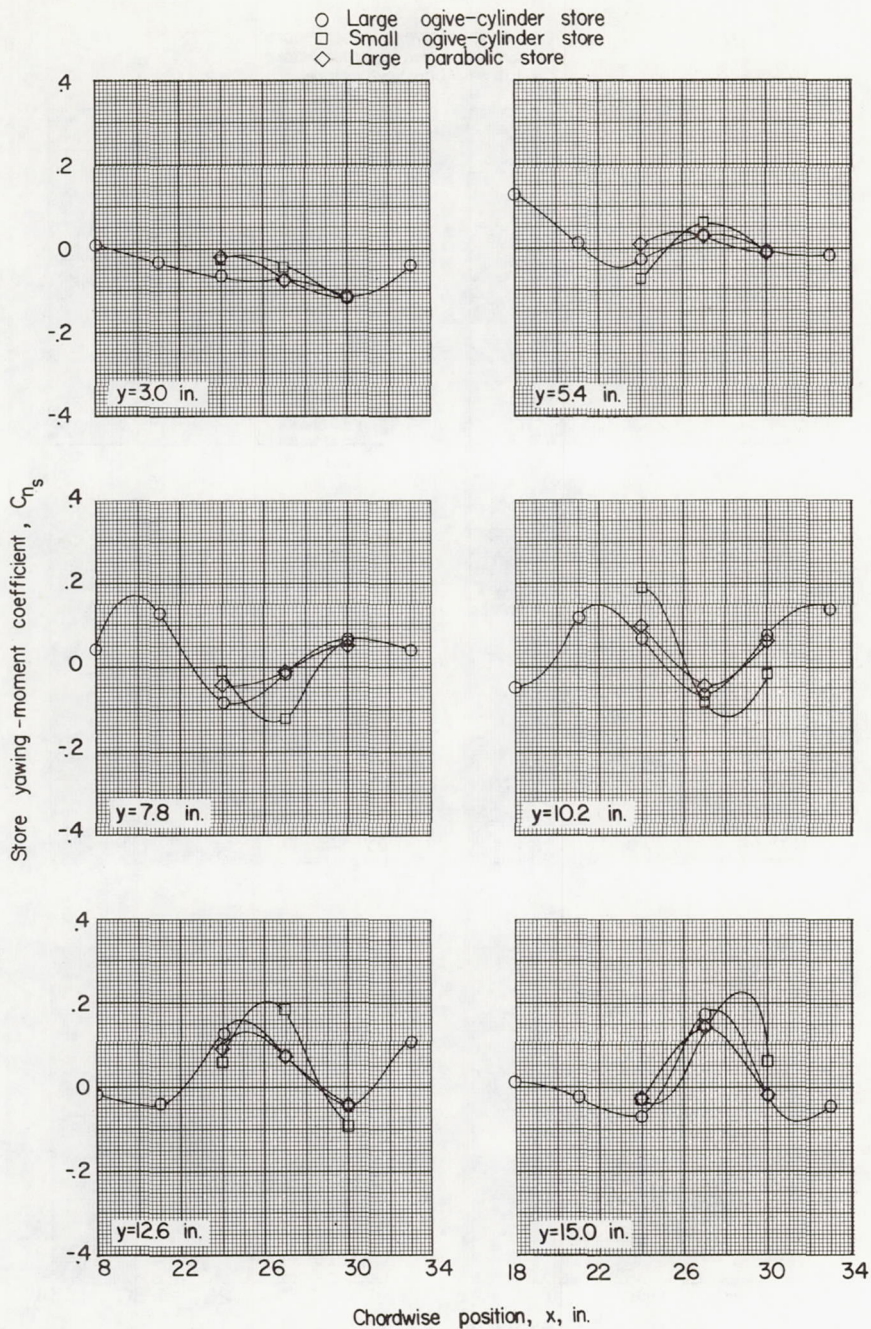
Figure 18.- Yawing moment of stores of different shapes and sizes in presence of wing-fuselage combination. (Center of moments is store nose.)

○ Large ogive-cylinder store
 □ Small ogive-cylinder store
 ◇ Large parabolic store



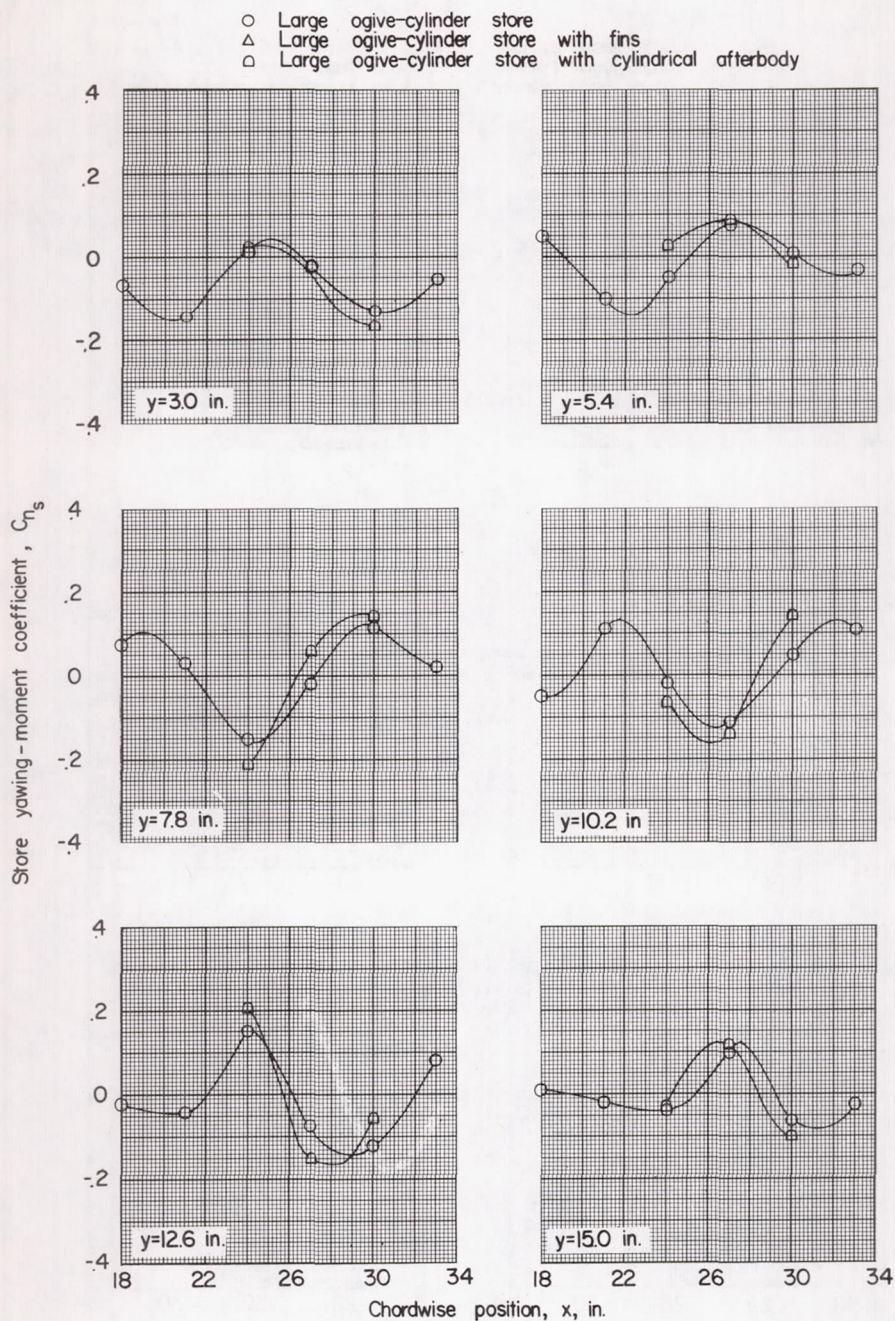
(b) $z = 2.09$ inches; $\alpha = 0^\circ$.

Figure 18.- Continued.



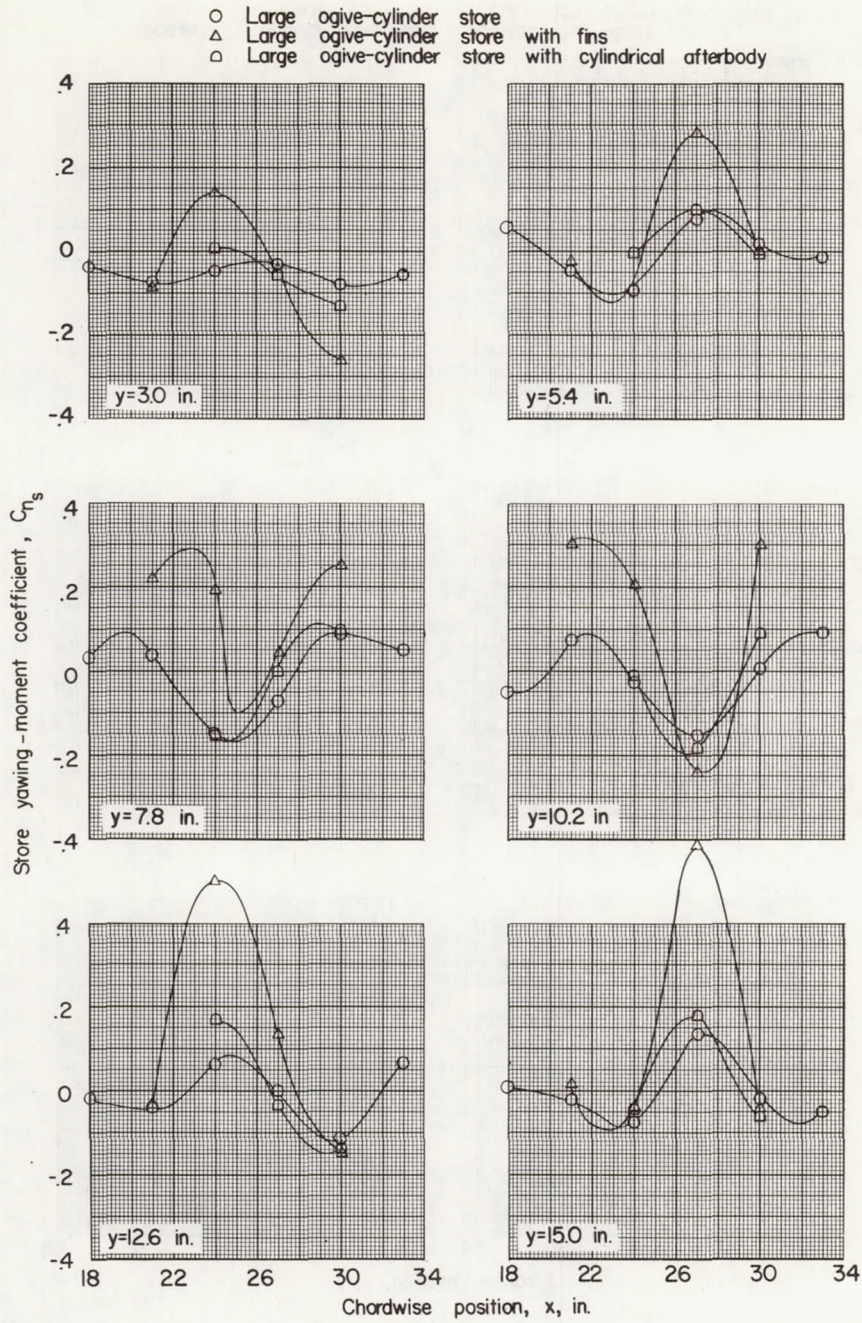
(c) $z = 2.09$ inches; $\alpha = 4^\circ$.

Figure 18.- Concluded.



(a) $z = 1.15$ inches; $\alpha = 0^\circ$.

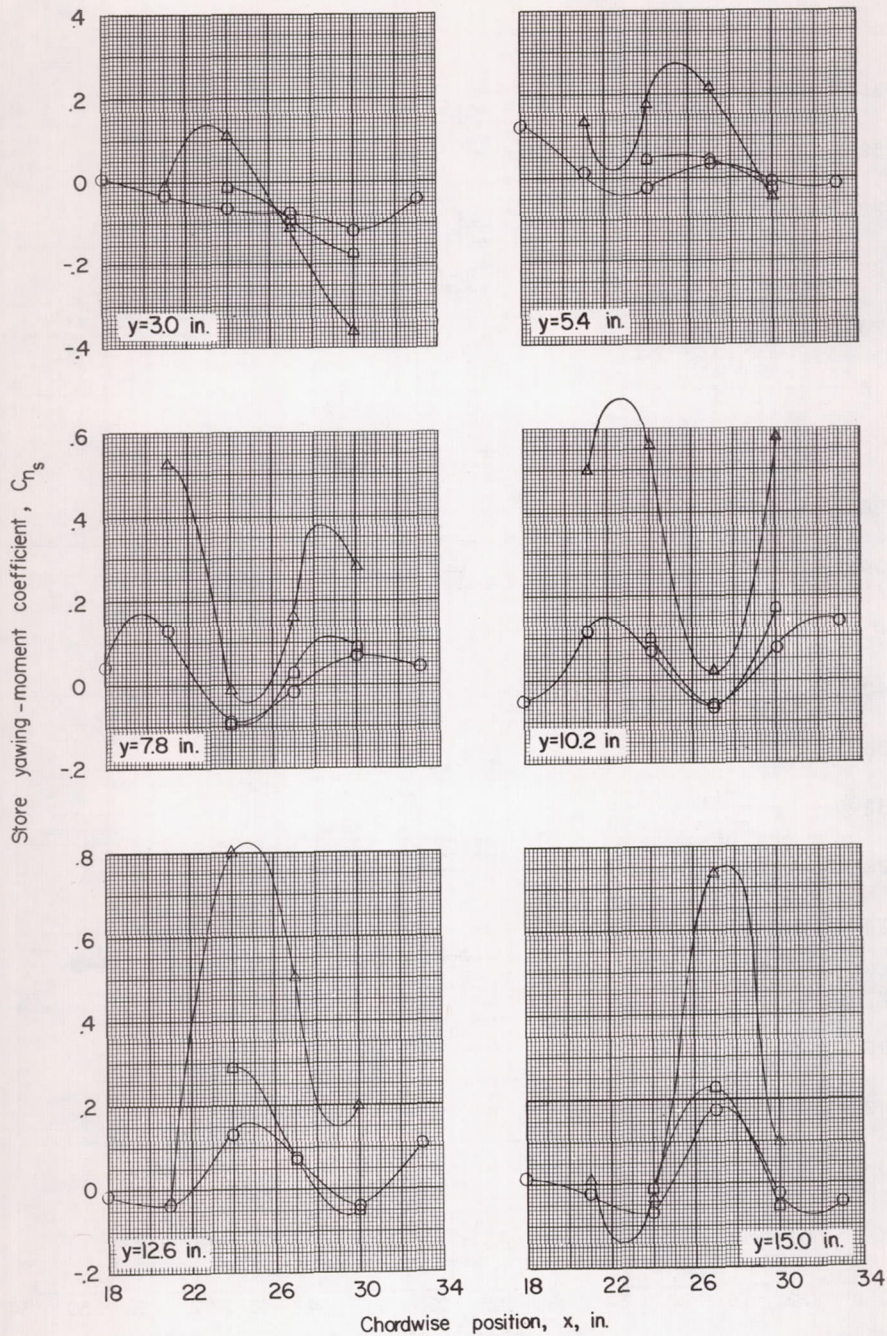
Figure 19.- Yawing moment of large ogive-cylinder store with various afterbody configurations in presence of wing-fuselage combination. (Center of moments is store nose.)



(b) $z = 2.09$ inches; $\alpha = 0^\circ$.

Figure 19.- Continued.

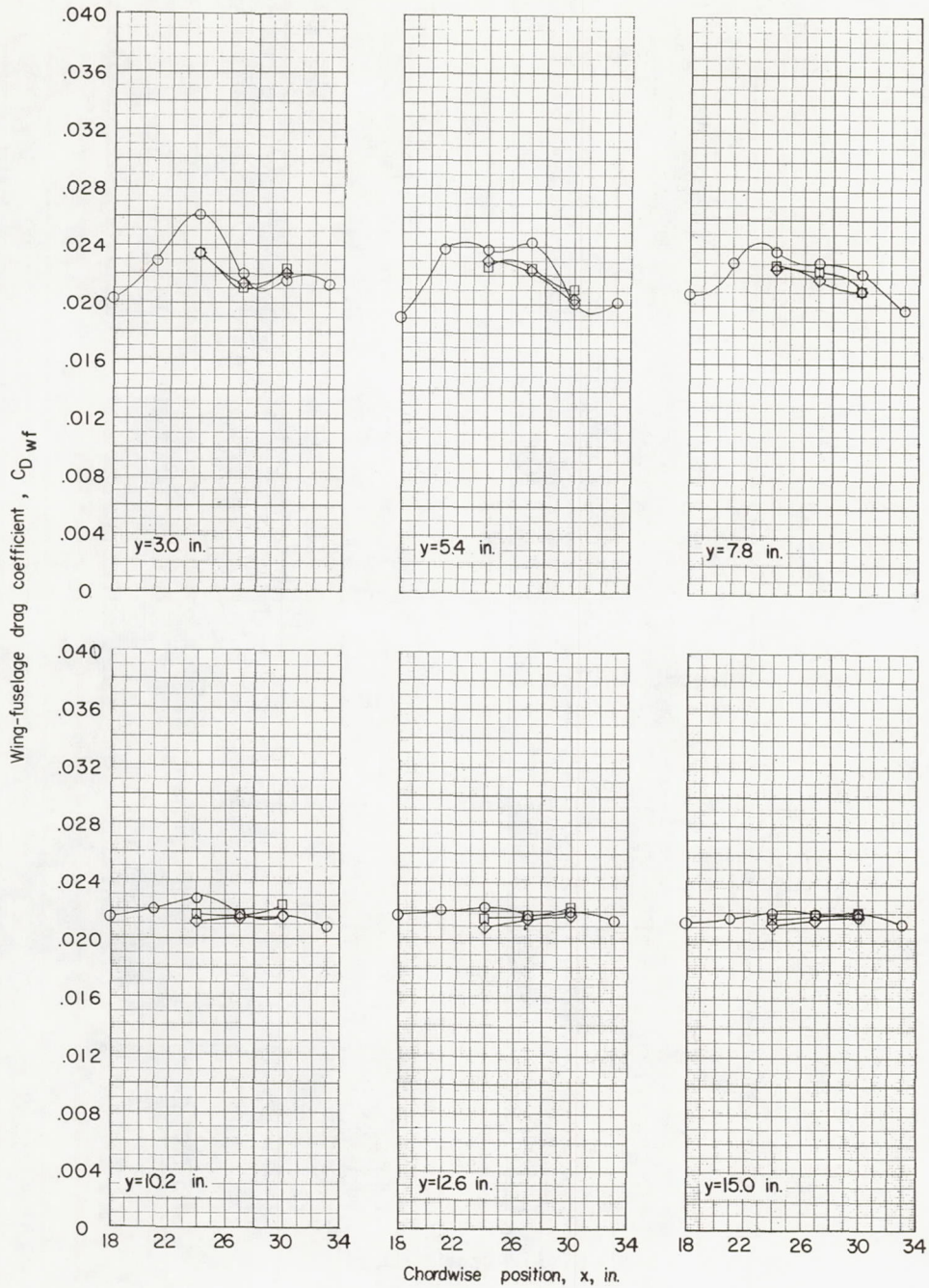
○ Large ogive-cylinder store
 △ Large ogive-cylinder store with fins
 □ Large ogive-cylinder store with cylindrical afterbody



(c) $z = 2.09$ inches; $\alpha = 4^\circ$.

Figure 19.- Concluded.

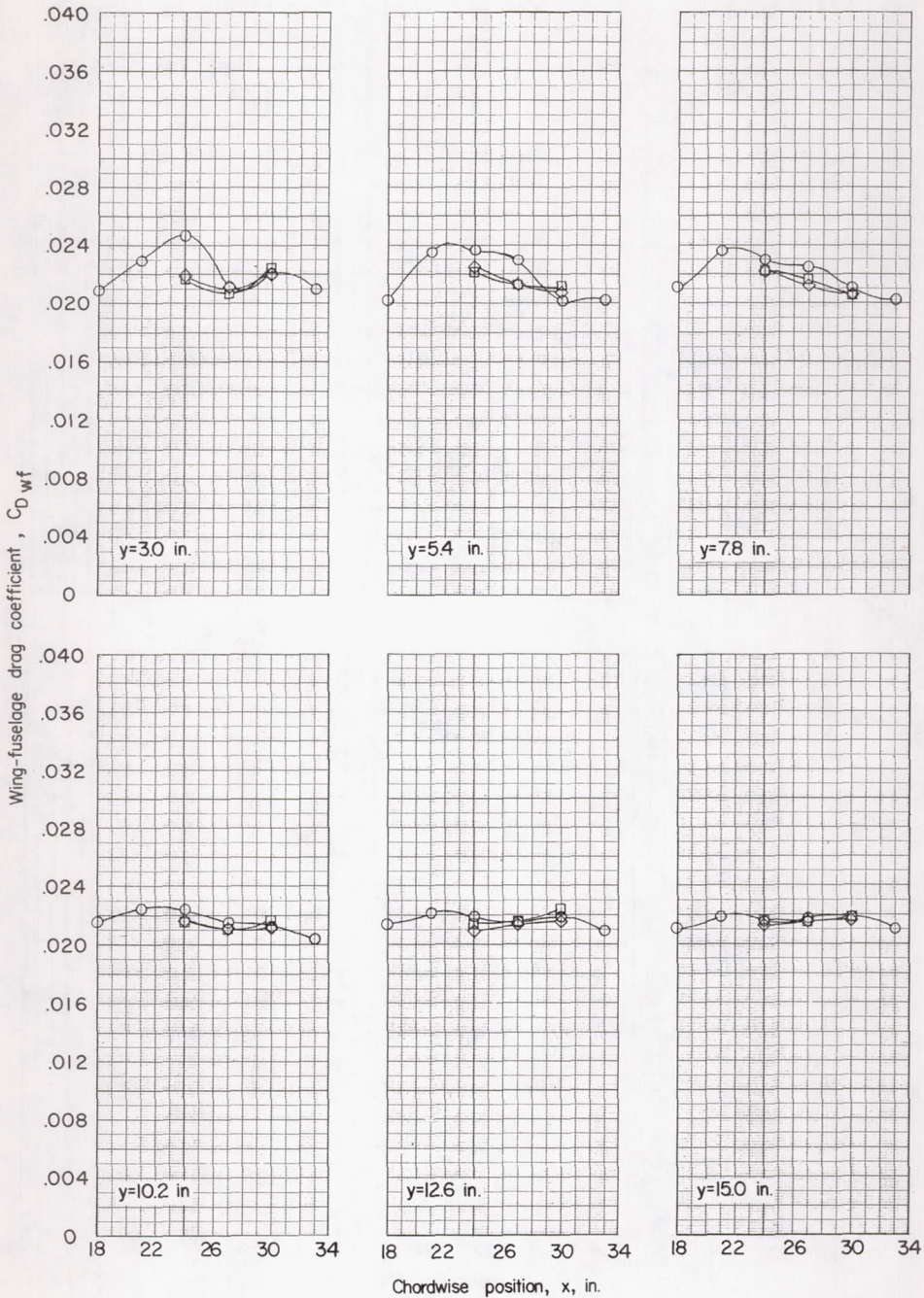
In presence of:
 ○ Large ogive-cylinder store
 □ Small ogive-cylinder store
 ◇ Large parabolic store



(a) $z = 1.15$ inches; $\alpha = 0^\circ$.

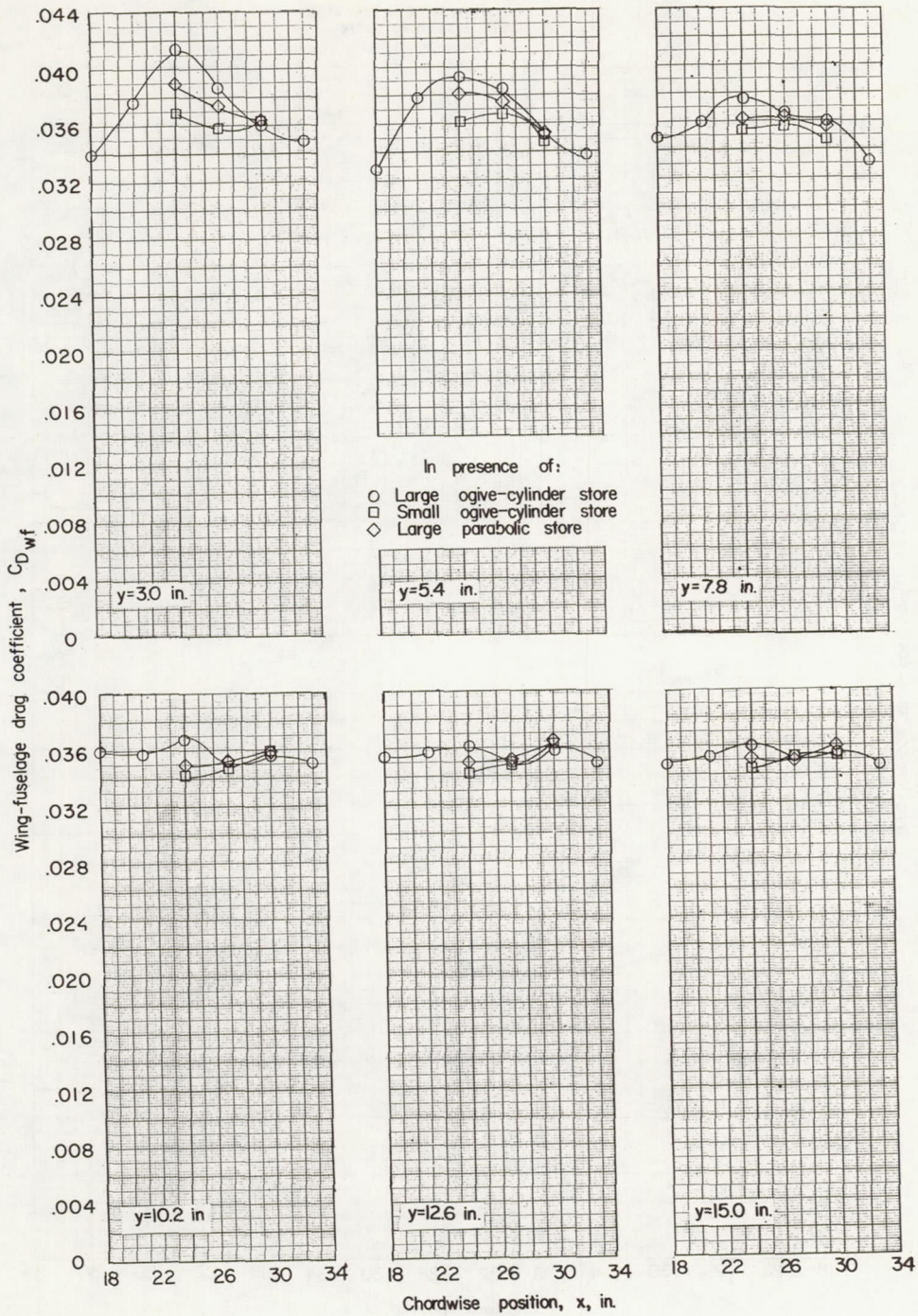
Figure 20.- Drag of wing-fuselage combination in presence of stores of different shapes and sizes. (Drag coefficient of isolated wing-fuselage is 0.0213 at $\alpha = 0^\circ$ and 0.0346 at $\alpha = 4^\circ$. See fig. 6.)

In presence of:
 ○ Large ogive-cylinder store
 □ Small ogive-cylinder store
 ◇ Large parabolic store



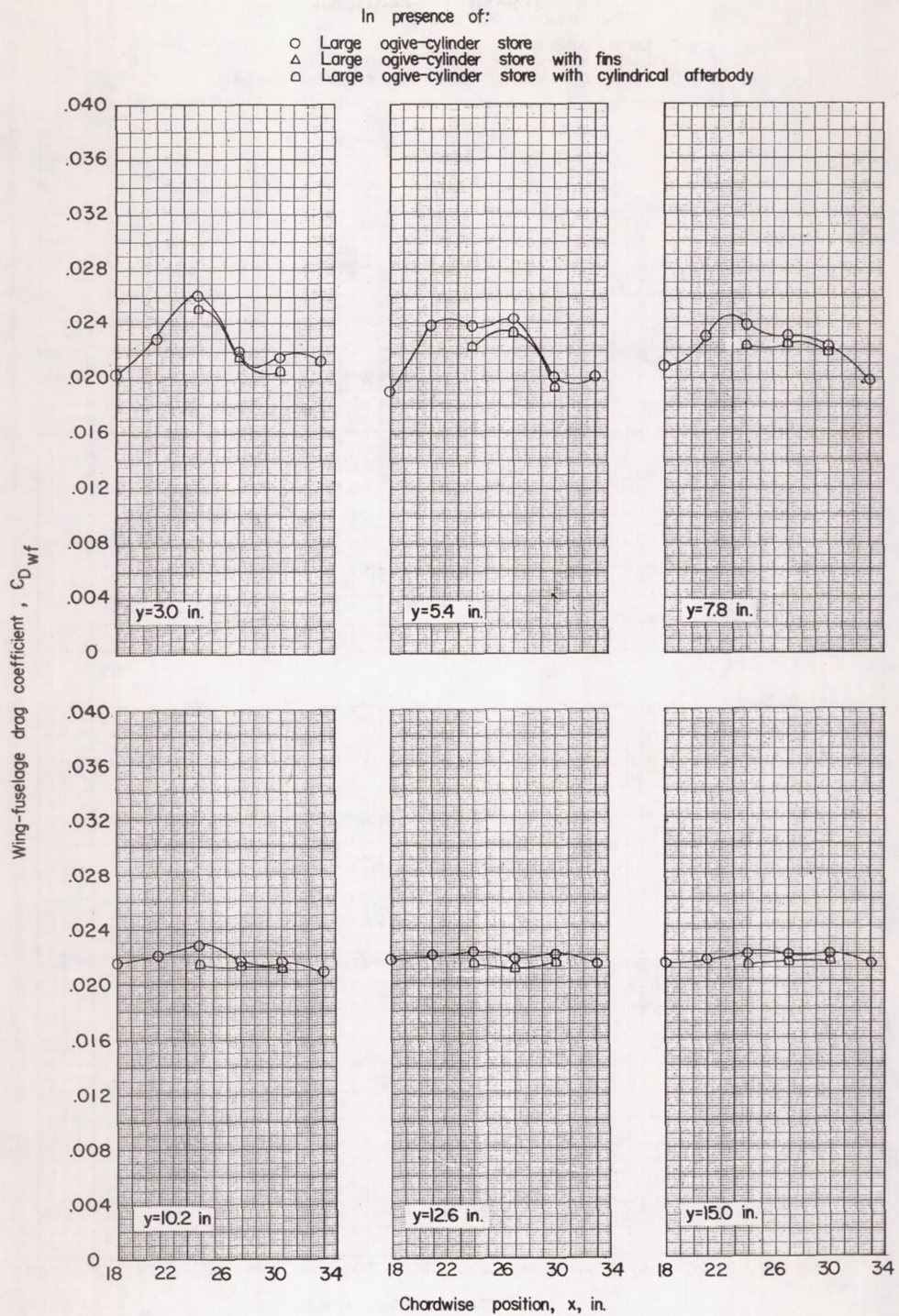
(b) $z = 2.09$ inches; $\alpha = 0^\circ$.

Figure 20.- Continued.



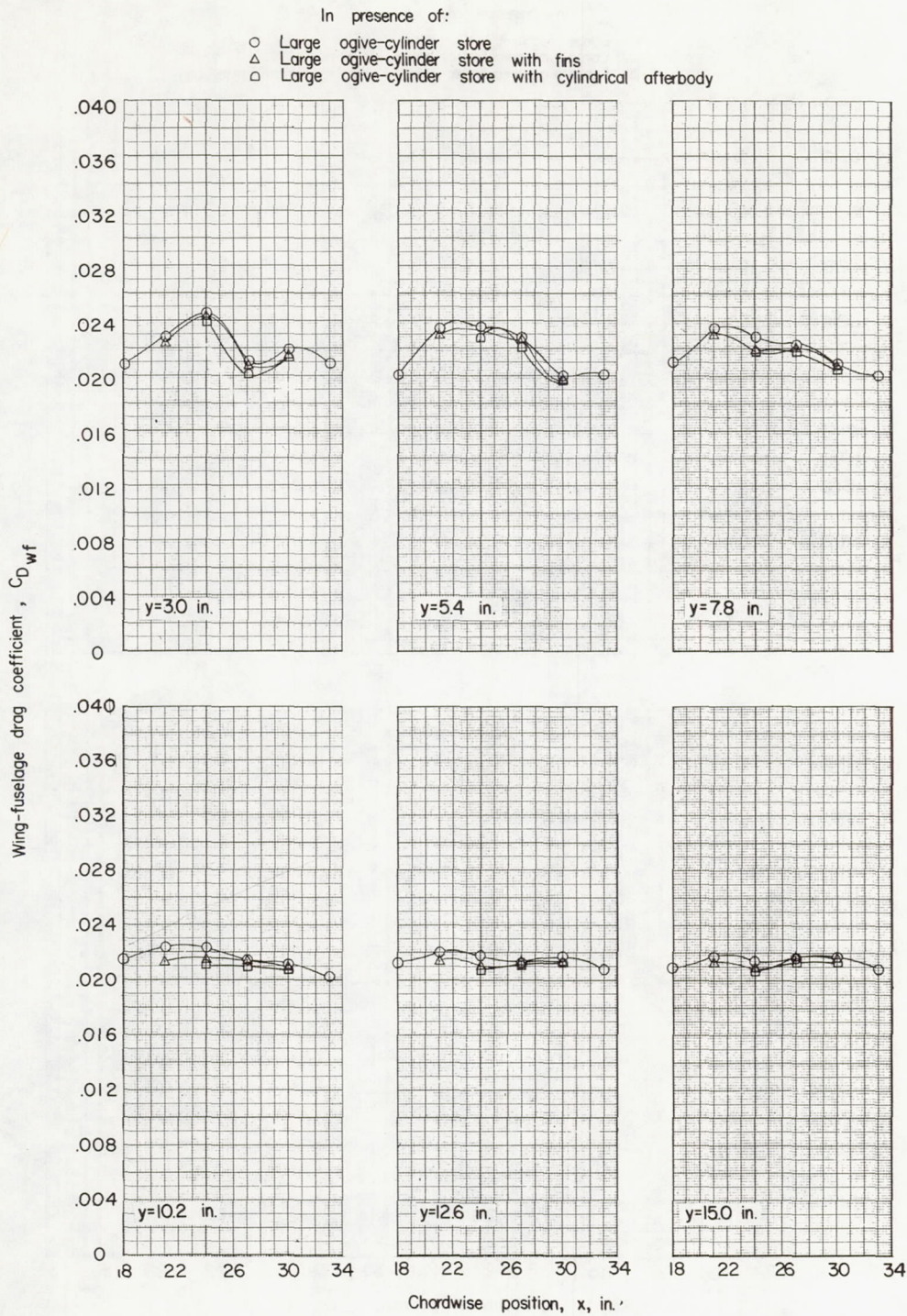
(c) $z = 2.09$ inches; $\alpha = 4^\circ$.

Figure 20.- Concluded.



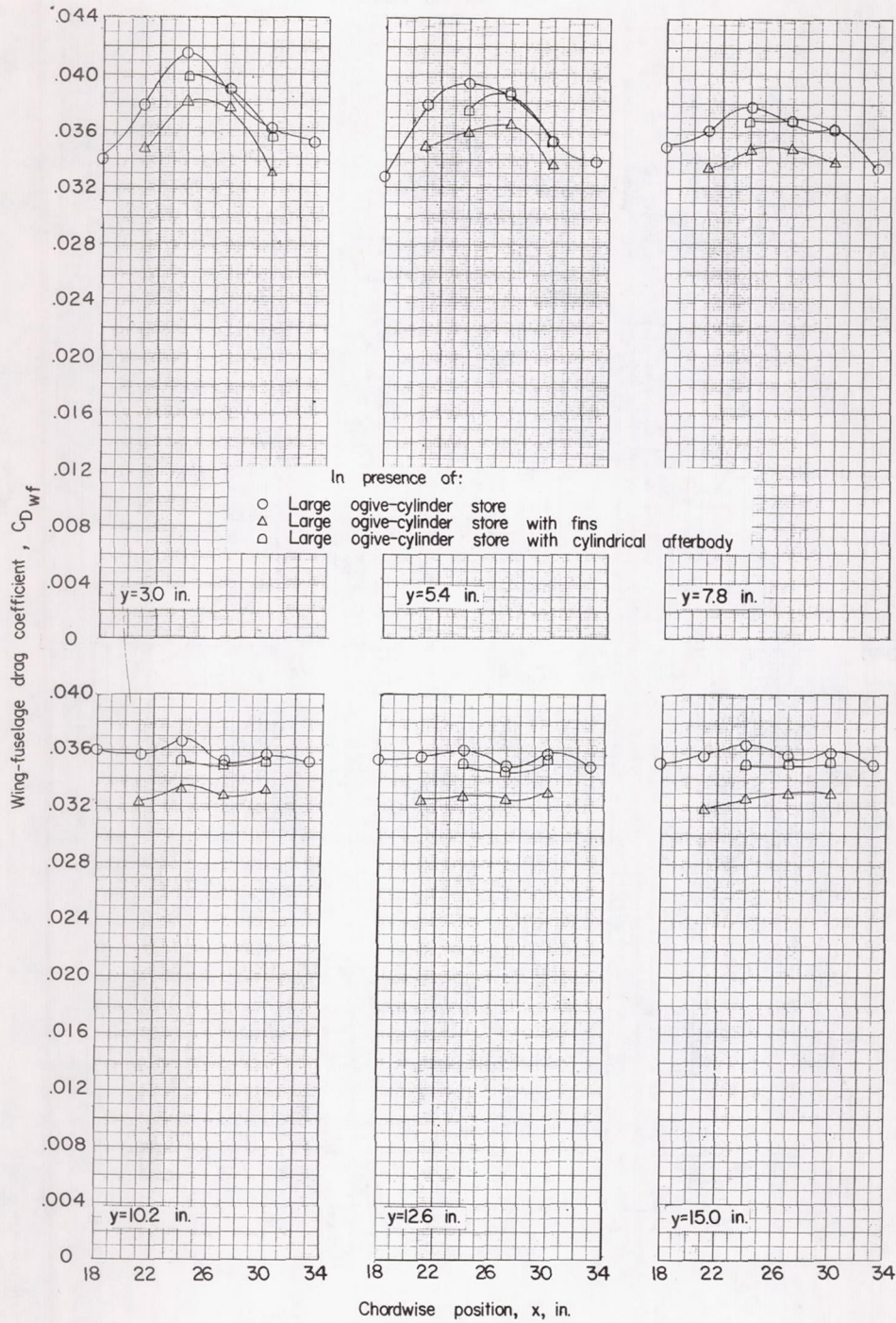
(a) $z = 1.15$ inches; $\alpha = 0^\circ$.

Figure 21.- Drag of wing-fuselage combination in presence of large ogive-cylinder store with various afterbody configurations. (Drag coefficient at isolated wing-fuselage is 0.0213 at $\alpha = 0^\circ$ and 0.0346 at $\alpha = 4^\circ$. See fig. 6.)



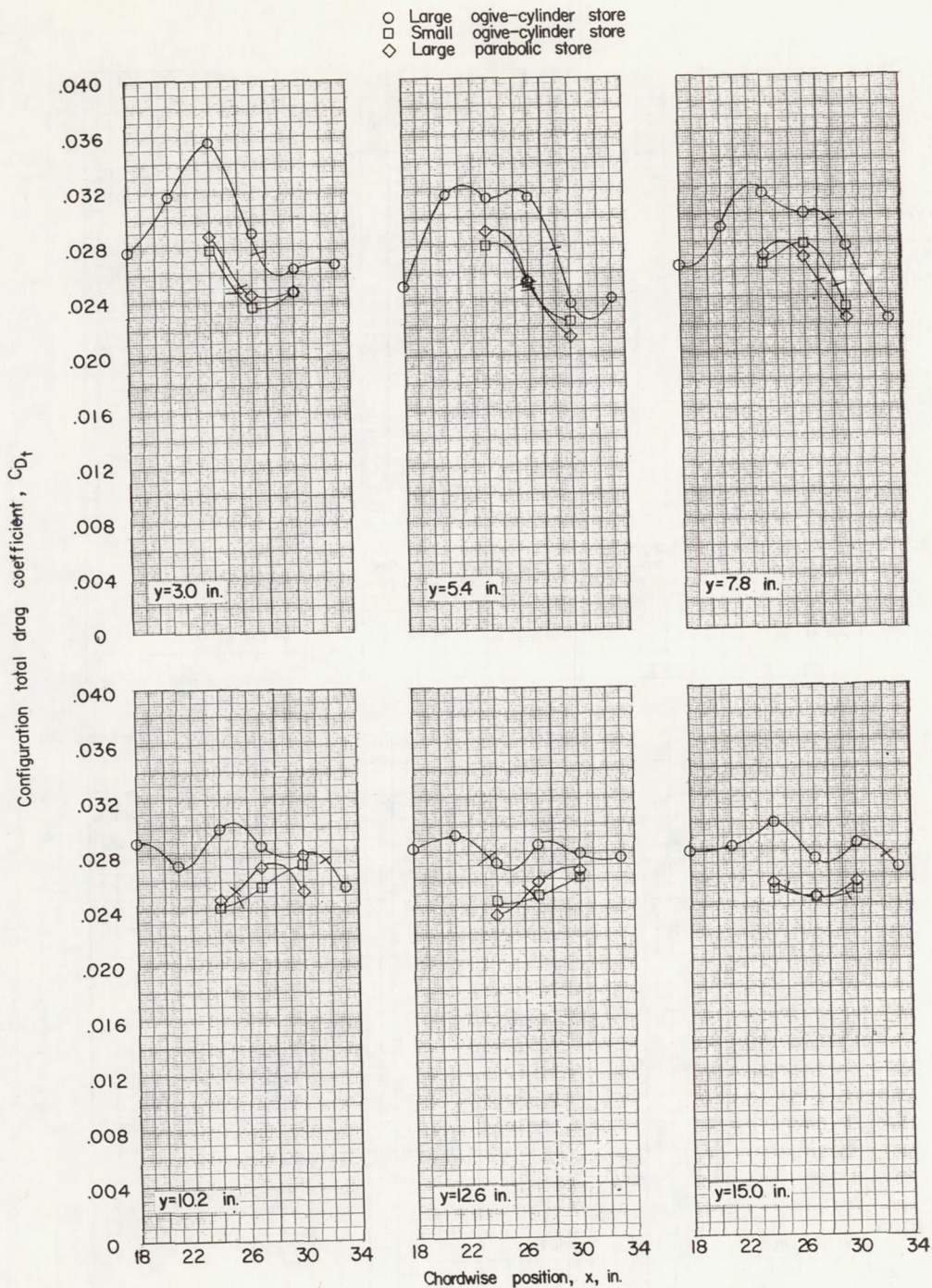
(b) $z = 2.09$ inches; $\alpha = 0^\circ$.

Figure 21.- Continued.



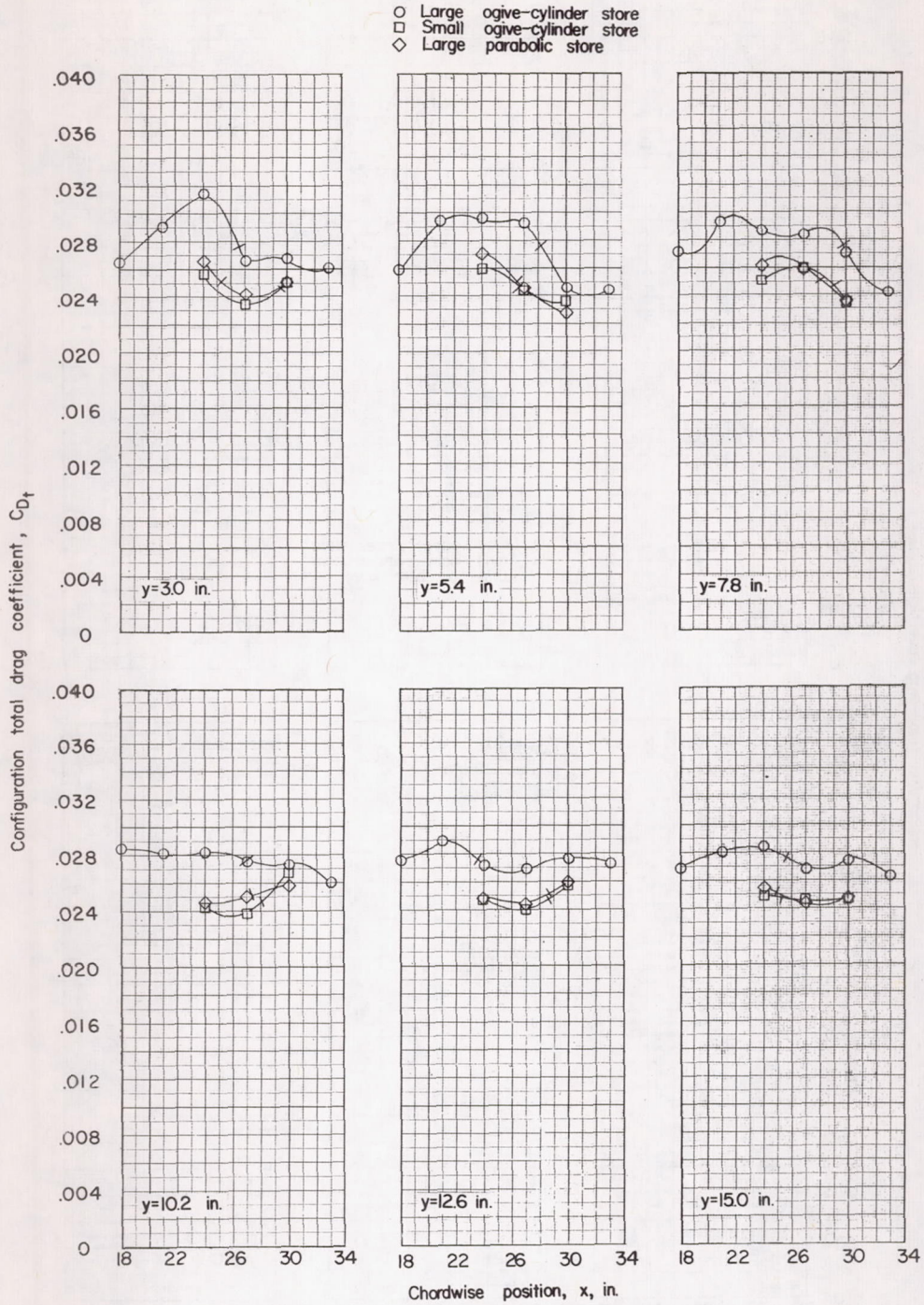
(c) $z = 2.09$ inches; $\alpha = 4^\circ$.

Figure 21.- Concluded.



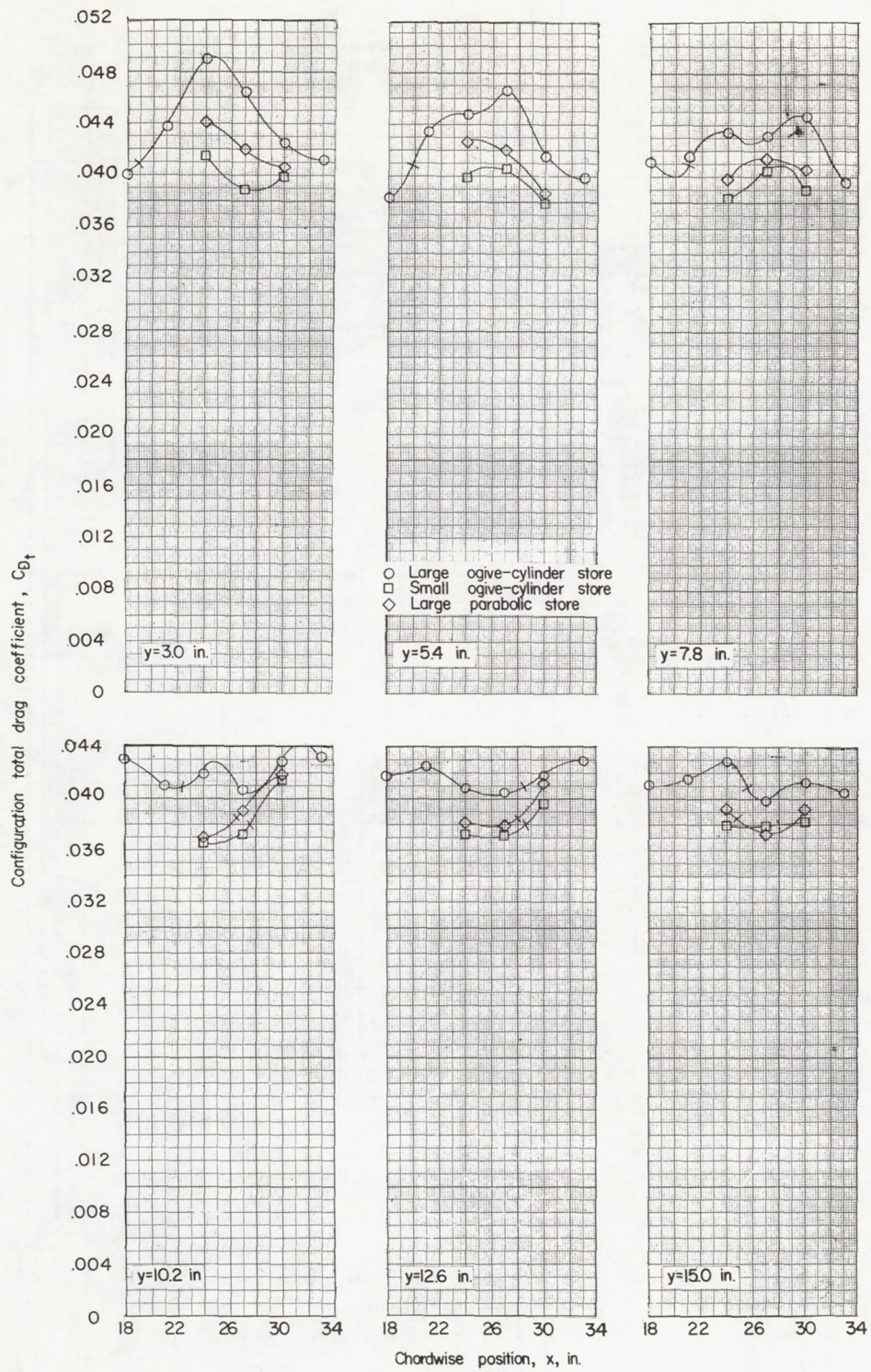
(a) $z = 1.15$ inches; $\alpha = 0^\circ$.

Figure 22.- Total drag of wing-fuselage-store combination in presence of stores of different shapes and sizes. (Tick marks indicate sum of drags of isolated wing-fuselage and isolated store, from figs. 5 and 6.)



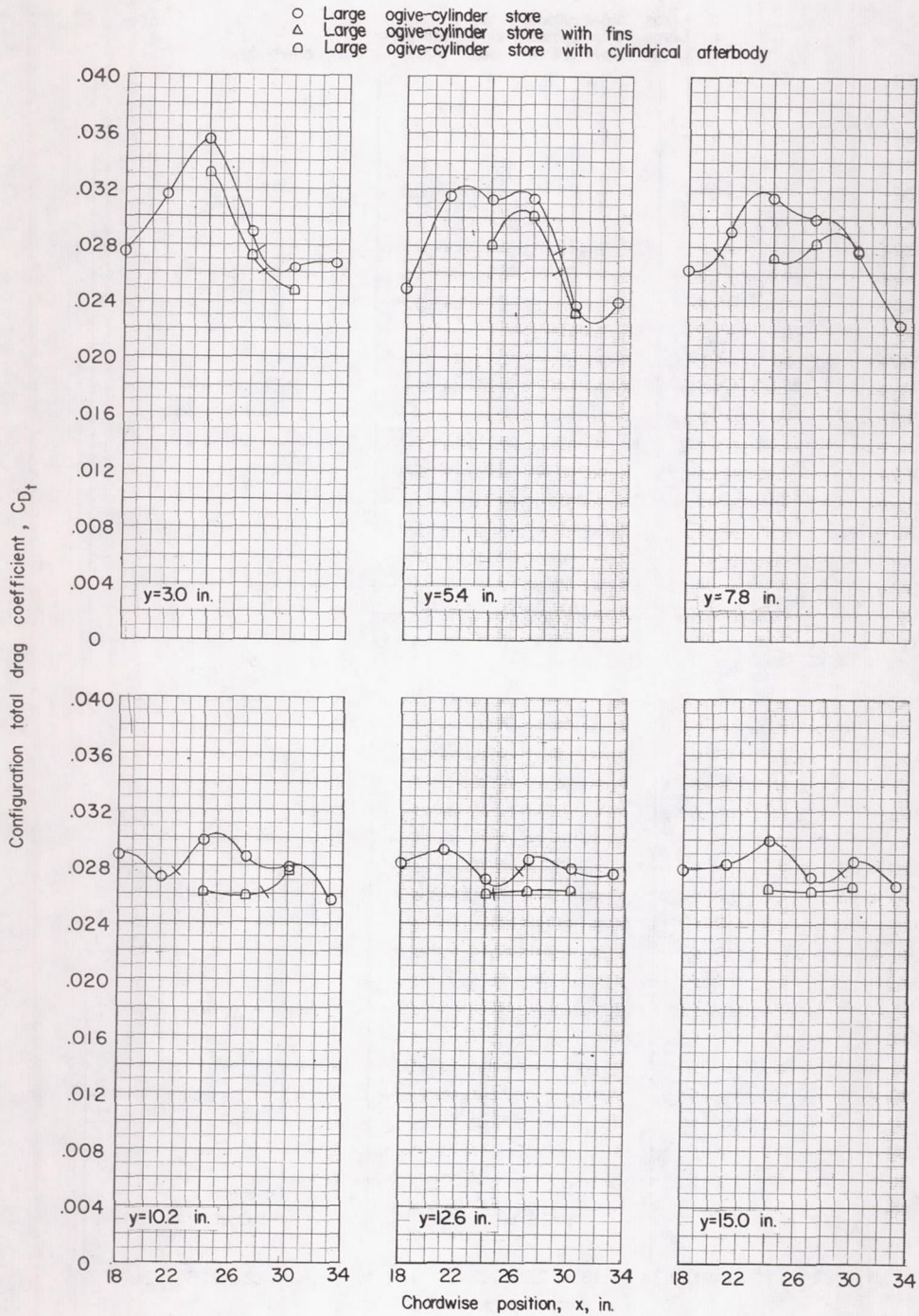
(b) $z = 2.09$ inches; $\alpha = 0^\circ$.

Figure 22.- Continued.



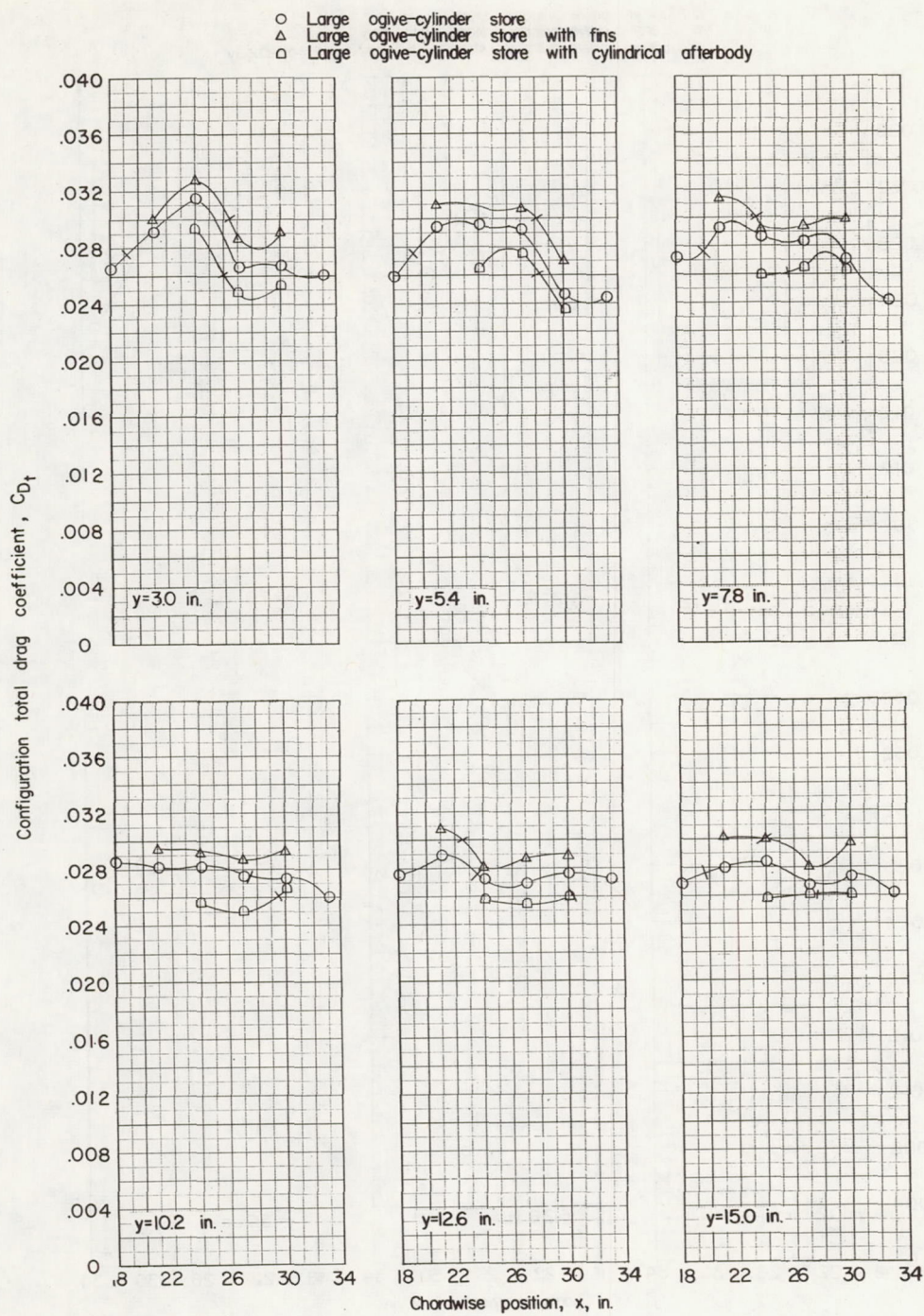
(c) $z = 2.09$ inches; $\alpha = 4^\circ$.

Figure 22.- Concluded.



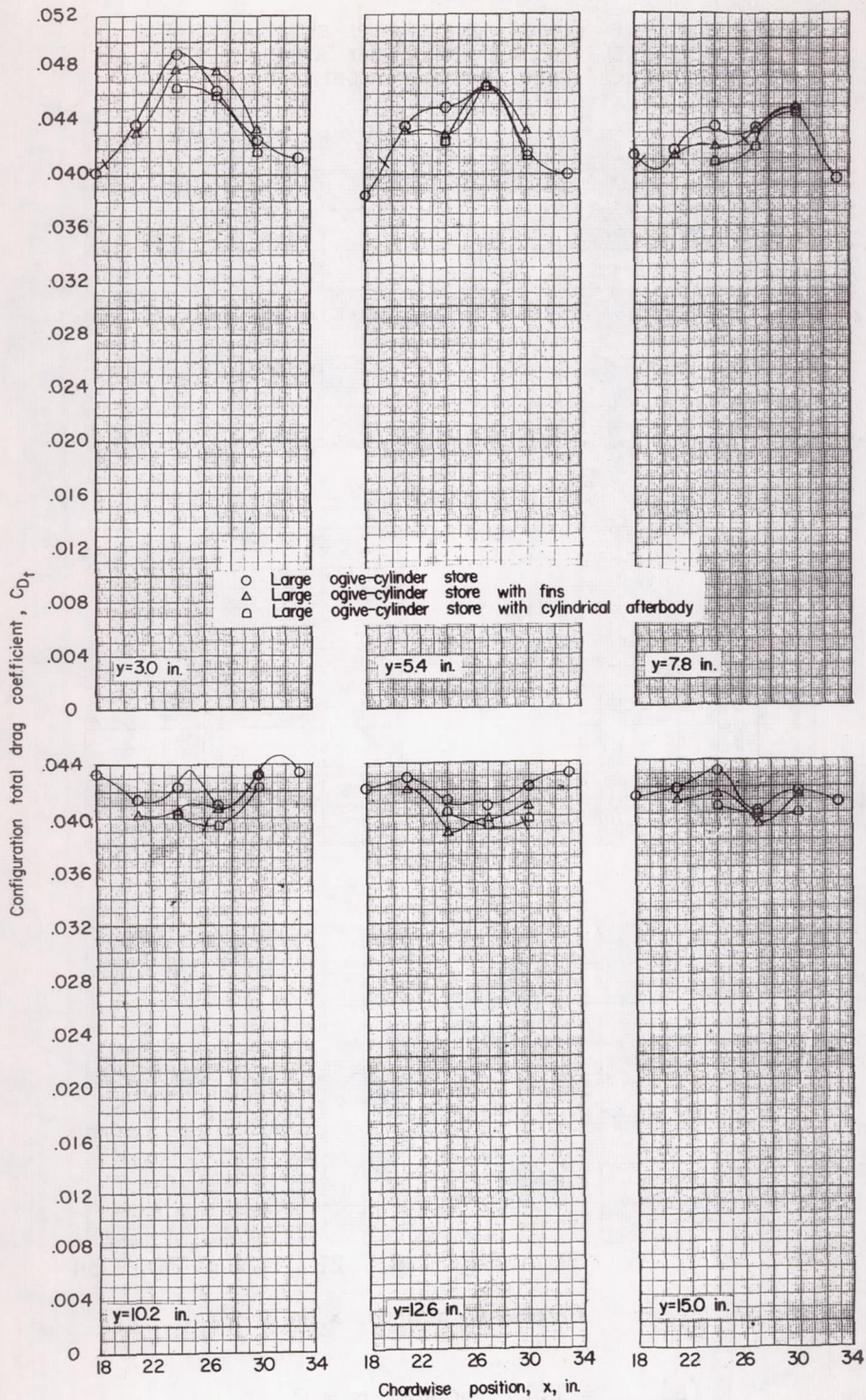
(a) $z = 1.15$ inches; $\alpha = 0^\circ$.

Figure 23.- Total drag of wing-fuselage-store combination in presence of large ogive-cylinder store with various afterbody configurations. (Tick marks indicate sum of drags of isolated wing fuselage and isolated store, from figs. 5 and 6.)



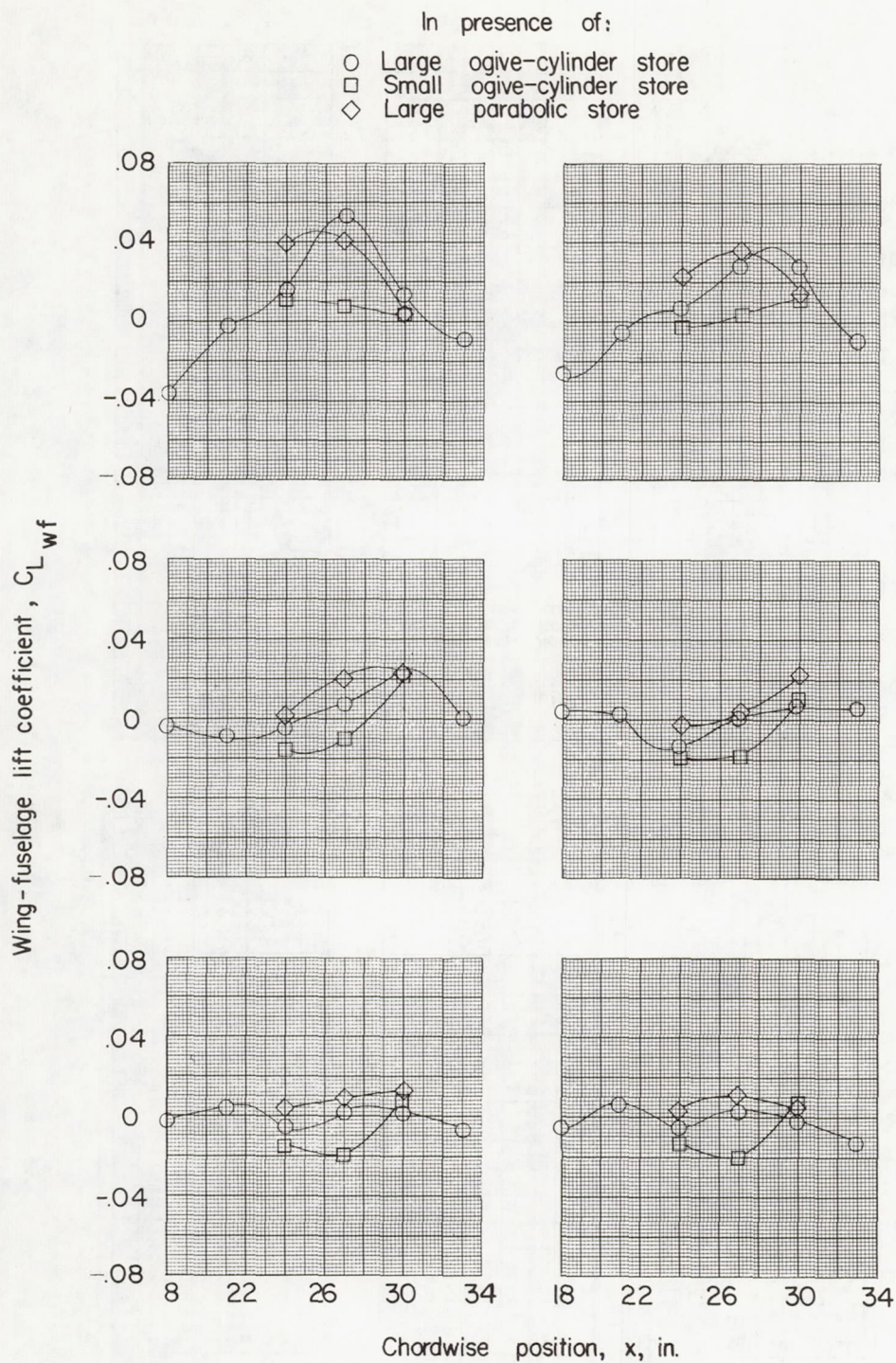
(b) $z = 2.09$ inches; $\alpha = 0^\circ$.

Figure 23.- Continued.



(c) $z = 2.09$ inches; $\alpha = 4^\circ$.

Figure 23.- Concluded.

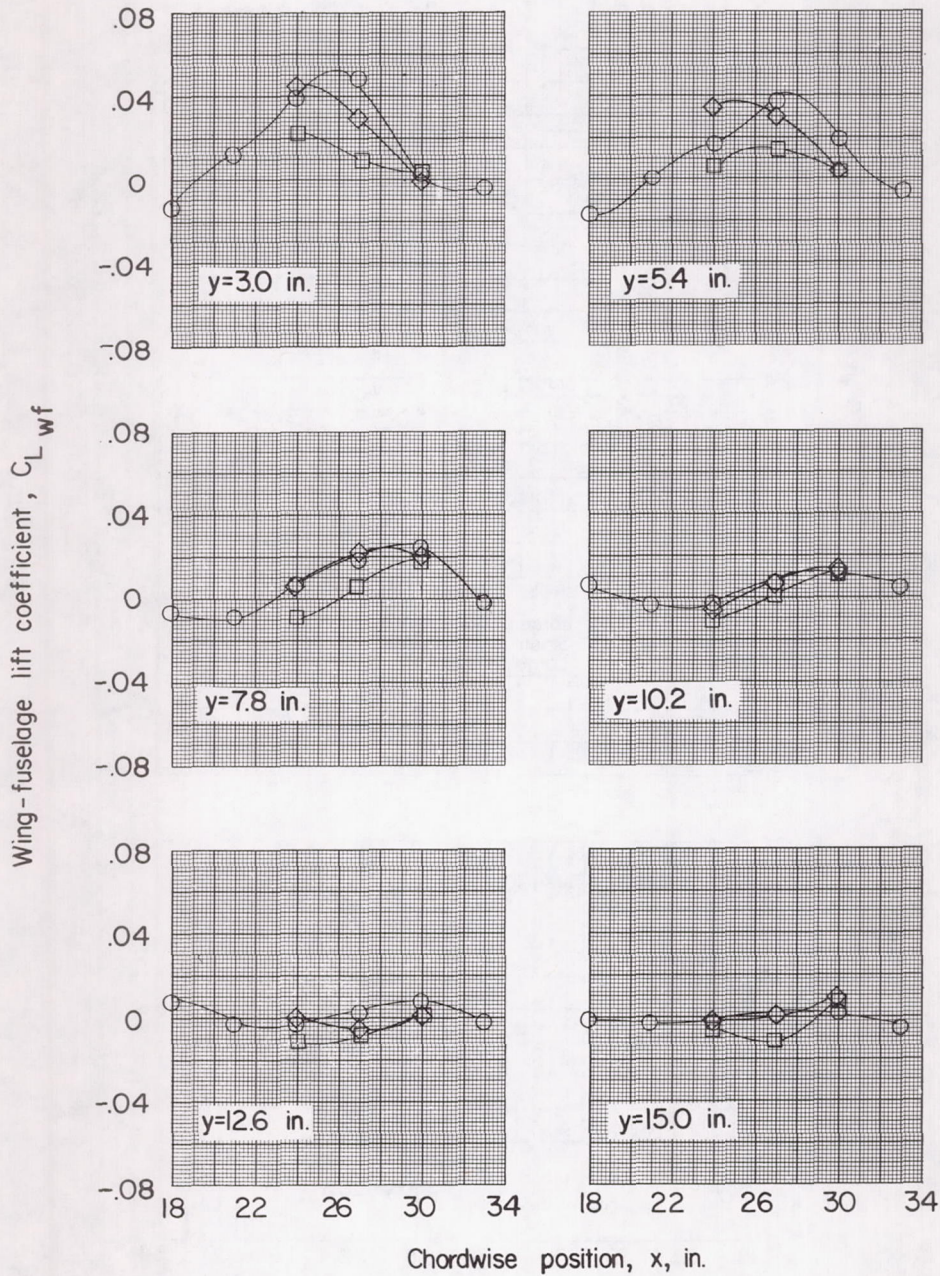


(a) $z = 1.15$ inches; $\alpha = 0^\circ$.

Figure 24.- Lift of wing-fuselage combination in presence of stores of different shapes and sizes.

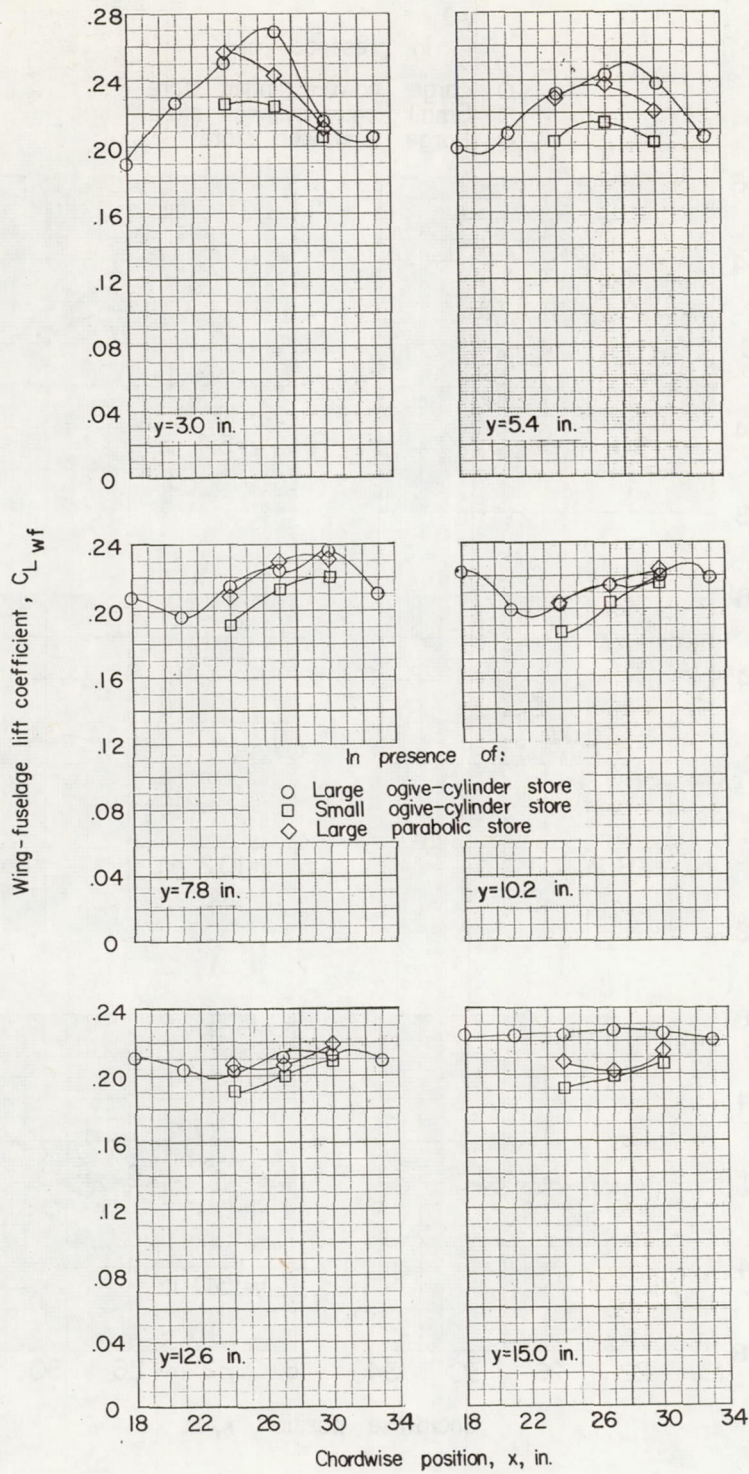
In presence of:

- Large ogive-cylinder store
- Small ogive-cylinder store
- ◇ Large parabolic store



(b) $z = 2.09$ inches; $\alpha = 0^\circ$.

Figure 24.- Continued.

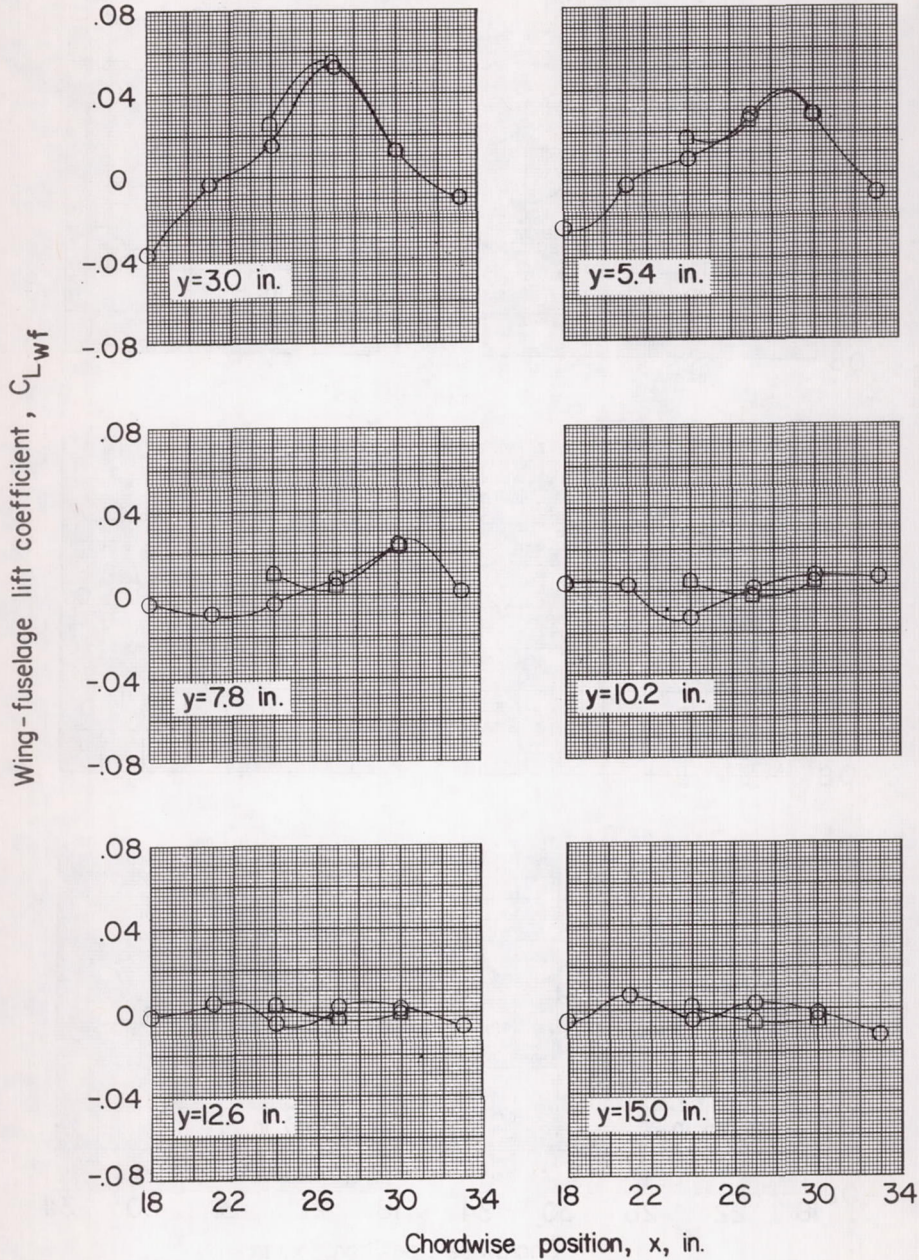


(c) $z = 2.09$ inches; $\alpha = 4^\circ$.

Figure 24.- Concluded.

In presence of:

- Large ogive-cylinder store
- △ Large ogive-cylinder store with fins
- ◻ Large ogive-cylinder store with cylindrical afterbody

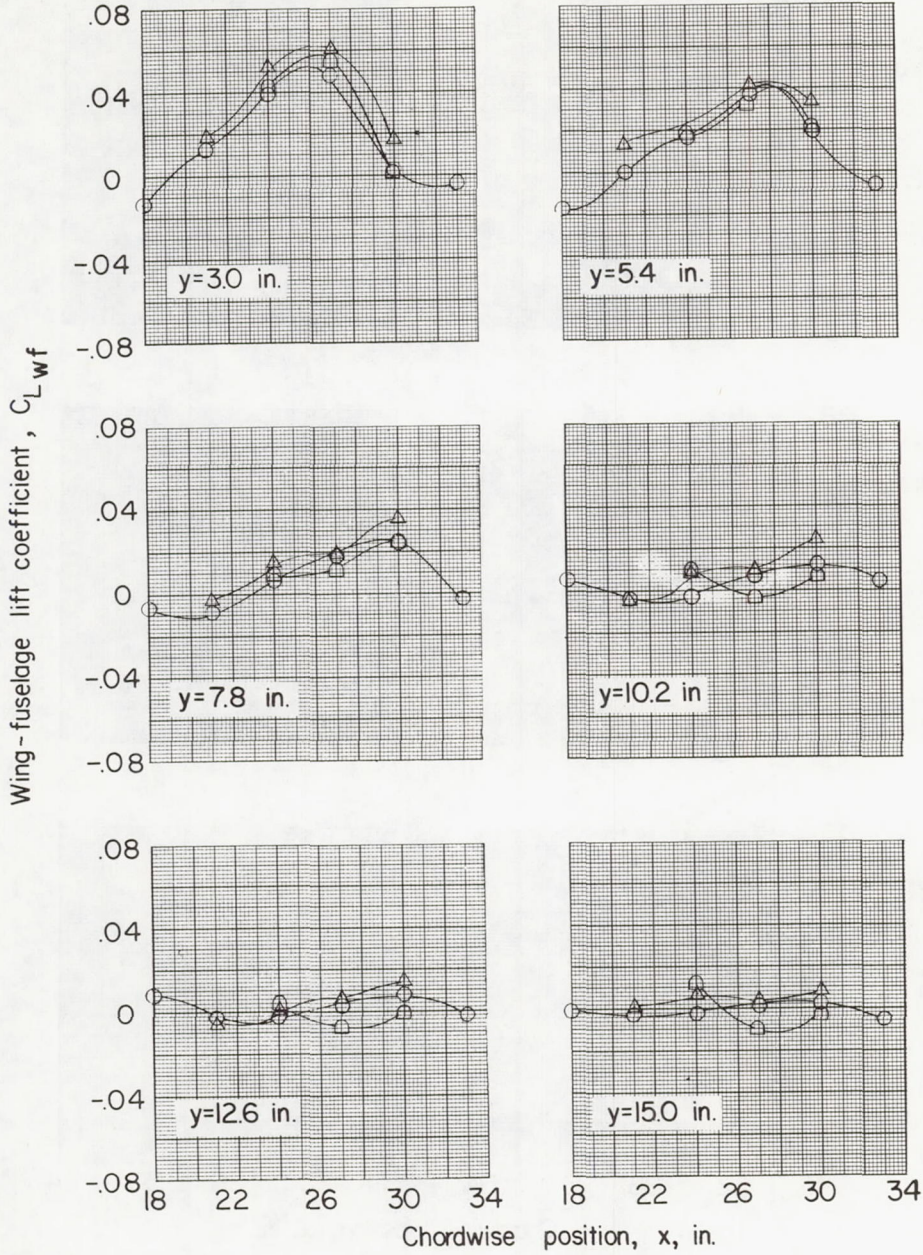


(a) $z = 1.15$ inches; $\alpha = 0^\circ$.

Figure 25.- Lift of wing-fuselage combination in presence of large ogive-cylinder store with various afterbody configurations.

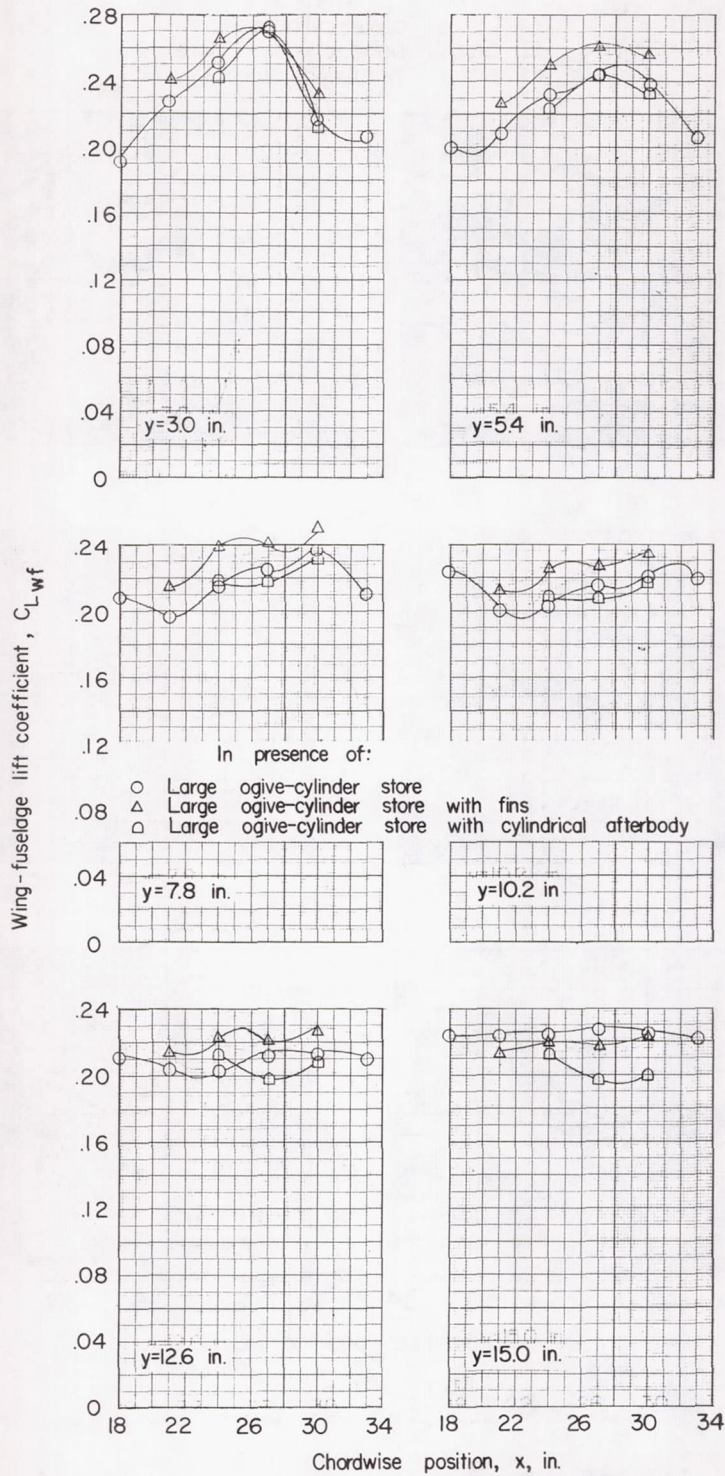
In presence of:

- Large ogive-cylinder store
- △ Large ogive-cylinder store with fins
- ◻ Large ogive-cylinder store with cylindrical afterbody



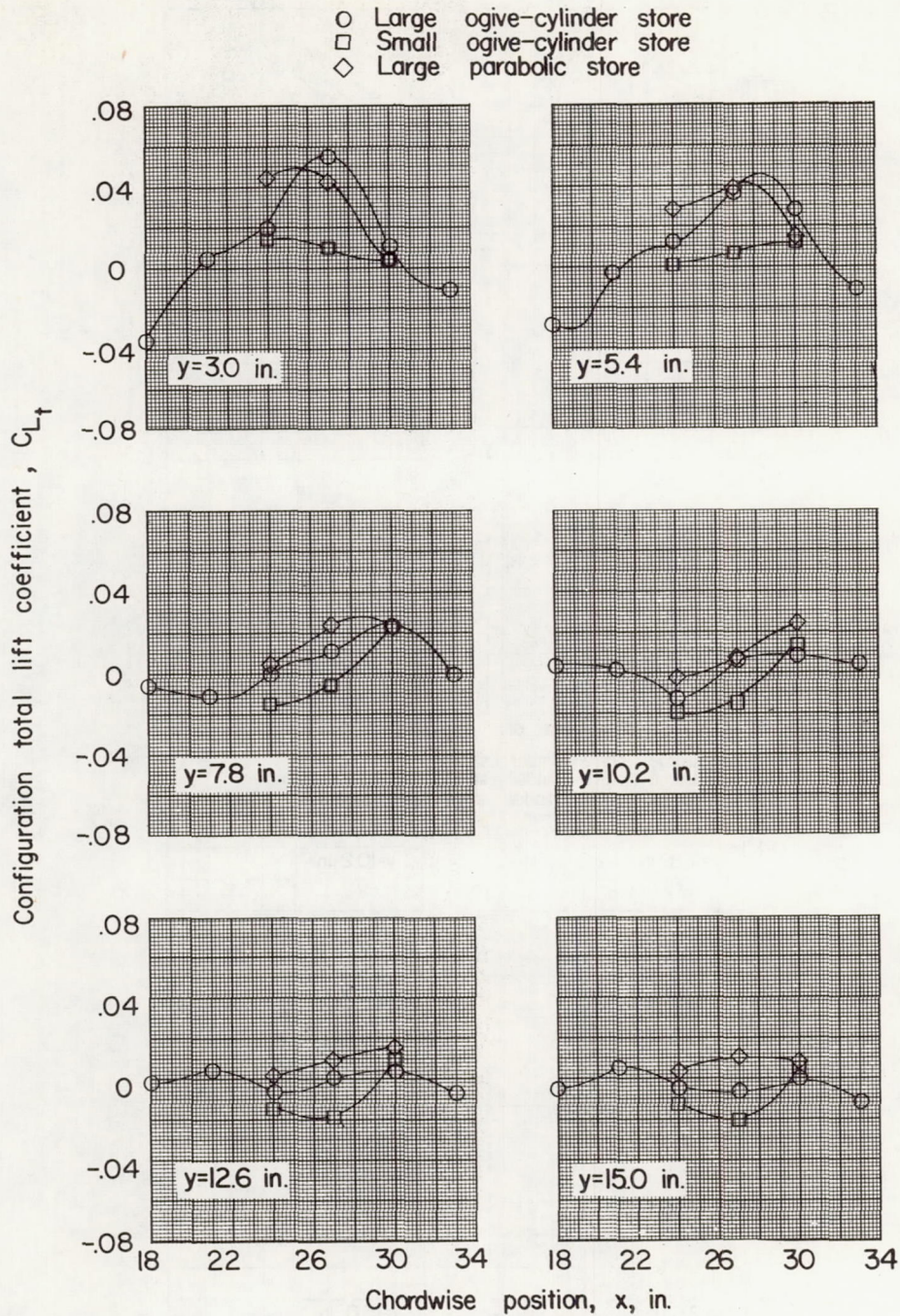
(b) $z = 2.09$ inches; $\alpha = 0^\circ$.

Figure 25.- Continued.



(c) $z = 2.09$ inches; $\alpha = 4^\circ$.

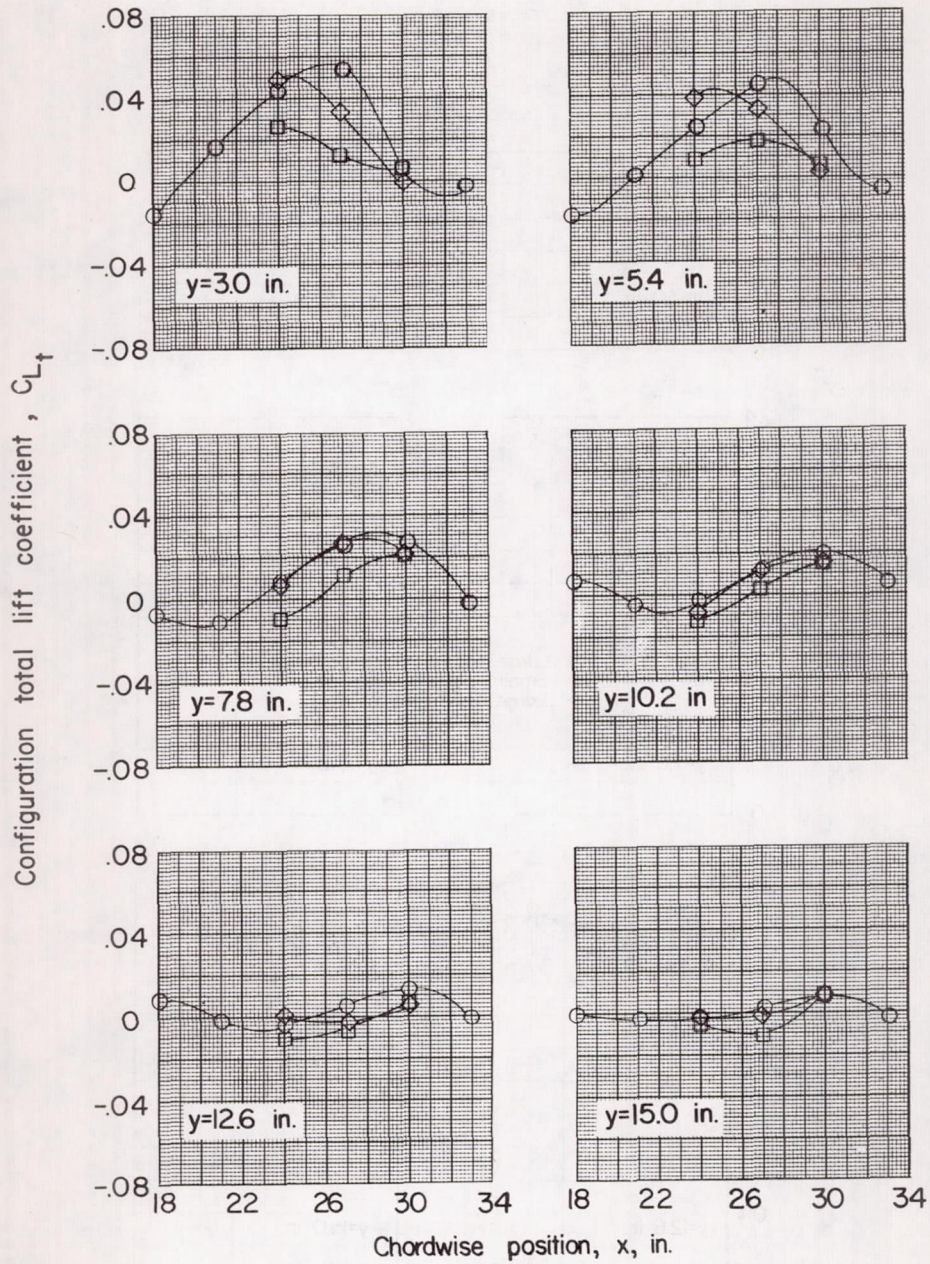
Figure 25.- Concluded.



(a) $z = 1.15$ inches; $\alpha = 0^\circ$.

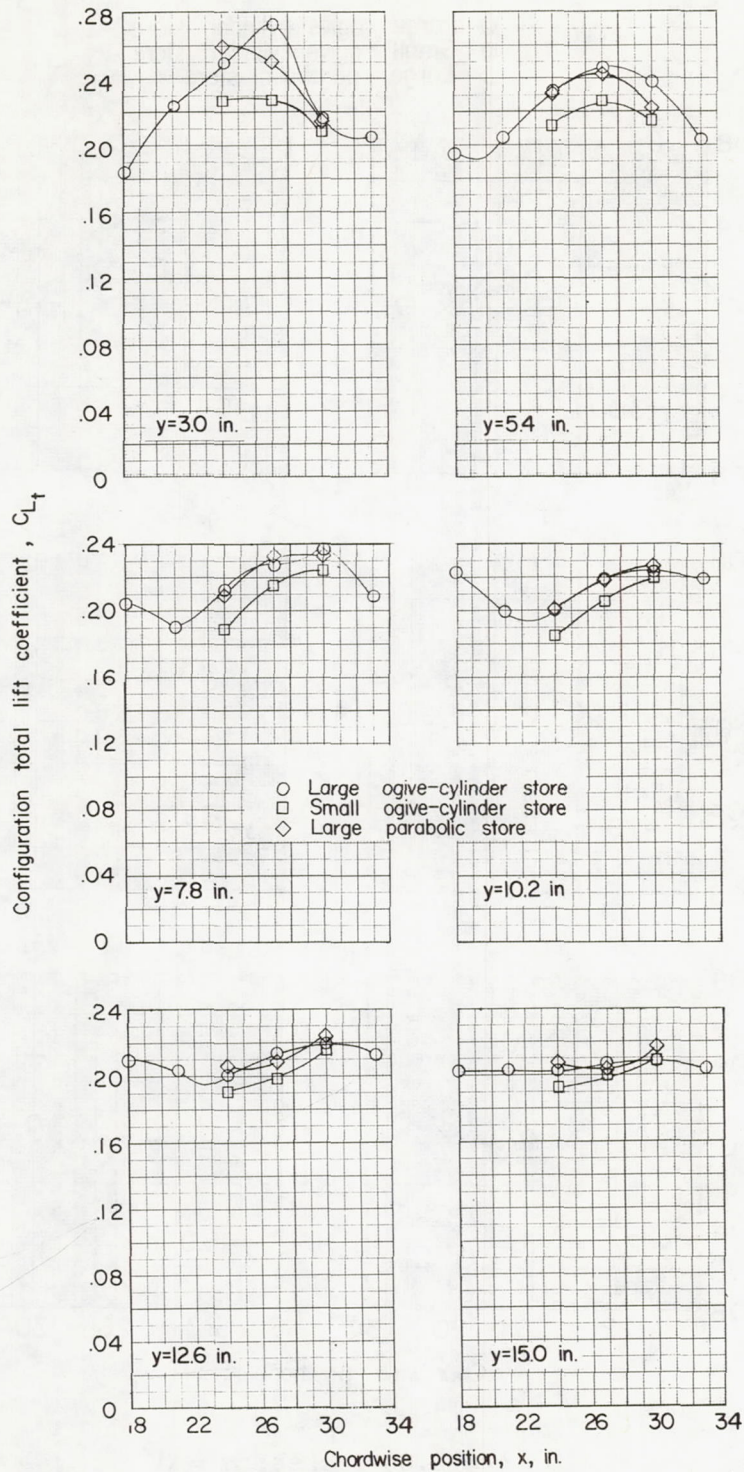
Figure 26.- Total lift of wing-fuselage-store combination in presence of stores of different shapes and sizes.

- Large ogive-cylinder store
- Small ogive-cylinder store
- ◇ Large parabolic store



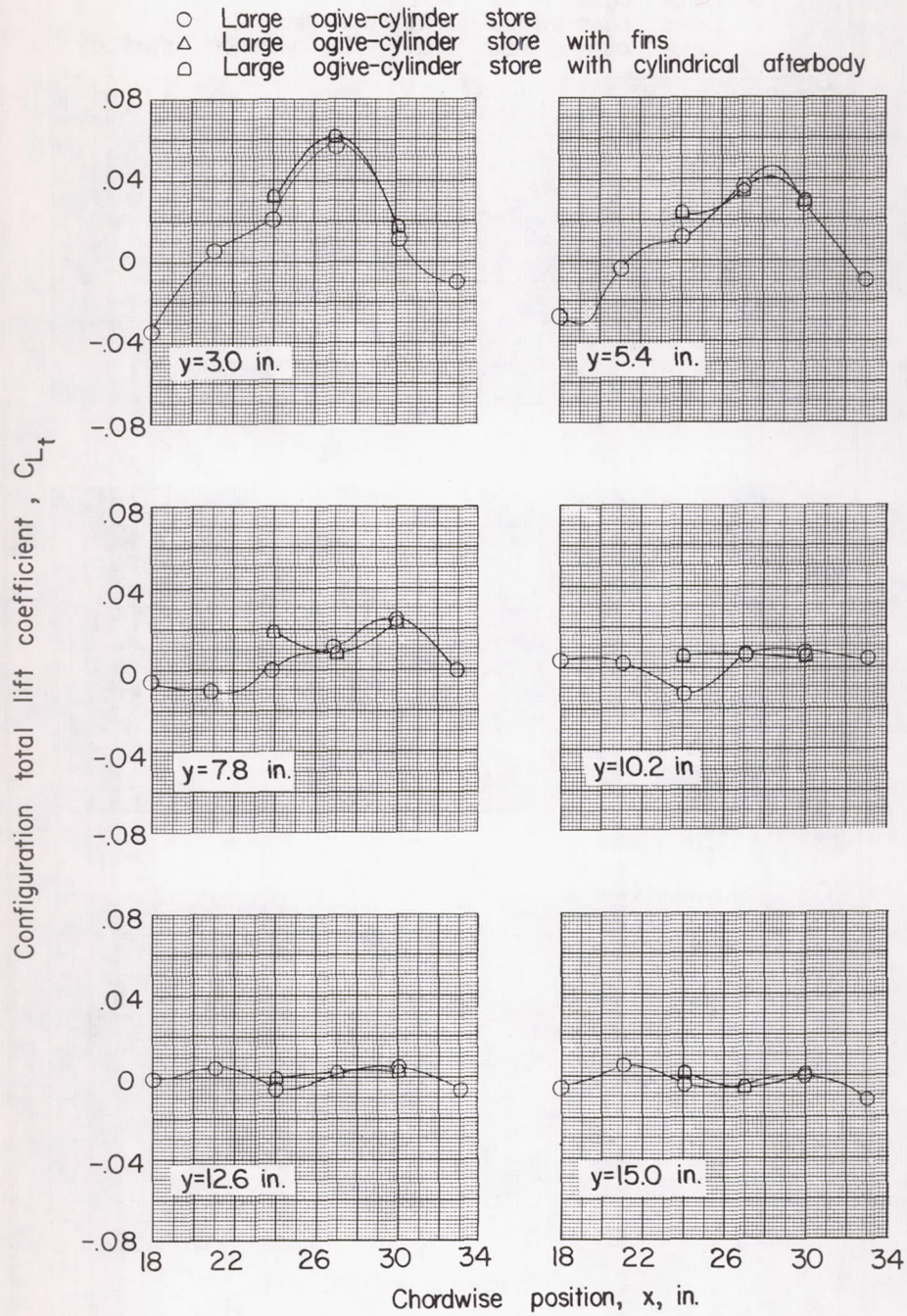
(b) $z = 2.09$ inches; $\alpha = 0^\circ$.

Figure 26.- Continued.



(c) $z = 2.09$ inches; $\alpha = 4^\circ$.

Figure 26.- Concluded.



(a) $z = 1.15$ inches; $\alpha = 0^\circ$.

Figure 27.- Total lift of wing-fuselage-store combination in presence of large ogive-cylinder store with various afterbody configurations.

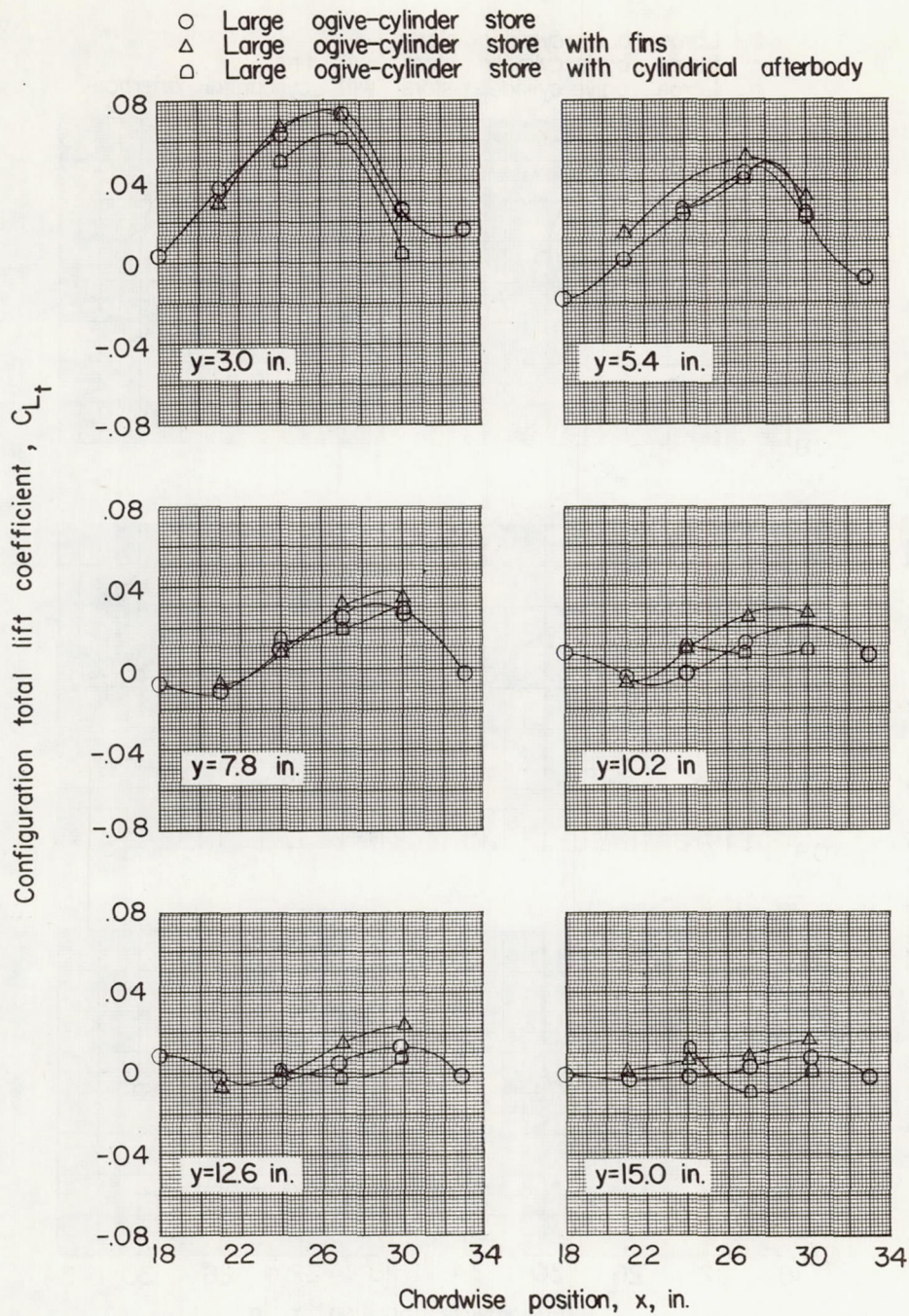
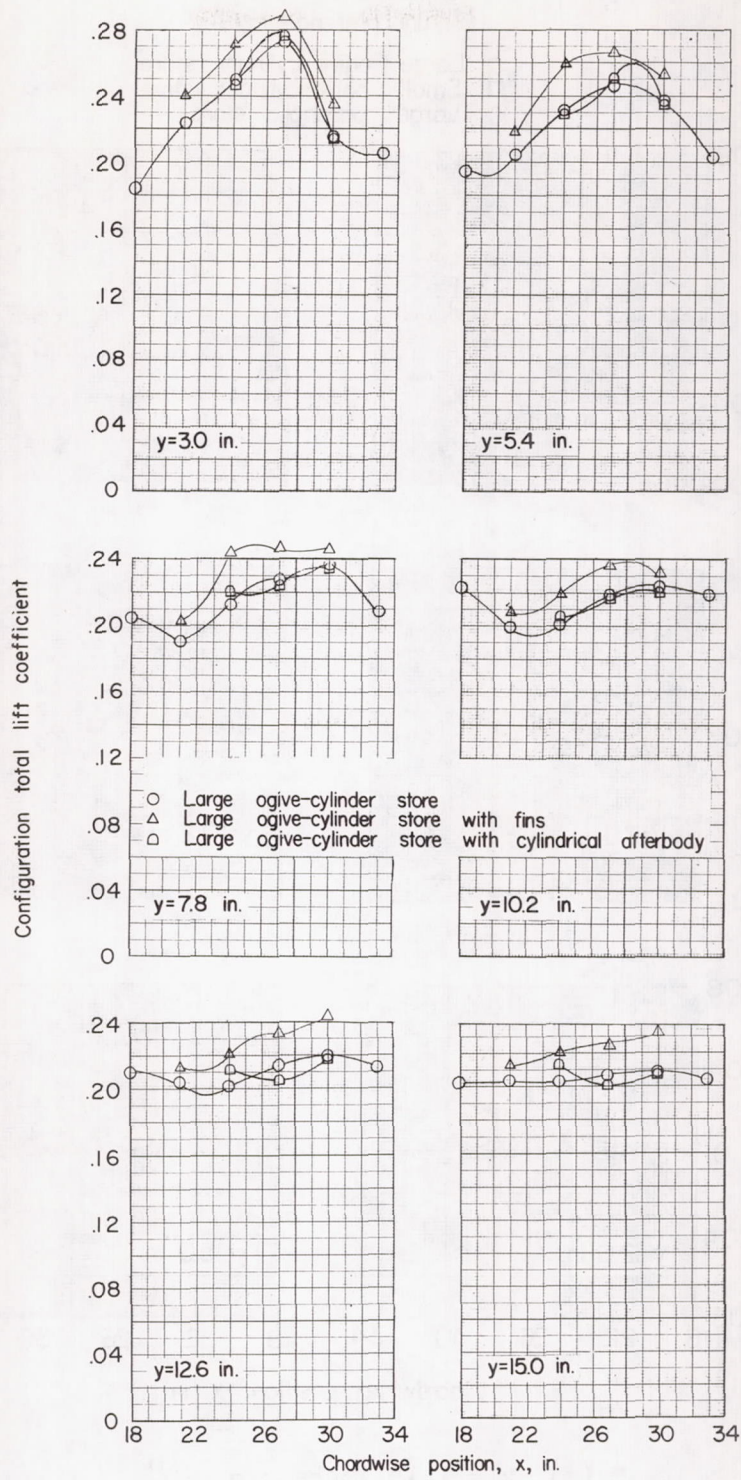
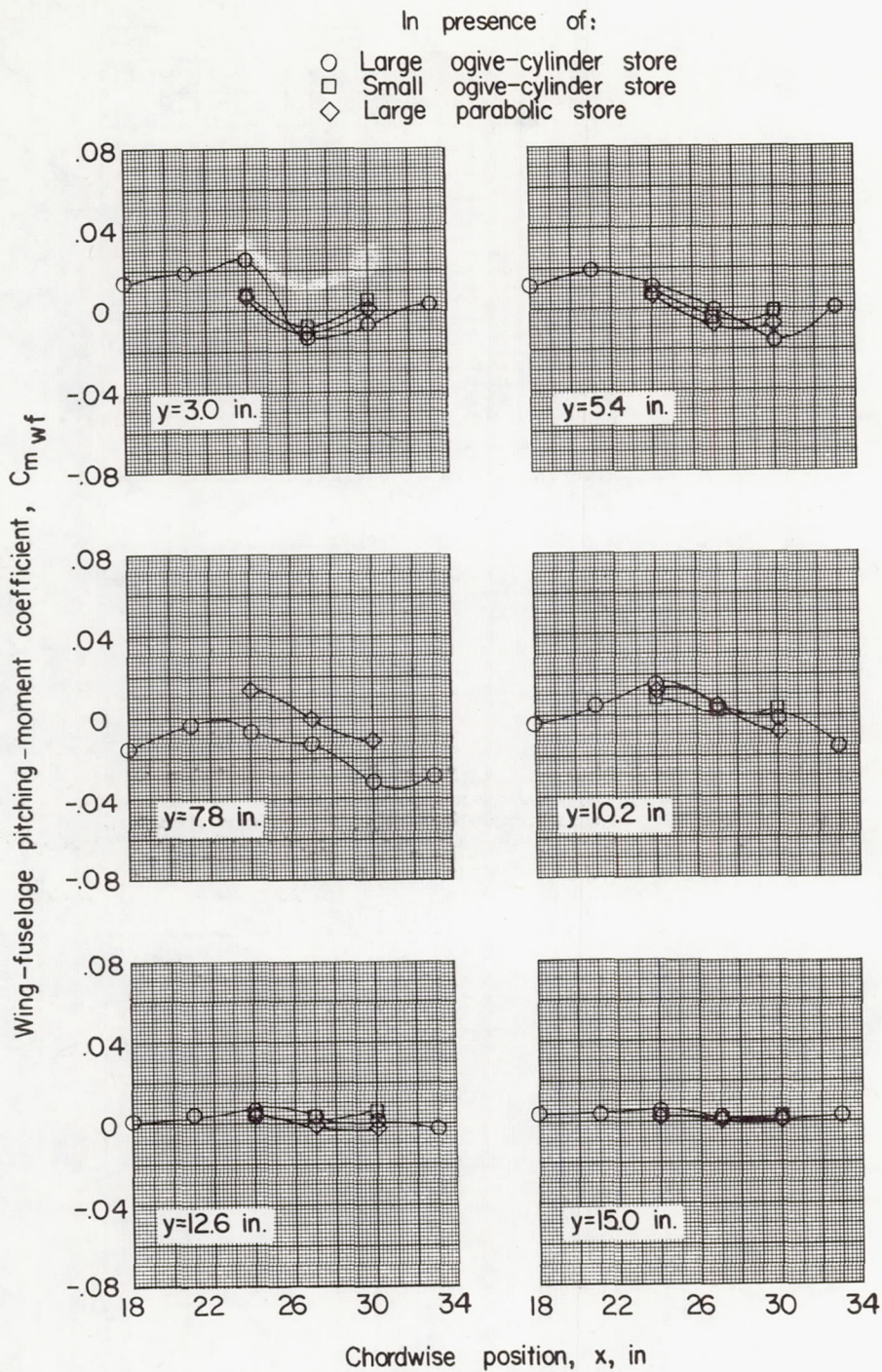


Figure 27.- Continued.



(c) $z = 2.09$ inches; $\alpha = 4^\circ$.

Figure 27.- Concluded.

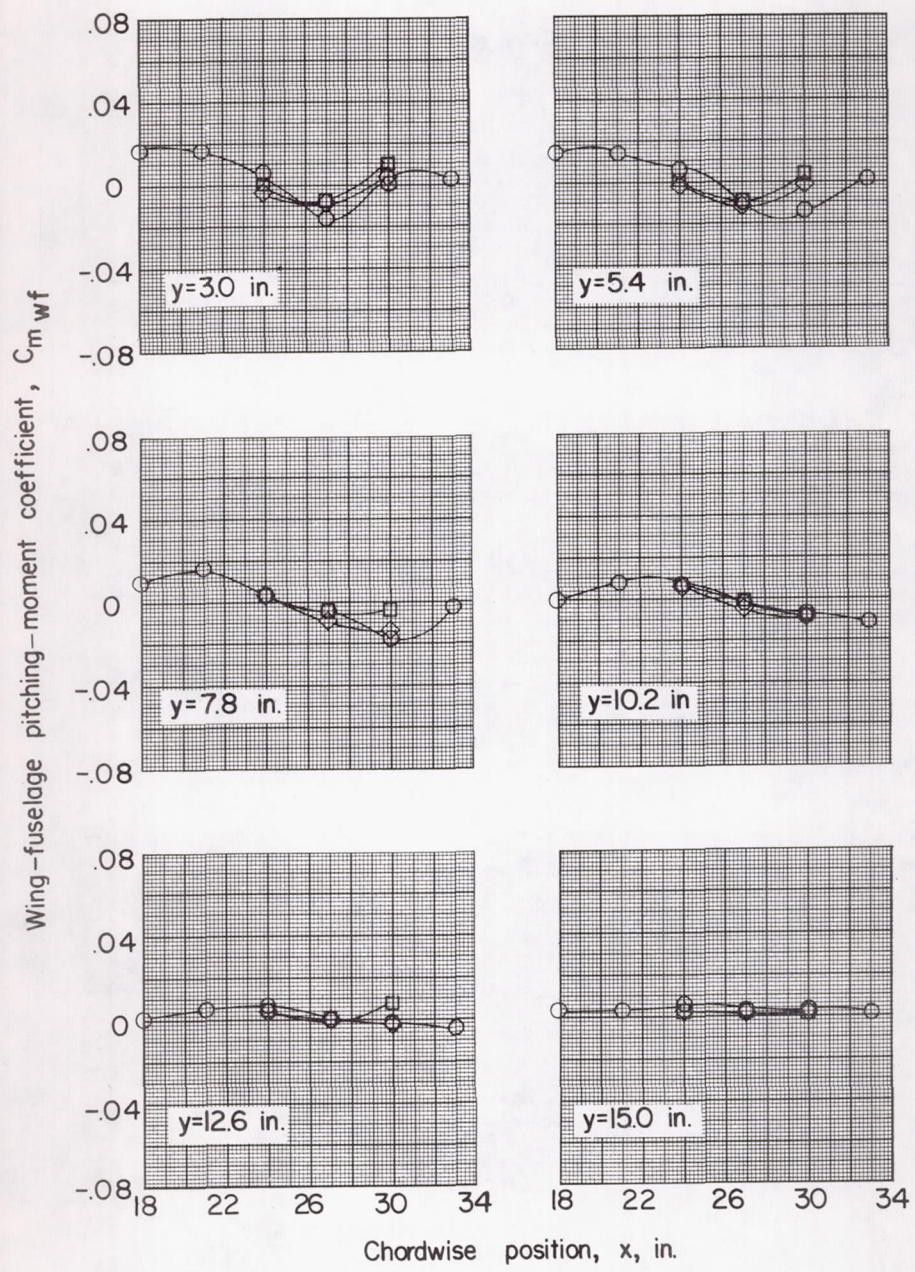


(a) $z = 1.15$ inches; $\alpha = 0^\circ$.

Figure 28.- Pitching moment of wing-fuselage combination in presence of stores of different shapes and sizes. (Center of moments is $\frac{\bar{c}}{4}$ of wing.)

In presence of:

- Large ogive-cylinder store
- Small ogive-cylinder store
- ◇ Large parabolic store

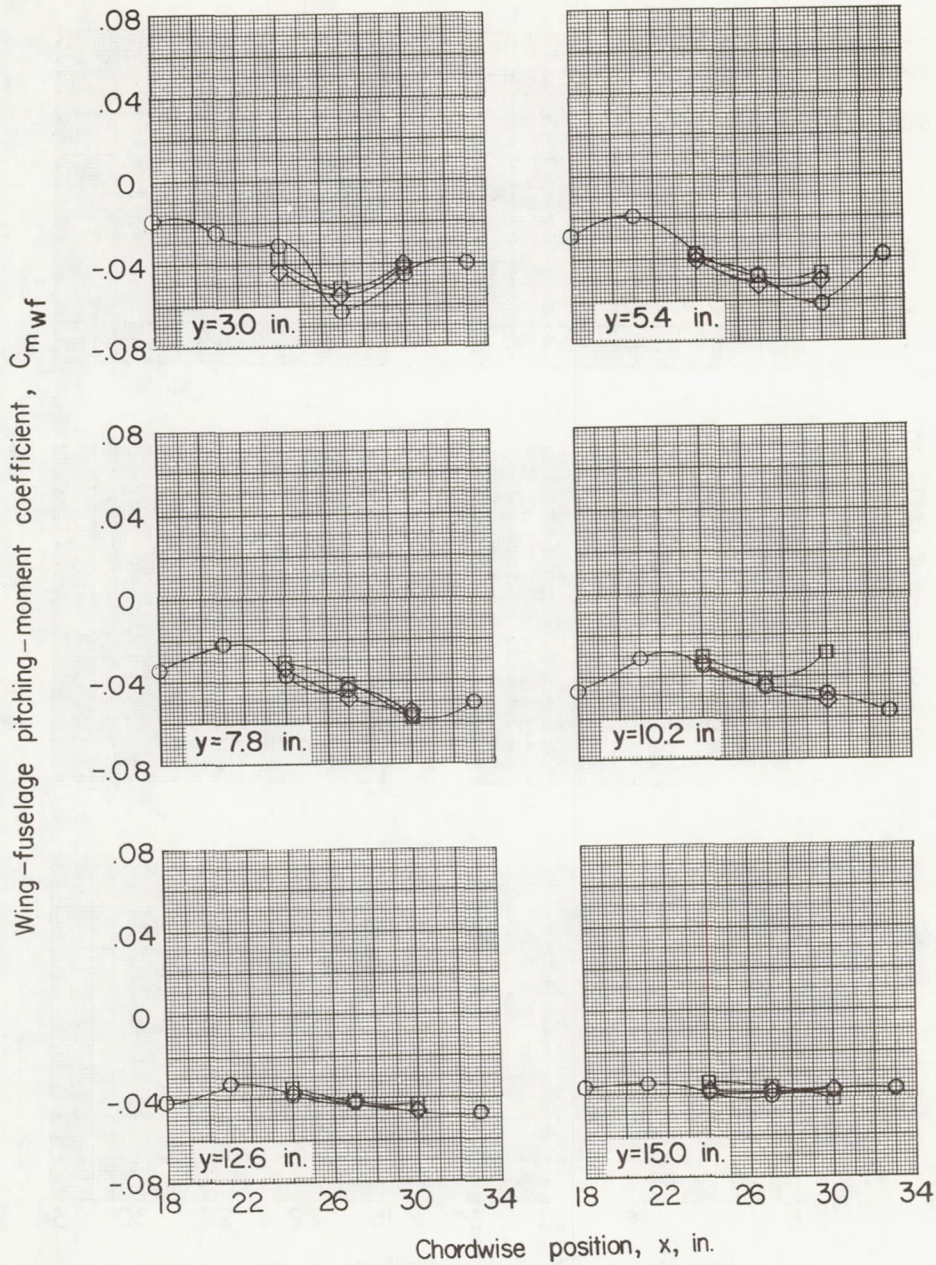


(b) $z = 2.09$ inches; $\alpha = 0^\circ$.

Figure 28.- Continued.

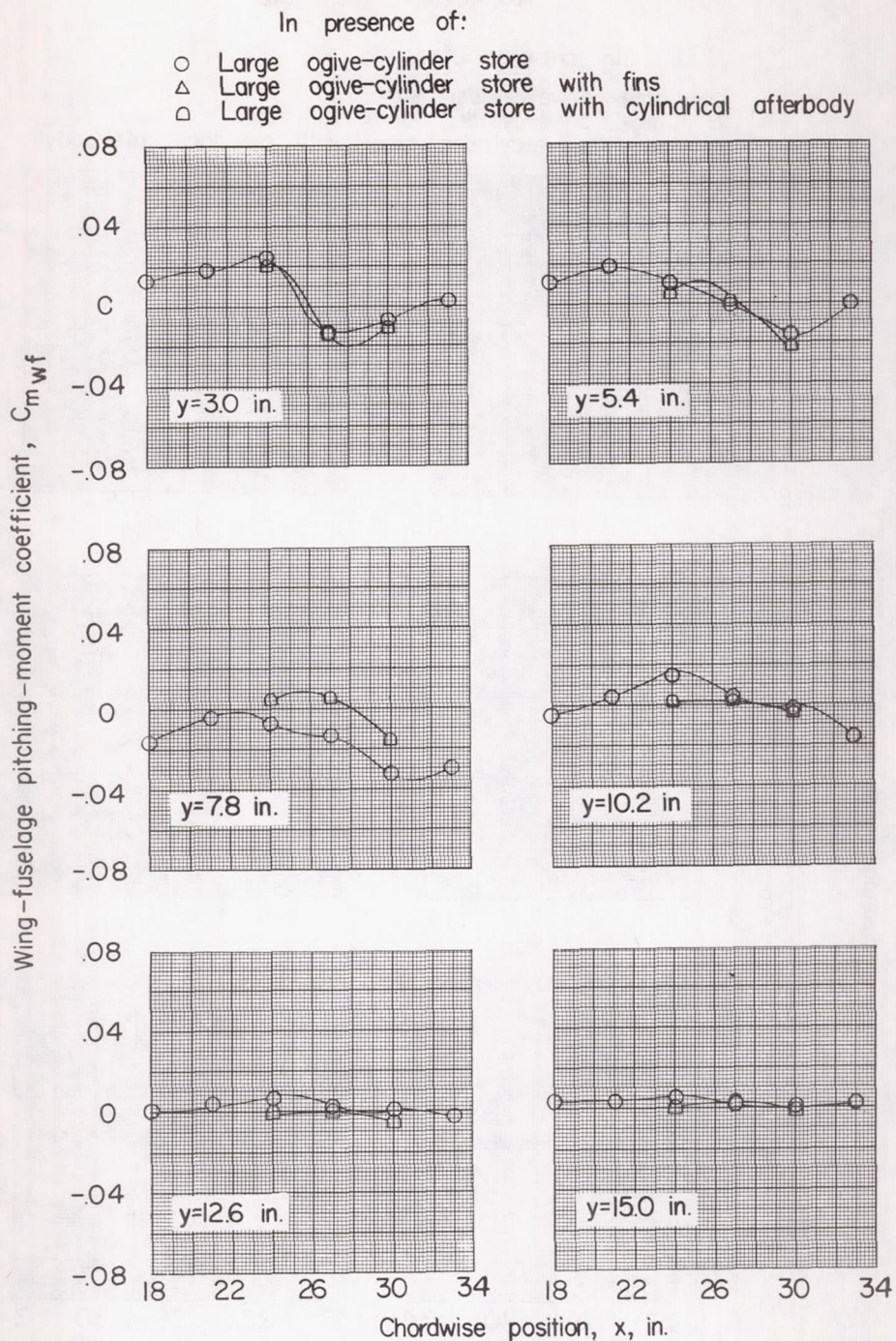
In presence of:

- Large ogive-cylinder store
- Small ogive-cylinder store
- ◇ Large parabolic store



(c) $z = 2.09$ inches; $\alpha = 4^\circ$.

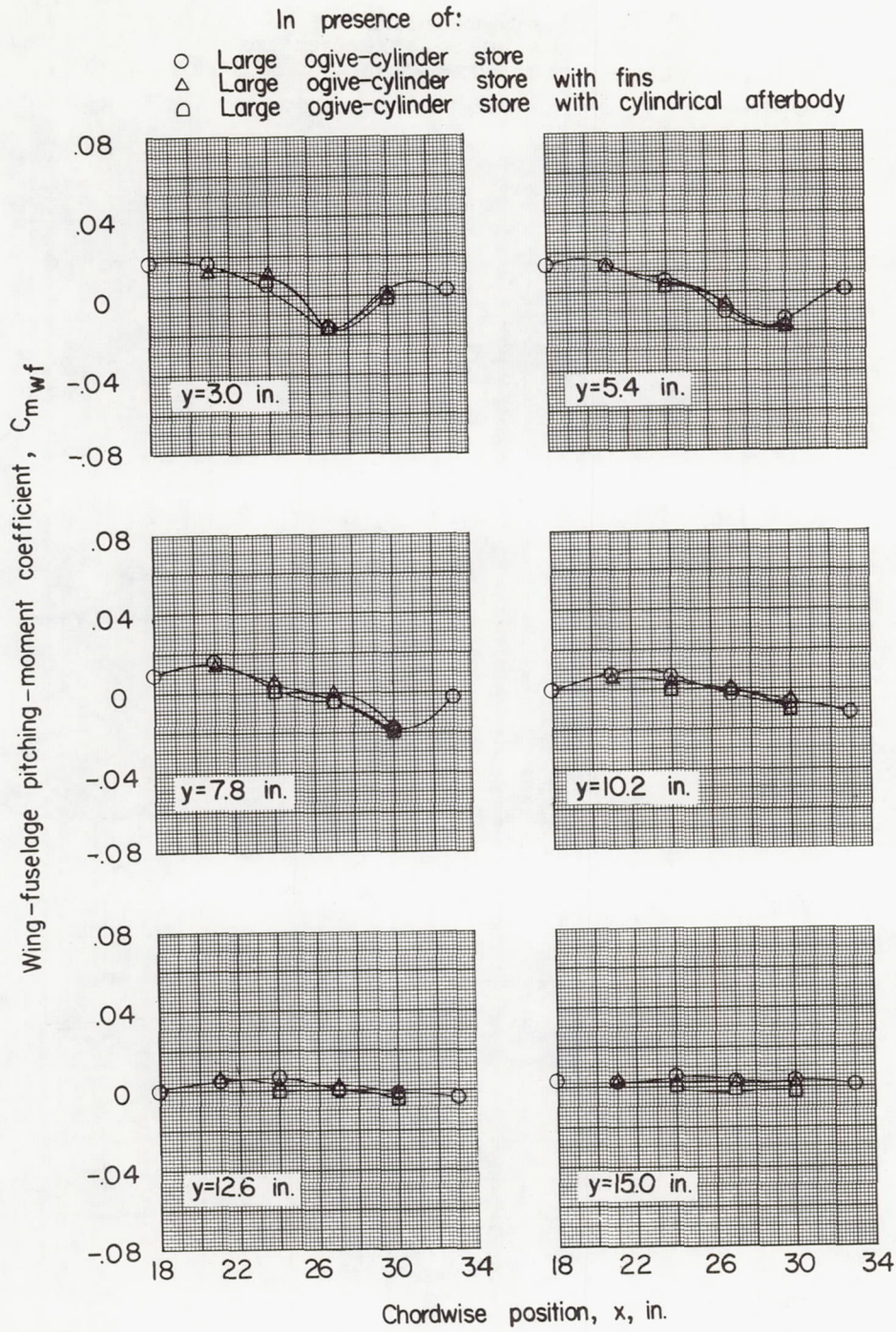
Figure 28.- Concluded.



(a) $z = 1.15$ inches; $\alpha = 0^\circ$.

Figure 29.- Pitching moment of wing-fuselage combination in presence of large ogive-cylinder store with various afterbody configurations.

(Center of moments is $\frac{\bar{c}}{4}$ of wing.)

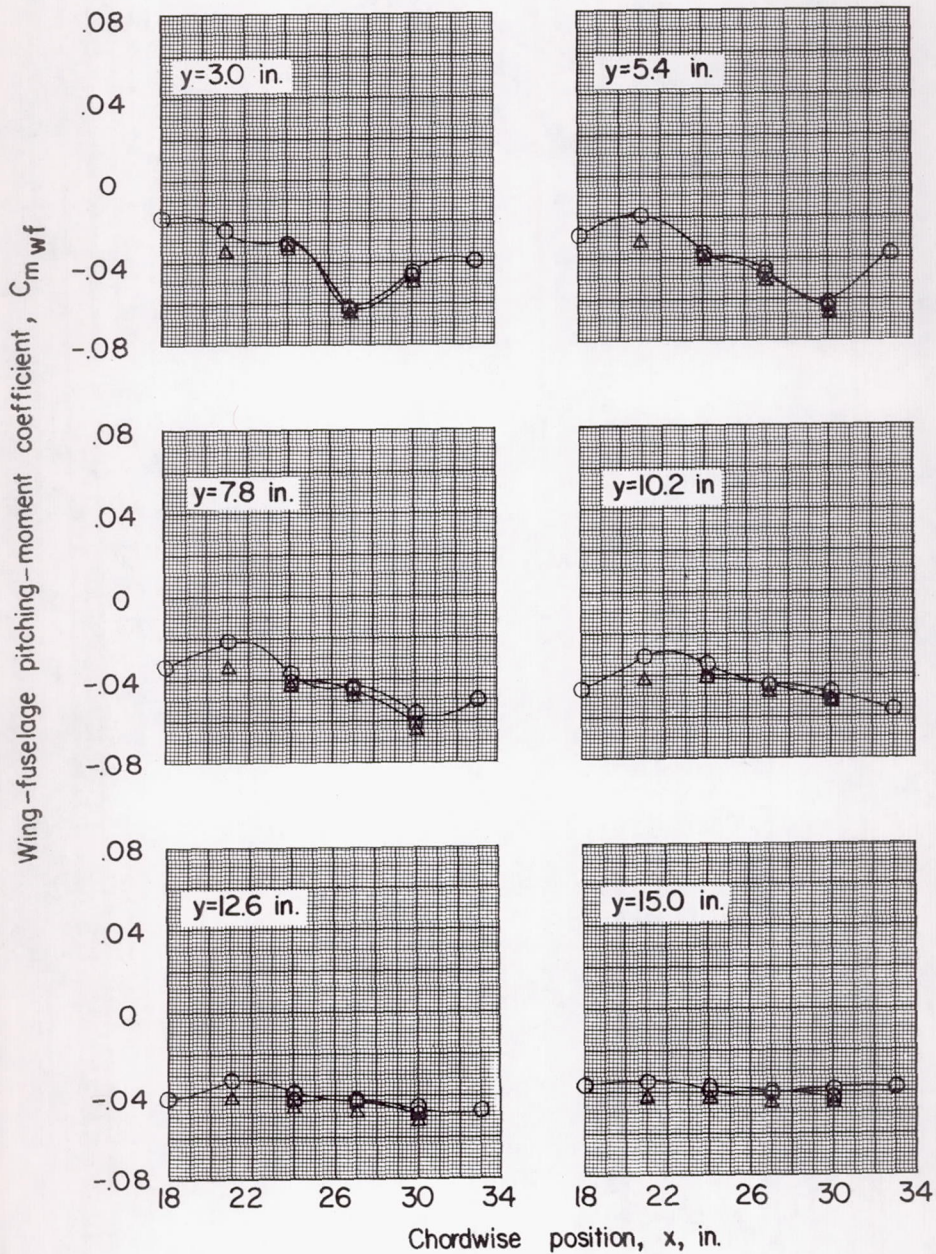


(b) $z = 2.09$ inches; $\alpha = 0^\circ$.

Figure 29.- Continued.

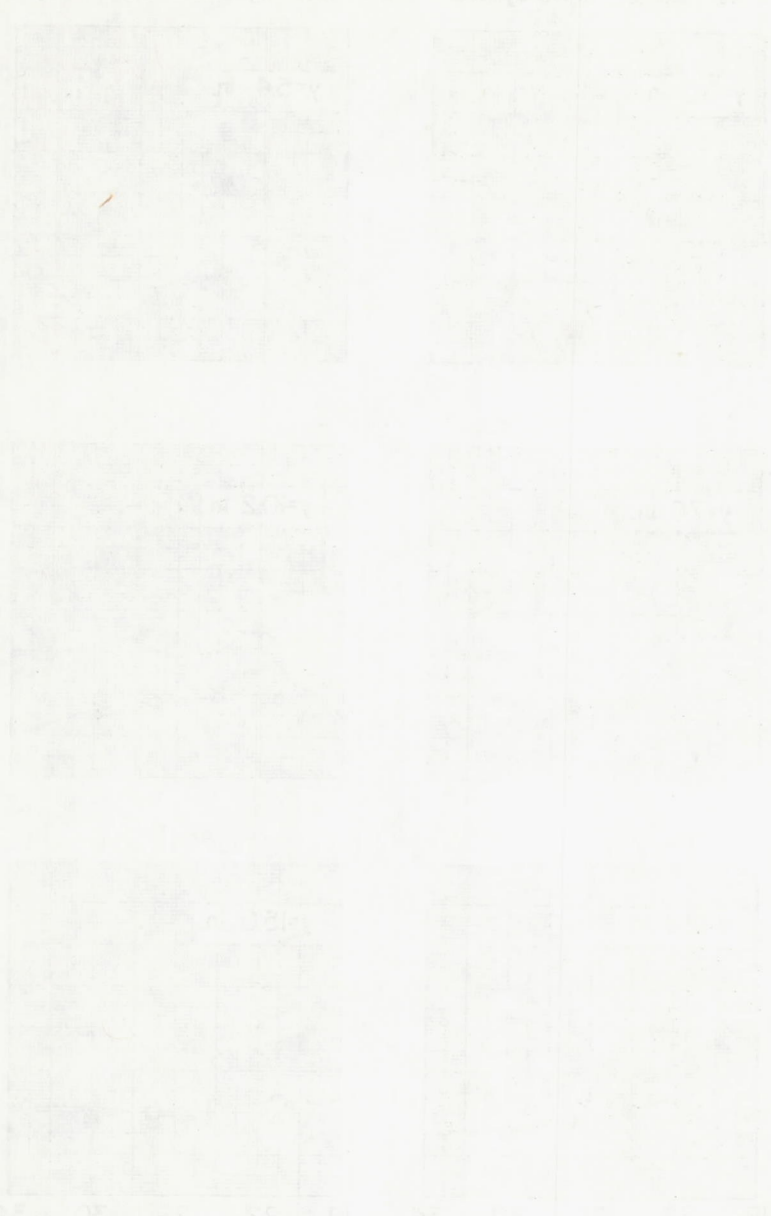
In presence of:

- Large ogive-cylinder store
- △ Large ogive-cylinder store with fins
- ◻ Large ogive-cylinder store with cylindrical afterbody



(c) $z = 2.09$ inches; $\alpha = 4^\circ$.

Figure 29.- Concluded.



20 15 10 5 0
 10 20 30 40 50 60 70 80 90 100

(1) ...

...

...